ALMA MATER STUDIORUM
UNIVERSITÀ DI BOLOGNA

DEPARTMENT OF PHYSICS AND ASTRONOMY "A. RIGHI"

SECOND CYCLE DEGREE

PHYSICS

Ultralight Vector Dark Matter from Non-Slow-Roll Inflation

Supervisor
Prof. S. Pascoli

Co-supervisor
Prof. G. Tasinato

Defended by
Martina La Rosa

Graduation Session September 2025

Academic Year 2024/2025

Abstract

Inflation not only provides a promising explanation for the observed structure of our universe; but also reveals a novel and elegant mechanism for the production of dark matter, distinct from the historically considered scenarios. Among the others, inflation naturally generates vector field fluctuations which, after being stretched to super-horizon scales and re-entering the horizon, are viable dark matter candidates. The longitudinal mode of a massive vector boson is especially noteworthy, being abundantly produced during inflation. Unlike scalars and tensors which are typically produced with a nearly scale-invariant spectrum, the longitudinal mode inherits unique dynamics from its inflationary origin, satisfying cosmological constraints and providing a robust dark matter candidate.

In this thesis, we propose a mechanism through which ultralight dark matter is generated during inflation. We introduce a brief departure from slow-roll inflation to address the challenge of producing a realistic dark matter candidate and explore its consequences. The violation of slow-roll conditions during inflation induces a rapid change in the vector boson mass, producing significant features in the power spectrum. We show that this rapid variation, occurring during a short non-slow-roll phase, enhances the power spectrum and naturally generates an ultralight dark matter relic with extremely small vector masses, allowing for the inclusion of candidates with masses as low as $m \simeq 10^{-19}$ eV or even smaller.

Our results demonstrate that the non-standard evolution of inflationary parameters strongly amplifies the longitudinal mode fluctuations, enabling ultralight bosons to be naturally produced by quantum fluctuations during inflation. This mechanism establishes a theoretically consistent pathway for generating ultralight dark matter and provides a framework to explore a unified inflationary origin for mixed dark matter scenarios.

Acknowledgments

I would like to express my sincere gratitude and appreciation to my external supervisor, Prof. G. Tasinato, for his guidance and vision in the complicated yet extraordinarily beautiful world of theoretical physics. The deep discussions we shared about the primordial universe and all the stories it can tell were truly inspiring. His ideas and approach to research have influenced the way I interpret scientific inquiry. It was a pleasure to work by his side at Swansea University, to learn from his experience and expertise and to be enriched by his deep and original perspective. I am profoundly grateful for his support and for giving me the opportunity to explore my research with sincerity and independence.

I am also indebted to my internal supervisor, Prof. S. Pascoli, for having outlined my path as a physicist. Her example and guidance allowed me to understand how the world of research truly works. I am grateful for her mentorship, for having opened to me the doors of an international research environment and for granting me the opportunity to grow both academically and personally. I deeply value the possibility of learning from her example.

I would like to extend my sincere appreciation also to Prof. F. Maltoni, my tutor for the award *"Più donne nella fisica 2024"*. It goes without saying that the passion he has put into teaching has inspired me and sparked my curiosity. For this reason, I would like to thank him for sharing his passion for physics with students in such a visible and inspiring way. But, above all, I am thankful for his support and for his presence as both tutor and guide, always ready to offer meaningful advices and insights.

Finally, special thanks are due to my colleagues, which I had the pleasure of meeting during these two years, both at the University of Bologna and at Swansea University. I wish to express my thanks for the countless reflections and insights on physics and on how it shapes our lives. Having them by my side during these years has opened my eyes to new and unexpected perspectives. Seeing everyone work with passion, driven by a common goal and a strong desire to understand more, has truly brightened my experience. I was surrounded by an environment full of dedication, from which I was fortunate to learn something from each of them. I am grateful for every moment of discussion and exchange we shared.

Thank you all for being part of my journey and for your invaluable contributions.

Note on Publications

The results discussed in this thesis are closely connected to the work *"Ultralight Dark Matter from Inflationary Particle Production"* , arXiv:2508.16455, 2025, which was carried out during my Master's research period at Swansea University and forms the basis of part of the present thesis. Unless otherwise stated, all the plots in this thesis are taken from our recent paper. The results discussed here expand upon and complement the material contained in that work.

Notation and Units

In this thesis, **boldface symbols** are consistently used to denote vector quantities, while scalar quantities are represented by regular (non-bold) symbols. Greek letters are reserved for parameters and constants that are widely accepted in the literature and subscripts are employed to indicate specific components or references where necessary. This notation is maintained throughout the thesis to ensure clarity and consistency in the presentation of mathematical expressions and physical concepts.

We will be using the convention $(-,+,+,+)$.

We will adopt natural, or high energy physics, units. After setting $\hbar = c = k_B = 1$, there is only one fundamental dimension: *energy*.
In these units:

$$[\text{Energy}] = [\text{Mass}] = [\text{Temperature}] = [\text{Length}]^{-1} = [\text{Time}]^{-1}$$

Common quantities used:

$1\text{GeV}^{-1} = 1.97 \times 10^{-14}$ cm $= 6.59 \times 10^{-25}$ sec
$M_{\text{Pl}} = 1.22 \times 10^{19}$ GeV
$\text{H}_0 = 100h$ km sec^{-1} Mpc$^{-1} = 2.1h \times 10^{-42}$ GeV
$\rho_c = 1.87h^2 \times 10^{-29}$ g/cm$^3 = 1.05h^2 \times 10^4$ eV/cm$^3 = 8.1h^2 \times 10^{-47}$ GeV^4

Contents

Chapter 1

Introduction

A description of our Universe has two complementary aspects:

- the *global* properties, encoded in the so-called cosmological parameters,
- the *irregularities* in the distribution of matter and radiation.

The cosmological parameters describe both the geometry and the content of the universe. The overall dynamics of cosmic expansion are governed by the Hubble parameter and the spatial curvature, the latter being determined by the relative fractions of different forms of energy and matter. Direct observations reveal the presence of baryonic matter (the ordinary matter of which we are made) and radiation, primarily in the form of the cosmic microwave background (CMB), characterized by a thermal spectrum with temperature $T_0 = 2.728\,\mathrm{K}$. In addition, particle physics predicts a background of cosmological neutrinos, with a similar energy density to the CMB.

However, several lines of evidence indicate that most of the matter in the universe is in the form of non-baryonic *dark matter*, whose nature is still unknown. The evolution of the universe, and in particular of the irregularities it contains, depends quite sensitively on the properties of this dark matter. Structure formation models generally require at least a component of *cold dark matter* (slow-moving particles), though other components such as *hot dark matter* (relativistic particles) are also possible. Determining the precise values of the cosmological parameters remains one of the central goals in cosmology: apart from the CMB temperature, most parameters -such as the Hubble constant and the total density parameter- are still debated.

The second key feature of the cosmological description is the fact that the distribution of matter is *not* uniform. The deviations from homogeneity are known as *density perturbations* and understanding their origin and evolution is one of the major challenges of modern cosmology. A wide variety of observational probes give us information about structure formation: the anisotropies in the CMB reflect the distribution of matter at very early times, the velocities of galaxies reveal the gravitational forces they experience, galaxy abundances and galaxy clusters inform us about present-day density fluctuations, and observations of high-redshift objects (quasars and distant galaxies observed by telescopes such as HST and Keck) probe structure at earlier cosmic epochs [1, 2].

The current cosmological model, ΛCDM, has been very successful at describing the observed large-scale structure. One of the main components of this model is dark matter, which is thought to make up approximately 5/6 of all matter in the Universe. The evidence for the existence of dark matter is strong and includes galaxy rotation curves [3, 4], redshift surveys [5, 6], the cosmic microwave background [7], weak lensing [8, 9] and other observational probes [2, 10].
Considerable effort has been dedicated to developing a wide range of theoretical models and experimental searches in an attempt to identify the correct dark matter candidate. The models themselves vary in complexity, but they are often parameterized according to the mass of the dark matter particle, which spans a range from roughly 10^{-24} eV to $\sim 10M_{\odot}$. Despite these global efforts, no confirmed non-gravitational detection of dark matter has yet been achieved and the nature, composition and origin of dark matter remain still unknown.
Thus, determining the fundamental nature of dark matter (DM) remains one of the most pressing open questions in modern physics. Its extremely weak interactions with Standard Model particles -possibly limited to gravity alone-, make direct detection exceptionally difficult [10, 11].

Inflation provides a compelling framework for understanding the very earliest moments of the universe. It offers solutions to a number of fundamental cosmological puzzles, including the striking homogeneity and isotropy observed on large scales. At the same time, quantum fluctuations during inflation generate small perturbations in the density field, which serve as the seeds for the formation of cosmic structure. These primordial inhomogeneities leave observable imprints on the cosmic microwave background and the measured spectrum of these fluctuations is in remarkable agreement with the predictions of inflation. This concordance is widely considered one of the strongest pieces of observational support for the inflationary paradigm.

Since its conception, the inflationary universe scenario has progressed from a bold hypothesis to a well-established theory of the evolution of the universe, accepted by the majority of cosmologists. If gravity is the sole interaction connecting the hidden and visible sectors, an efficient mechanism is required to generate dark matter in the early universe. Cosmic inflation naturally provides such a mechanism through the process of particle production in a rapidly expanding, curved spacetime. During inflation, the exponential expansion stretches quantum fluctuations beyond the Hubble horizon, effectively converting vacuum fluctuations into excited modes. This phenomenon is not limited to the inflaton field itself but can also produce other fields that are only gravitationally coupled, including potential dark matter candidates [12–14].

Besides explaining the origin of the structures in the universe, inflation addresses many theoretical puzzles such as the observed large scale homogeneity and isotropy of the universe on large scales, the horizon problems and the flatness problem.
Furthermore, the imprint left on the CMB by the inhomogeneities arising from quantum fluctuations during the inflationary epoch, where probed, matches with those of the predictions of inflation. This remarkable agreement is often regarded as the best observational evidence for the inflationary paradigm and makes inflation one of the cornerstones of modern cosmology.

However, while inflation is widely accepted as the origin of structure in the universe, the nature and origin of dark matter remains unknown. Conventionally, dark matter is assumed to originate from mechanisms such as thermal freeze-out or misalignment. In this thesis, we explore a striking alternative: the possibility that inflation, a theory that so beautifully explains the origins of structure in the universe, could also simultaneously be the source of the dark mat-

ter that is essential for the growth of this structure, through purely gravitational processes [15–17].

To achieve this goal, it is intriguing to explore the possibility that inflation may include brief epochs of non-slow-roll (NSR) evolution. Such departures from the standard slow-roll dynamics can leave distinctive signatures on the small-scale spectrum of fluctuations, which can be exploited to enhance dark matter production. In particular, NSR phases can induce a strong amplification of scalar curvature perturbations, potentially exceeding the threshold for primordial black hole formation in single-field inflation models [18–20]. Similarly, an enhancement of the primordial gravitational wave spectrum at high frequencies could bring it within the sensitivity of current or next-generation gravitational wave detectors. From a theoretical perspective, incorporating NSR phases into the standard inflationary model is highly significant, as these non-slow-roll periods can significantly alter our understanding of dark matter production.

Therefore, in our work we extend the perspective of [15] by demonstrating that NSR phases play a key role in the gravitational production of ultralight dark matter [10, 21, 22]. We investigate a variation of the scenario proposed in [15], where DM consists of the longitudinal modes of a massive dark photon produced purely through gravitational effects during inflation. The framework of [15] is especially minimal, relying only on the existence of a massive vector field as the DM candidate, which is efficiently generated in the very early universe. Since then, this setup has been further elaborated in a broad range of theoretical works [23–34], while its phenomenological consequences have been addressed in [35–45].
Here we study how this setup is modified by introducing a brief phase of non-slow-roll dynamics during inflation, leading to a rapid variation of the effective vector mass. The rapid changes in the inflaton dynamics during these brief epochs can induce strong modifications in the mass-dependent spectra of longitudinal vector modes, offering a new and efficient channel for generating ultralight dark matter during the early universe.

This generalization enables the production of dark matter with ultralight masses, down to $m \sim 10^{-19}\,\mathrm{eV}$ or below. A central prediction of the mechanism is the simultaneous generation of a stochastic gravitational wave background [46–50], peaking at ultra-low frequencies, which provides a distinctive observational signature of the scenario. Thus, by studying these effects, NSR inflation not only enriches the phenomenology of primordial perturbations but also opens a unified window to study both gravitational wave signals and dark matter production. Furthermore, this opens a novel connection between ultralight vector dark matter and PBH physics, suggesting a framework in which mixed dark matter scenarios naturally arise and offering new ways to probe inflationary dynamics across widely separated scales.

It is important to emphasize that the mechanism of ultralight dark matter (DM) production we propose differs fundamentally from previously studied frameworks, such as those based on the misalignment mechanism [22, 51]. Unlike these approaches, our mechanism does not rely on background fields oscillating around the minimum of their potential. Moreover, the fact that the spectrum of the longitudinal vector field is not scale-invariant implies that the misalignment mechanism is ineffective in generating a late-time vector abundance. This is because the energy density stored in a homogeneous vector field redshifts away while $H > m$, rendering any relic abundance produced in this manner negligible. This point is crucial, as it highlights that our proposal relies on a genuinely distinct mechanism for the production of ultralight DM. Our results are then different from the results of previous models in which ULDM was proposed as produced from cosmological initial conditions. By opening up this new avenue, our mechanism broadens

the landscape of viable dark matter models, offering fresh opportunities to connect early-universe dynamics with present-day cosmological observations.

Executive summary

This thesis explores the role of inflationary cosmology and ultra-light vector bosons in the early universe, with the goal of exploring the origin of dark matter. It is organized as follows:

We begin with an introduction to the inflationary theoretical framework in Chapter 2, outlining the standard inflationary paradigm, its puzzles and the motivations for inflation as our starting point. Building on this foundation, in Chapter 3 we study cosmological perturbation theory, focusing on quantum fluctuations of scalar fields during inflation and their power spectra. After this, we move into the core of our analysis by investigating the origin of dark matter in Chapter 4, and then examining in detail the role of vector fields in the early universe in Chapter 5. Here, we analyse the compatibility of ultra-light vector bosons with cosmological constraints, their dynamics during inflation and radiation domination and their implications for dark matter abundance. In Chapter 6, we extend this analysis to scenarios of non-slow-roll inflation, exploring departures from standard conditions, both in terms of how the behaviour of longitudinal modes changes under different initial conditions and of the phenomenological consequences of this new mechanism.

The thesis concludes by highlighting the key findings and open questions, and by presenting three technical appendices that support the main calculations. Overall, the aim is to show how ultra-light vector bosons may be produced during inflationary epoch and may serve as viable dark matter candidates, bridging inflationary physics, cosmological perturbations and observational constraints.

Chapter 2

Foundations of Inflationary Cosmology

> *"We are just an advanced breed of monkeys on a minor planet of a very average star. But we can understand the Universe. That makes us something very special."*
> — Stephen Hawking

Inflation [1, 52] stands as the most beautiful and profound theoretical paradigm in modern cosmology. It offers a convincing explanation of the reasons for which our universe appears as it does today. The inflationary paradigm asserts that, in its earliest moments, an infinitesimally small region of spacetime underwent a phase of rapid accelerated expansion -transforming into the universe we live in and that we now observe. This dramatic growth smoothed out primordial irregularities, rendering the observable universe remarkably homogeneous and isotropic at large scales.

Yet the elegance of inflation extends far beyond this initial contribution: inflation not only stretches spacetime, but also quantum fields themselves. During this epoch, quantum fluctuations are excited and their perturbations extended from microscopic to cosmological scales. The vacuum fluctuations, once stretched beyond the horizon, effectively freeze and become classical, imprinting energy density variations across the universe. As the universe evolves and these fluctuations re-enter the observable horizon, they manifest as temperature and matter anisotropies- believed to be the origin of the large-scale structure of galaxies and dark matter [1, 53]. Inflation, in its richness, offers yet another remarkable prediction: it sources primordial gravitational waves as quantum fluctuations of spacetime itself. These waves may leave subtle imprints in the polarization patterns of the CMB and their detection is now the focus of an ambitious and far-reaching observational effort.
Thus, inflation suggests a breathtaking possibility: that all the structure we see in the universe today -every galaxy, cluster and filament- is the result of quantum fluctuations born in the earliest moments of cosmic history. This provides the motivation for taking it as the basis of our study.

Inflation is defined in an extraordinarily clear and elegant way: it refers to the epoch in the early universe during which the *scale factor* -the parameter that quantify the size of the universe- undergoes accelerated expansion. As we shall see, this does not constitute the sole definition of inflation, as there exist equivalent formulations describing the same period of accelerated expansion. Regardless the definition, inflation represents an extraordinary phase of expansion in the

universe that irreversibly shaped its structure. More insightfully, one might describe the inflationary expansion by involving the *Hubble radius* -the characteristic scale of causal contact-, saying that it shrinks relative to any fixed physical scale embedded in the expansion. In this sense, inflation should be viewed as a powerful "zoom-in" on a tiny patch of the primordial universe. Importantly, inflation is not a replacement for the Hot Big Bang theory; rather, it is a remarkable extension appended to its earliest phase.

A sufficiently long period of inflation can successfully solve various issues related to the initial conditions required by the Hot Big Bang model in order to produce a universe like the one we live in. In particular, it naturally explains why the universe is so close to being spatially flat and why it appears remarkably homogeneous on large scales. These puzzles were precisely the motivation for Guth's original proposal of inflation in 1981 [54]. Even so, these issues are no longer the primary driving force behind inflationary cosmology. What makes inflation truly compelling today is its role as a mechanism for generating the primordial structure of the universe. In this sense, inflation has become a genuinely predictive paradigm and remains the leading theoretical framework for explaining the origin of all structure in the universe, including life itself.

2.1 Overview of Inflationary Paradigms

The history of the universe from 10^{-10} seconds after the Big Bang (corresponding to energies around 1 TeV) up to the present day is grounded in observational evidence and well-tested physical theories [1, 13]. It relies mainly on the Hot Big Bang cosmology [2] and its success ensures that the model gives a correct description of the Universe starting at some epoch before nucleosynthesis takes place. At epochs well before nucleosynthesis, the universe was composed of a hot gas that gradually cooled as cosmic expansion proceeded. This gas contained several components, corresponding to the various particle species present, among them the photons that we now detect as the cosmic microwave background radiation. Initially, the energy density was dominated by relativistic species (including photons), collectively referred to as radiation; at later times it became dominated by non relativistic species, referred to as matter. However, in sharp contrast to this well-defined picture, we have no certain knowledge of the universe well before nucleosynthesis: before 10^{-10} seconds from the Big Bang, the physics becomes as uncertain as it is fascinating. No direct experimental probe can give us information about the very first instants of the universe. It's in this regime, where experimental physics is blind, that theory offers insights in the understanding of the universe. It is from those first 10^{-10} seconds that we want to extrapolate information about the universe today. For example, to explain the perturbations in the CMB temperature we require a primordial seed of fluctuations and a mechanism by which those microscopic quantum fluctuations in the energy density are stretched to macroscopic scales.

The entire gaseous period of the universe is often referred to as the Big Bang, with the term *Hot* typically omitted, since the universe need not have been in thermal equilibrium or radiation-dominated. Before this, there is thought to have been an era of **inflation**, during which the

energy density of the universe was dominated by the potential of the scalar fields. Inflation is supposed to determine the initial conditions for the Big Bang, including the perturbations. However, as anticipated, one of the most fascinating things about inflation is that, although initially proposed to fix issues involving the initial conditions of the standard Hot Big Bang cosmology, its enduring importance stems from a feature identified shortly after its introduction: it also offers a compelling mechanism for generating the primordial inhomogeneities that ultimately gave rise to all observable structures, from the earliest collapsed objects and the clustering of galaxies, to the anisotropies detected in the microwave background. Then, if we assume this spectrum was produced by inflation, we can use late time observations of the CMB and the LSS to infer the primordial input spectrum. This gives us an observational probe of the physical conditions when the universe was 10^{-34} seconds old and a new, fascinating opportunity to use cosmology to probe physics at the highest energies [53].

2.2 The Standard Inflationary Universe

Homogeneity and isotropy are observed when the universe is considered at sufficiently large scales. At these scales, our universe exhibits a striking degree of uniformity, an observation that underpins the Cosmological Principle. The most compelling evidence for this isotropy comes from the extraordinary uniformity of the cosmic microwave background (CMB) radiation: intrinsic temperature anisotropies are suppressed to the level of one part in 10^5. This remarkable smoothness indicates that, at the epoch of last scattering, approximately 200,000 years after the Big Bang, the universe was isotropic and homogeneous to an exceptional degree of precision, on the order of 10^{-5}.

This observed large-scale homogeneity and isotropy provides the foundation for modeling the universe using the Friedmann–Robertson–Walker (FRW) framework. By assuming that the universe is homogeneous and isotropic, the FRW model successfully describes its large-scale dynamics and allows us to extend our understanding back to extremely early times, as close as 10^{-43} seconds after the Big Bang, approaching the limits of known physics [1, 12, 52, 53, 55].

2.2.1 An Homogeneous Universe

Assuming large-scale homogeneity and isotropy, one is naturally led to describe the spacetime geometry of the universe using the Friedmann–Robertson–Walker (FRW) metric:

$$\mathrm{d}s^2 = -\,\mathrm{d}t^2 + a^2(t)\left[\frac{\mathrm{d}r^2}{1-k\,r^2} + r^2\,\mathrm{d}\theta^2 + r^2\sin^2\theta\,\mathrm{d}\varphi^2\right]. \tag{2.1}$$

where the spacetime coordinates (t, r, θ, φ) are comoving coordinates, with t representing the proper time as measured by an observer at rest in the comoving reference frame -i.e. with fixed spatial coordinate (r, θ, φ). The expansion of the universe is reflected by the growth of the *scale factor* $a(t)$, while galaxies and comoving observers retain fixed spatial coordinates, provided no external forces act upon them [12, 14].
The radial coordinate r is dimensionless, meaning that the cosmic scale factor $a(t)$ carries the dimension of length, and only relative distances are physically meaningful. For spaces of constant spatial curvature, the curvature parameter k can be rescaled to take values $+1, -1$ or 0, corresponding respectively to positive, negative or flat spatial geometry. In the case $k = +1$, the coordinate r ranges from 0 to 1.

The essential quantity characterizing the Friedmann–Robertson–Walker spacetime is the expansion rate, defined by the *Hubble parameter*:

$$H(t) \equiv \frac{\dot{a}(t)}{a(t)}, \tag{2.2}$$

where $\dot{a}(t)$ is the time derivative of the cosmic scale factor. The Hubble parameter $H(t)$ has units of inverse time. It sets the characteristic time-scale and the characteristic length-scale of the homogeneous universe, respectively the *Hubble time:* $t_H \sim H^{-1}$ and the *Hubble radius* given by $R_H \sim H^{-1}$. This means that the Hubble time sets the scale for the age of the universe, while the Hubble length sets the size of the observable universe. It is positive in an expanding universe, negative in a contracting one.
Given the comoving distance, the corresponding physical distance is due to

$$R = a(t)r \ , \tag{2.3}$$

which evolves in time even for objects with zero peculiar velocity. This encapsulates the essence of cosmic expansion: the stretching of space itself rather than motion through space.

Besides, the form of the scale factor $a(t)$ is dictated by the matter content of the universe via the Einstein field equations. Its evolution, on the other hand, is determined by the Friedman equation

$$H^2 + \frac{k}{a^2} = \frac{8\pi G_{\rm N}}{3}\rho \tag{2.4}$$

and, for the acceleration

$$\frac{\ddot{a}}{a} = -\frac{4\pi G_{\rm N}}{3}(\rho + 3P) \tag{2.5}$$

The Friedmann equation 2.4 can be recast as

$$\Omega - 1 = \frac{\rho}{3H^2/8\pi G_{\rm N}} = \frac{k}{a^2 H^2} \ , \tag{2.6}$$

where the parameter Ω is the ratio between the energy density ρ and the critical energy density $\rho_{\rm c}$ (both Ω and $\rho_{\rm c}$ are not constant in time):

$$\Omega = \frac{\rho}{\rho_{\rm c}}, \qquad \rho_{\rm c} = \frac{3H^2}{8\pi G_{\rm N}} \ . \tag{2.7}$$

Since $a^2H^2 > 0$, there is a correspondence between the sign of k and the sign of $(\Omega - 1)$:

$$\begin{array}{rcll} k = +1 & \Rightarrow & \Omega > 1 & \text{closed}, \\ k = 0 & \Rightarrow & \Omega = 1 & \text{flat}, \\ k = -1 & \Rightarrow & \Omega < 1 & \text{open}. \end{array} \tag{2.8}$$

This is valid at all times. This classification corresponds to three distinct possible geometries for the universe:

- **Closed universe ($k = +1$, $\Omega > 1$)**: The spatial geometry is spherical, meaning the universe is finite in volume and may eventually recollapse under its own gravity if dominated by matter.
- **Flat universe ($k = 0$, $\Omega = 1$)**: The spatial geometry is Euclidean, implying that the universe is spatially infinite and the expansion rate asymptotically balances the gravitational attraction. This case is especially favoured by inflationary cosmology.
- **Open universe ($k = -1$, $\Omega < 1$)**: The spatial geometry is hyperbolic, indicating an infinite universe that expands forever, with curvature dominating at large scales if no dark energy is present.

By introducing the *conformal time* τ, as a clock which slows down with the expansion of the universe and as the coordinate for which light rays propagate as if in flat space

$$\tau = \int \frac{dt}{a(t)} \, , \tag{2.9}$$

we can rewrite the FRW metric as:

$$\mathrm{d}s^2 = a^2(\tau) \left[-\mathrm{d}\tau^2 + \frac{\mathrm{d}r^2}{1 - k\, r^2} + r^2\, \mathrm{d}\theta^2 + r^2 \sin^2\theta\, \mathrm{d}\varphi^2 \right] = a^2(\tau) \left[-\mathrm{d}\tau^2 + \mathrm{d}\mathbf{x}^2 \right] \, . \tag{2.10}$$

The reason why is called conformal is manifest from Eq. 2.10: the corresponding FRW line element is conformal to the Minkowski line element describing a static four dimensional hypersurface [12–14].

2.2.2 The Particle Horizon and the Hubble Radius

Having introduced the *conformal time*, we can now proceed to give a set of useful definitions [14].

A light signal emitted from coordinate position $(r_{\mathrm{H}}, \theta_0, \phi_0)$ at time $t = 0$ will reach $r_0 = 0$ in a time t determined by

$$\int_0^t \frac{\mathrm{d}t'}{a(t')} = \int_0^{r_{\mathrm{H}}} \frac{\mathrm{d}r'}{\sqrt{1 - kr'^2}}. \tag{2.11}$$

This is the maximum distance light can propagate between an initial time t_i, usually taken to be the origin of the universe, $t_i \equiv 0$, and some later time t.
Starting from this, we define the *particle horizon* as the proper distance to the horizon at time t

$$R_{\rm H}(t) = a(t)\int_0^t \frac{{\rm d}t'}{a(t')} = a(t)\int_0^a \frac{{\rm d}a'}{a'}\frac{1}{a'H(a')} = a(t)\int_0^{r_{\rm H}} \frac{{\rm d}r'}{\sqrt{1-kr'^2}}. \tag{2.12}$$

.

The particle horizon is fundamental for understanding the causal structure of the universe. In the standard Big Bang model, the universe begins at a finite time in the past and at any point in its early history, the particle horizon is likewise finite. This constrains the maximum distance over which regions of spacetime could have interacted causally, forming the basis of the so-called *Big Bang puzzles*.
Specifically, if $R_H(t)$ is finite, it marks the boundary between the **observable Universe** and regions from which light has not reached us. The finiteness of the particle horizon depends on the behaviour of the scale factor $a(t)$ near the initial singularity. In standard cosmology, one finds $R_H(t) \sim t$, confirming that the particle horizon is indeed finite.

We also recall the defintion of *Hubble radius*:

$$\frac{1}{H} = \frac{a}{\dot{a}} \tag{2.13}$$

as the distance over which particles can travel in the course of one expansion time.

The main difference between these two recently introduced quantities is subtle but important. The Hubble radius provides a measure of whether particles are causally connected at a given time. If they are separated by distances larger than the Hubble radius H^{-1}, they cannot currently communicate, i.e., they cannot interact at time t. However, they could have interact in the past. In contrast, if particles are separated by distances greater than $R_H(t)$, they *could never* have communicated with one another.

In standard cosmology, the particle horizon is finite and, up to numerical factors, approximately equal to the Hubble radius, H^{-1}. For this reason, the terms horizon and Hubble radius are often used interchangeably in this context. However, in inflationary models the horizon and Hubble radius behave quite differently. During inflation, the horizon distance grows exponentially relative to the Hubble radius; by the end of inflation, the two differ by a factor of e^N, where N denotes the number of e-folds of inflation.

Let us also define the *comoving particle horizon* as the quantity which delineates the boundary beyond which signals emitted at a given time τ will never reach a specified observer in the future. In comoving coordinates, the comoving particle horizon corresponds to the set of points satisfying

$$\tau_{\rm H} = \int_0^t \frac{{\rm d}t'}{a(t')} = \int_0^a \frac{{\rm d}a'}{H(a')a'^2} = \int_0^a {\rm d}\ln a' \left(\frac{1}{Ha'}\right) \tag{2.14}$$

where the quantity

$$\frac{1}{aH} \tag{2.15}$$

gives the definition of the *comoving Hubble radius*, which plays a crucial role in inflation. We see that the comoving horizon then is the logarithmic integral of the comoving Hubble radius $(aH)^{-1}$.

Since particles separated by distances larger than $(aH)^{-1}$ are not in causal contact at a *given time*, it is possible for $\tau_{\rm H}$ to be much larger than the comoving Hubble radius at the present epoch: in this case, particles may not be able to communicate today, even though they could have interacted at earlier times. This situation can occur if the comoving Hubble radius was much larger in the early universe, such that $\tau_{\rm H}$ receives most of its contribution from those early times. This does not occur during matter-dominated or radiation-dominated epochs. In these periods, the comoving Hubble radius increases with time, so that the dominant contribution to H typically comes from the most recent times.

Furthermore, a physical length scale λ lies *inside* the Hubble radius if $\lambda < H^{-1}$. We can also express this condition in terms of its comoving wavenumber k, since: $\lambda = 2\pi\, a/k$. This leads to the following useful expressions:

$$\frac{k}{aH} \ll 1 \quad \rightarrow \quad \text{scale } \lambda \text{ outside the Hubble radius,} \tag{2.16}$$

$$\frac{k}{aH} \gg 1 \quad \rightarrow \quad \text{scale } \lambda \text{ inside the Hubble radius.} \tag{2.17}$$

2.3 The Big Bang Puzzles

Initial Conditions as Fine-Tuning Problems

For the universe to evolve to its current state, in the context of the conventional Big Bang model, extreme fine-tuning is required. Indeed, in order to obtain a homogeneous and isotropic universe, we would need to specify the initial amount of matter and its spatial distribution in the universe, which can be done by explicitly giving its energy density and pressure, $\rho(\vec{x})$ and $p(\vec{x})$, both depending on spatial location. However, at the same time, observations of the cosmic microwave background show that the inhomogeneities were much smaller in the past than they are today. To ensure that the universe remains homogeneous at late times requires the initial fluid velocities $\vec{v}(\vec{x})$ to take very precise values. It seems, then, that in order to obtain the universe as it is today, we need exact initial values, so the initial conditions for the conventional FRW cosmology appear highly fine-tuned [13].

While this is not inherently problematic, it is somewhat unsatisfying to attribute the universe's current configuration only to a specific and highly delicate configuration of the initial conditions: it does necessitate the precise calibration of fundamental parameters, and this invites deeper examination.
Inflation offers a compelling resolution to this issue by providing a mechanism through which the

observed features of the universe can emerge naturally, without invoking such extreme fine-tuning.

The fine-tuning problem manifests in distinct forms, commonly referred to as the *horizon problem* and the *flatness problem* to which we may add the primordial perturbation problem.

Homogeneity and the Horizon Problem: *Why does the Universe look the same in all directions?*

The only way two regions of the universe can share the same physical properties, such as temperature, is if they are close enough for information to be exchanged between them and allow their conditions to equilibrate, in particular to reach thermal equilibrium, which requires causal contact. Since no signal can travel faster than light, causal contact is limited by the light-travel time. Whenever two regions are separated by a distance so large that light has not had sufficient time to cross between them, they are causally isolated. In that case, the regions lie beyond each other's horizons and cannot influence one another [13, 56].

According to standard cosmology, photons decoupled from baryons and electrons at a temperature of order $\sim 0.3\,\mathrm{eV}$, corresponding to the so-called surface of last scattering at redshift $z \simeq 1100$, when the universe was about 3×10^5 years old. From that moment onward, CMB photons have free-streamed essentially unperturbed and thus provide a direct snapshot of the state of the universe at that early epoch.

Observations reveal that the universe is highly homogeneous and isotropic on large scales. The best measure of this is provided by observed spectrum of the cosmic microwave background, which is extremely close to a perfect blackbody with temperature $T \simeq 2.728\,\mathrm{K}$, with temperature anisotropies of order 10^{-5}, over more than three orders of magnitude in wavelength. This suggests that the universe was even smoother at earlier epochs. So, when we observe the CMB in opposite directions, we find that its temperature is almost identical to an astonishing level of precision. However, CMB photons have been travelling for almost the entire lifetime of the Universe in order to reach us today and they had no time to traverse the whole universe and reach the regions on the opposite side of the sky. Yet, the universe appear homogeneous in all the directions. This is particularly surprising since in the conventional Big Bang picture the early universe consisted of a large number of causally-disconnected regions of space.

How can distant regions be so finely correlated if they were never in causal contact? In the Big Bang theory, there is no dynamical reason to explain why these causally-separated patches show such similar physical conditions. By tracing the expansion backwards, one finds that even regions that are only one degree apart on today's sky were already outside each other's horizons when the CMB was emitted. We then refer to the *homogeneity problem* as the *horizon problem.*

In order to have a more quantitative perspective, let us follow the discussion of [57] and consider

the physical length corresponding to present Hubble radius, which is essentially the size of the observable universe. We can evaluate it at the time of last scattering (ls) by scaling it back with the scale factor:

$$\lambda_{\rm H}(t_{\rm ls}) = R_{\rm H}(t_0)\,\frac{a_{\rm ls}}{a_0} = R_{\rm H}(t_0)\,\frac{T_0}{T_{\rm ls}}. \tag{2.18}$$

During matter domination, however, the Hubble length evolves differently, since

$$H^2 \propto \rho_m \propto a^{-3} \;\propto\; T^3. \tag{2.19}$$

Consequently, at last scattering one finds

$$H_{\rm ls}^{-1} = R_{\rm H}(t_0)\left(\frac{T_{\rm ls}}{T_0}\right)^{-3/2} \;\ll\; R_{\rm H}(t_0). \tag{2.20}$$

In other words, the physical size of today's Hubble radius was *much larger* than the causal horizon at the epoch of last scattering. From the comparison of the corresponding volumes, one finds:

$$\frac{\lambda_H^3(T_{\rm ls})}{H_{\rm ls}^{-3}} = \left(\frac{T_0}{T_{\rm ls}}\right)^{-3/2} \;\approx\; 10^6. \tag{2.21}$$

This implies that within the region which has now grown into our present Hubble volume, there were of order 10^6 causally disconnected patches at the time of last scattering. It is difficult to imagine any mechanism *within the standard Big Bang framework* capable of producing a black-body spectrum for the cosmic photon bath when those regions had no causal contact the last time they interacted with the surrounding plasma.

The Flatness Problem: *Why is the universe so flat?*

At the present time, the universe is remarkably close to being spatially flat, lying almost exactly between a positively curved (closed) and a negatively curved (open) geometry.
Out of the full range of possibilities, our nearly flat universe seems to be clearly a very special case.

Let's assume that Einstein equations are valid until the Plank era, and let's turn to the Friedmann equation for the curvature:

$$H^2 = \frac{\rho(a)}{3} - \frac{k}{a^2} \tag{2.22}$$

also written as

$$\Omega(a) - 1 = \frac{k}{(aH)^2}\,, \tag{2.23}$$

where

$$\Omega(a) \equiv \frac{\rho(a)}{\rho_{\rm crit}(a)}\,, \qquad \rho_{\rm crit}(a) \equiv 3H(a)^2\,. \tag{2.24}$$

Stating that the universe is perfectly flat means to require $\Omega = 1$ at all times; but if there is even a small curvature term, the time dependence of $\Omega(a)$ is quite different.
During a radiation–dominated (RD) era we have:

$$H^2 \propto \rho_{\rm r} \propto a^{-4}\,, \tag{2.25}$$

and therefore

$$\Omega - 1 \;\propto\; \frac{1}{a^2\rho_{\rm r}} \;\propto\; \frac{1}{a^2 a^{-4}} \;\propto\; a^2. \tag{2.26}$$

During matter domination (MD):

$$\rho_{\rm m} \propto a^{-3} \tag{2.27}$$

and, analogously,

$$\Omega - 1 \;\propto\; \frac{1}{a^2\rho_{\rm m}} \;\propto\; \frac{1}{a^2 a^{-3}} \;\propto\; a. \tag{2.28}$$

In both regimes, $(\Omega - 1)$ becomes smaller as we go *backwards* in time.
Since today $(\Omega_0 - 1)$ is of order unity, we can estimate its value at $t_{\rm Pl}$ (the time when the temperature of the universe was $T_{\rm Pl} \simeq 10^{19}\,\text{GeV}$):

$$\frac{|\Omega - 1|_{\,T=T_{\rm Pl}}}{|\Omega - 1|_{\,T=T_0}} \;\simeq\; \left(\frac{a_{\rm Pl}^2}{a_0^2}\right) \;\simeq\; \left(\frac{T_0^2}{T_{\rm Pl}^2}\right) \;\sim\; \mathcal{O}(10^{-64}). \tag{2.29}$$

with $T_0 \simeq 10^{-13}\,\text{GeV}$, which is the current temperature of the CMB radiation. Thus, the deviation from flatness at Planck scales is extremely small.
This is particularly striking because any small departure from flatness in the early universe becomes increasingly amplified as the Universe evolves. For example, if the density had been only slightly larger than the critical value even as late as one billion years after the Big Bang, the universe would already have collapsed by now; if it had been slightly smaller, the rapid expansion would have diluted all matter and prevented structure formation.

In standard cosmology, the comoving Hubble radius, $(aH)^{-1}$, grows with time and from Eq.2.23 the quantity $|\Omega - 1|$ must thus diverge with time. In the absence of any selection principle or dynamical mechanism, one would expect $|\Omega - 1|_{\,T=T_{\rm Pl}} \sim \mathcal{O}(1)$.
The critical value $\Omega = 1$ is an unstable fixed point. Therefore, in standard Big Bang cosmology without inflation, the near-flatness observed today requires a drastic fine-tuning. The value of $|\Omega$- 1| at early times have to be fine-tuned to values amazingly close to zero, but without being exactly zero. Why, then, we need such tuned initial conditions?

2.4 Inflation as the solution of the Big Bang Puzzles

To specify the universe's initial conditions, well-posed Cauchy problem requires the specification of the positions and velocities of all matter particles, everywhere in space. The subsequent homogeneity of the universe turns out to be extremely sensitive to these initial velocities. If they are even slightly underestimated, matter collapses rapidly under gravity; if they are slightly overestimated, the expansion proceeds too fast, leaving behind a nearly empty universe without structure.

This deep sensitivity, as we outlined, reflects a fine-tuning problem. The situation is further complicated by the horizon problem: the required coordination of velocities must extend across regions that, according to causal limits, could never have exchanged information.

The flatness and horizon problems thus represent significant limitations in the predictive power of the Big Bang model [1, 12, 13]. The extreme flatness of the early universe must be imposed as part of the initial conditions. Similarly, the remarkable large-scale homogeneity of the universe is neither explained nor predicted by the model, but must be assumed. A theory capable of dynamically accounting for these initial conditions is therefore highly desirable.

In this respect, one might observe that both of these problems stem from the fact that, within conventional cosmology, the comoving Hubble radius grows monotonically with time. This observation points to an elegant resolution: if, in the very early universe, the comoving Hubble radius were instead to decrease sufficiently, the puzzles of the Big Bang would naturally be resolved.
Thus, we require a primordial period during which physical length scales evolve more rapidly than the Hubble radius, H^{-1}. This hypothesis could allow photons to have been in causal contact in the past, thereby explaining the observed homogeneity of the CMB. Indeed, if there exists an epoch during which physical scales grow faster than the Hubble radius, then scales that are within the horizon today ($\lambda < H^{-1}$) but were outside it at some earlier time ($\lambda > H^{-1}$) -for instance, at the time of last scattering when two photons were emitted- could have re-entered the Hubble radius during a primordial epoch ($\lambda < H^{-1}$) once again.

If this occurs, homogeneity and isotropy of the CMB follow naturally: photons we observe today, which were emitted from causally disconnected regions on the last-scattering surface, share the same temperature because they had an opportunity to exchange information at an earlier stage in the universe's evolution.

The resolution of the horizon problem thus lies in the distinction between the (comoving) particle horizon and the (comoving) Hubble radius: while the particle horizon is larger than the Hubble radius today -so that particles were in causal contact at early times- they are no longer in contact at later epochs.
Since a given scale evolves as a, while the Hubble radius scales as $H^{-1} \sim a/\dot{a}$, we must impose a period during which their ratio increases with time. Equivalently, this requires that the comoving Hubble radius decreases.

2.4.1 Conditions for Inflation

The fundamental condition we gave for inflation relies on the definition of the Hubble radius, since it most directly relates to the flatness and horizon problems and is the key for the mechanism to generate fluctuations. This is the requirement for which the comoving horizon has to decrease

[13]:

$$\frac{d}{dt}\left(\frac{1}{aH}\right) < 0 \ . \tag{2.30}$$

If we now take the time derivative of the shrinking Hubble sphere, we can see that this corresponds to:

$$\frac{d}{dt}\Big(\frac{1}{aH}\Big) = \frac{-\ddot{a}}{(aH)^2}, \tag{2.31}$$

and then we immediately deduce that a shrinking comoving Hubble radius implies accelerated expansion

$$\frac{d^2a}{dt^2} > 0 \ . \tag{2.32}$$

This explains why inflation is often defined as a period of accelerated expansion and gives us another way to describe the inflationary epoch.

This can be seen also in a different way, by expressing the second time derivative of the scale factor in terms of the first time derivative of the Hubble parameter H and by introducing the parameter ε:

$$\frac{\ddot{a}}{a} = H^2(1-\varepsilon), \qquad \text{where} \quad \varepsilon \equiv -\frac{\dot{H}}{H^2}. \tag{2.33}$$

Acceleration therefore corresponds to

$$\varepsilon = -\frac{\dot{H}}{H^2} = -\frac{d\ln H}{dN} < 1, \tag{2.34}$$

Here, we have defined $\mathrm{dN} = \mathrm{H\ dt} = \mathrm{d\ln a}$, which measures the number of e-folds N of inflationary expansion. Eq.2.34 therefore means that the fractional change of the Hubble parameter per e-fold is small.

Moreover, from the second Friedman equation 2.5, we infer that $\ddot{a} > 0$ requires

$$p < -\frac{1}{3}\rho, \tag{2.35}$$

i.e. negative pressure.

Thus, we have three equivalent formulations of inflation, three conditions that can be equivalently verified in order to characterize the inflationary expansion. The three conditions for inflation are:

- **Decreasing comoving horizon**
- **Accelerated expansion**
- **Negative pressure**

If this occurs, the isotropy and homogeneity of the CMB are naturally accounted for: photons observed today, which were emitted from causally disconnected regions at the time of last scattering, could nevertheless have the same temperature because they were once in causal contact in the very early universe.

To investigate easily some properties and features of the inflationary epoch, let us consider the special case $P = -\rho$, so let us work in a *de Sitter* phase.

From the FRW equations together with the energy conservation law, one finds that during a de Sitter stage,

$$\rho = \text{constant}, \qquad H_{\rm I} = \text{constant}, \tag{2.36}$$

where $H_{\rm I}$ denotes the Hubble parameter during inflation. As a consequence, the scale factor evolves as

$$a(t) = a_{\rm I}\, e^{H_{\rm I}(t-t_{\rm I})}, \tag{2.37}$$

with $t_{\rm I}$ marking the onset of inflation.
Although the scale factor grows exponentially and the expansion is therefore superluminal, this does not contradict General Relativity. The rapid growth refers to the expansion of space-time itself, not to the propagation of signals within it.

It is precisely this period of exponential expansion that allows us to address the primordial shortcomings of the standard Big Bang model:

Flatness problem and Inflation

Recall the Friedmann Equation 2.23 for a non-flat universe

$$|1 - \Omega(a)| = \frac{1}{(aH)^2} \propto \frac{1}{a^2}\ . \tag{2.38}$$

If the comoving Hubble radius decreases this *drives the universe toward flatness* (rather than away from it). This solves the flatness problem. The solution $\Omega = 1$ is an attractor during inflation [13].

It is important to underline the fact that inflation does not change the global geometric properties of the spacetime. If the universe is open or closed, it will always remain flat or closed, independently from inflation. What inflation does is to magnify the radius of curvature R_{curv} so that locally the universe is flat with a great precision.

The Horizon problem and Inflation

A decreasing comoving horizon implies that the large scales we observe in the present universe were, in fact, within causal contact before the onset of inflation. This means that causal information operating prior to inflation was able to establish spatial homogeneity across regions that today appear disconnected. Once a phase of accelerated expansion began, these initially uniform regions were stretched to enormous scales, thereby preserving their homogeneity.

During inflation:

$$R_H(t) = a(t) \int_{t_\mathrm{I}}^{t} \frac{dt'}{a(t')} = a_\mathrm{I}\, e^{H_\mathrm{I}(t-t_\mathrm{I})} \left(-\frac{1}{H_\mathrm{I}}\right) \left[e^{-H_\mathrm{I}(t-t_\mathrm{I})}\right]_{t_\mathrm{I}}^{t} \simeq \frac{a(t)}{H_\mathrm{I}}, \tag{2.39}$$

while the Hubble radius itself remains constant,

$$\text{Hubble Radius} = \frac{a}{\dot{a}} = H_\mathrm{I}^{-1}. \tag{2.40}$$

Besides, in comoving coordinates, the comoving Hubble radius decreases exponentially,

$$\text{Comoving Hubble Radius} = H_\mathrm{I}^{-1} e^{-H_\mathrm{I}(t-t_\mathrm{I})}, \tag{2.41}$$

while comoving length scales remain constant.

In this way, inflation naturally resolves the horizon problem: regions of the cosmic microwave background (CMB) sky that seem causally disconnected today were actually in thermal contact before inflation. They reached equilibrium prior to being stretched beyond each other's horizons during inflation, which explains why the CMB exhibits such remarkable uniformity across the sky. Moreover, small primordial fluctuations generated during this epoch were imprinted on top of this nearly homogeneous background, providing the seeds for the anisotropies observed in the CMB and, ultimately, for the formation of cosmic structure.

2.4.2 Beyond the Big Bang Puzzles: The Deeper Role of Inflation

Beyond solving the horizon and flatness problems, inflation stands as the leading theory of the primordial universe because, by simply requiring the condition outlined in Section 2.4.1 to be verified, inflation also accounts for another fundamental feature of the our universe: the existence of galaxies and clusters of galaxies. In other words, inflation provides a natural explanation for the origin of large-scale structure (LSS).

This is possible because inflation stretched microscopic fluctuations into macroscopic scales. Thus, today's large-scale structures are the amplified remnants of primordial quantum fluctuations, expanded during the accelerated phase of cosmic inflation [1, 17, 58].

Indeed, the quantum fluctuations present in the very early universe could have served as the primordial source for galaxy formation. However, without inflation, these fluctuations would have been far too small to account for the ripples we observe in the cosmic microwave background. Therefore, inflation resolves this issue: the extremely rapid expansion of the universe during this epoch stretched the quantum fluctuations to much larger physical scales, large enough to manifest as the anisotropies in the CMB, which later grew under the influence of gravity to form galaxies and clusters over billions of years.

In this sense, inflation not only explains the initial conditions of the universe but also provides the mechanism by which microscopic quantum fluctuations are promoted to macroscopic, classical perturbations. These perturbations form the seeds of all cosmic structures observed today.

Thus, inflation should be regarded, first and foremost, as a theory of primordial quantum fluctuations.

2.5 A Scalar field as the source of Inflation

2.5.1 Standard models of inflation

The main idea underlying all existing versions of the inflationary universe scenario is that in the very earliest stages of its evolution, the universe could be in an unstable vacuum like state having high energy density. In most conventional inflationary models, the accelerated expansion is driven by a particular type of matter given by a scalar field. This type of field, which plays a central role in symmetry breaking in particle physics, is assumed to possess a potential energy that sustains the inflationary phase. However, particle physics does not yet provide a definitive prediction for the form of this potential, nor for the detailed properties of the scalar field itself. This lack of specificity leaves considerable freedom to construct a variety of inflationary scenarios, each based on different choices of the potential and motivated by different high-energy physics backgrounds.

Inflationary models differ primarily in the choice of the potential for the scalar field (or fields) driving inflation, as well as the mechanism by which inflation ends. Throughout the early 1990s, single-field models dominated [59, 60]. In these models, the scalar-field potential is often chosen for simplicity, e.g., as a monomial or exponential function, with initial conditions set so that the field is well displaced from its minimum, while keeping its energy density below the Planck scale. Some single-field models can also produce a significant level of gravitational waves.
In the mid-1990s, a new class of particle-physics-motivated models emerged, known as hybrid inflation [53, 61, 62]. These involve interactions between two scalar fields and exploit the flat potentials expected in supersymmetric theories. Hybrid models can generate enough inflation with only modest evolution of the fields, which remain far below the Planck mass.
Finally, there are less conventional models, such as those based on extended gravitational theories. These aim to source the inflation-driving scalar field directly from the gravitational sector rather than from matter fields.

Is it clear that many different models of inflation have been proposed and the challenge of explaining the underlying physics of inflation is considerable. The mechanisms capable of producing an inflationary expansion are quite diverse. Inflation can arise in many different theoretical settings, ranging from models based on simple scalar fields with carefully chosen potentials to more elaborate frameworks involving multiple fields, higher-order corrections or even modifications of General Relativity itself. This variety reflects both the flexibility of the inflationary paradigm and the fact that we still lack a definitive understanding of the physics driving inflation. Inflation should be regarded as a paradigm, a theoretical framework for describing the early universe, rather than a single unique theory.

A wide variety of phenomenological models have been developed, motivated by different theoretical considerations and yielding diverse observational predictions. This diversity provides a certain freedom to investigate alternative scenarios and to examine their phenomenological implications, but it also poses the challenge of identifying which, if any of these models, correctly describes the physics of the early universe.

2.5.2 The Scalar Field Dynamics

Several are the advantages of having a phase of accelerated expansion in the primordial universe, but it is true that this is a rather unusual physical phenomenon: within a tiny fraction of a second, the universe expanded exponentially at an accelerated rate. In the framework of Einstein gravity, such behavior demands the presence of a source with negative pressure; it requires $p < -\frac{1}{3}\rho$. This condition can be realized through a simple scalar field, which we shall call the *inflaton.*

The single scalar field model of the *inflaton* ϕ minimally coupled with gravity is the simplest model of inflation. For this to work, we do not need to specify the physical nature of this field, but rather use it as an order parameter (or clock) to describe the time evolution of the inflationary energy density [13].
Its dynamics is governed by the action:

$$S = \int \mathrm{d^4x}\sqrt{-\mathrm{g}}\left[\frac{1}{2}\mathrm{R} + \frac{1}{2}\mathrm{g}^{\mu\nu}\partial_\mu\phi\,\partial_\nu\phi - \mathrm{V}(\phi)\right] = \mathrm{S_{EH}} + \mathrm{S}_\phi \tag{2.42}$$

which is just the sum of the gravitational Einstein-Hilbert action, S_{EH}, and the action of a scalar field with canonical kinetic term, S_ϕ, where $V(\phi)$ describes the self-interactions of the inflaton.

From the Eulero-Lagrange equations, the dynamics of the (homogeneous) scalar field in the FRW geometry is given by:

$$\ddot{\phi} + 3H\dot{\phi} + V'(\phi) = 0, \tag{2.43}$$

where $V'(\phi) = (dV(\phi)/d\phi)$ and where the friction term $3H\dot{\phi}$ comes into play: for large values of the potential, the field experiences significant Hubble friction, being:

$$H^2 = \frac{1}{3}\left(\frac{1}{2}\dot{\phi}^2 + V(\phi)\right). \tag{2.44}$$

This means that a scalar field rolling down its potential suffers a friction due to the expansion of the universe.

The energy-momentum tensor for the scalar field is

$$T^{(\phi)}_{\mu\nu} \equiv -\frac{2}{\sqrt{-g}}\frac{\delta S_\phi}{\delta g^{\mu\nu}} = \partial_\mu\phi\partial_\nu\phi - g_{\mu\nu}\left(\frac{1}{2}\partial^\sigma\phi\partial_\sigma\phi + V(\phi)\right). \tag{2.45}$$

We assume the FRW metric for $g_{\mu\nu}$. Consistency with the symmetries of the FRW spacetime requires that the background value of the inflaton only depends on time $\phi(t, \mathbf{x}) \equiv \phi(t)$. Restricting to the case of a homogeneous field, the scalar energy-momentum tensor takes the form of a perfect fluid

$$T^{\mu}_{\ \nu} = \begin{pmatrix} \rho_\phi & 0 & 0 & 0 \\ 0 & -p_\phi & 0 & 0 \\ 0 & 0 & -p_\phi & 0 \\ 0 & 0 & 0 & -p_\phi \end{pmatrix}$$

with

$$\rho_\phi = \frac{1}{2}\dot{\phi}^2 + V(\phi)\,, \tag{2.46}$$

$$p_\phi = \frac{1}{2}\dot{\phi}^2 - V(\phi)\,. \tag{2.47}$$

and the resulting equation of state is given by

$$w_\phi \equiv \frac{p_\phi}{\rho_\phi} = \frac{\frac{1}{2}\dot{\phi}^2 - V}{\frac{1}{2}\dot{\phi}^2 + V}. \tag{2.48}$$

Thus we can see that, if the potential energy V dominates over the kinetic energy

$$V(\phi) \gg \dot{\phi}^2 \quad , \tag{2.49}$$

we obtain the condition

$$P_\phi \simeq -\rho_\phi. \tag{2.50}$$

which means that a scalar field can lead to negative pressure ($w_\phi < 0$) and accelerated expansion. So inflation can be driven by a scalar field whose energy is dominant in the universe and whose potential energy dominates over the kinetic term. In particular, inflation is sourced by the vacuum energy of the inflaton field.

2.6 Slow-roll vs Non-slow-roll inflation

Slow-Roll Inflation

Slow Roll (SR) inflation is a deformation of exact de Sitter which lasts for a finite amount of time. It can be followed by reheating and by the usual Hot Big Bang model.

To build SRI it is sufficient to consider the dynamics of the inflaton scalar field minimally coupled to Einstein gravity via the action 2.42. To each value of the field ϕ corresponds a potential energy density $V(\phi)$.
If the condition 2.49 holds, so if the potential energy dominates over the kinetic energy -i.e., if the

field *rolls slowly-,* we can have a field configuration which leads to inflation.

The SR condition can be formulated in terms of the parameter ε, which is related to the evolution of the Hubble parameter through 2.33. Accelerated expansion occurs whenever $\varepsilon < 1$, while the exact de Sitter limit, $p_\phi \to -\rho_\phi$, corresponds to $\varepsilon \to 0$. Thus, the *first slow-roll condition* can be written as

$$\boxed{\text{First slow-roll condition:} \quad V(\phi) \gg \dot{\phi}^2 \quad \Longleftrightarrow \quad \varepsilon \ll 1} \tag{2.51}$$

This requirement alone, however, is not sufficient to guarantee successful inflation. One must also ensure that inflation lasts long enough to solve the horizon problem. Sustained accelerated expansion is possible only if the second time derivative of the field is small compared to the friction and potential terms:

$$|\ddot{\phi}| \;\ll\; |3H\dot{\phi}|\,,\, |V_{,\phi}|\,. \tag{2.52}$$

This motivates the introduction of a second slow-roll parameter,

$$\eta = -\frac{\ddot{\phi}}{H\dot{\phi}} = \varepsilon - \frac{1}{2\varepsilon}\frac{d\varepsilon}{dN}\,, \tag{2.53}$$

where the condition $|\eta| < 1$ ensures that the fractional variation of ε per e-fold remains small.

The *second slow roll condition* can be then expressed as

$$\boxed{\text{Second slow-roll condition:} \quad |\ddot{\phi}| \ll |3H\dot{\phi}|\,,\, |V_{,\phi}| \quad \Longleftrightarrow \quad |\eta| < 1}\,. \tag{2.54}$$

Generally, ε and η are referred to as *Hubble slow-roll parameters.*
The two slow-roll conditions, can equivalently be expressed as constraints on the shape of the inflationary potential:

$$\boxed{\varepsilon_{\rm v}(\phi) \equiv \frac{M_{\rm pl}^2}{2}\left(\frac{V_{,\phi}}{V}\right)^2 \ll 1}\,, \tag{2.55}$$

and

$$\boxed{\eta_{\rm v}(\phi) \equiv M_{\rm pl}^2\frac{V_{,\phi\phi}}{V} \;\ll 1}\,. \tag{2.56}$$

Here, ε_V and η_V are called *potential slow roll parameters.* Also, the Planck mass $M_{\rm pl}$ has been reintroduced to make $\epsilon_{\rm v}$ and $\eta_{\rm v}$ explicitly dimensionless.

Inflation terminates when the slow-roll conditions are violated:

$$\varepsilon(\phi_{\rm end}) \equiv 1\,, \qquad \varepsilon_{\rm v}(\phi_{\rm end}) \approx 1\,. \tag{2.57}$$

The amount of inflation is measured in terms of e-folds of expansion, $\mathrm{d}N = \mathrm{d}lna$. The total number of e-folds between a point on the potential and the end of inflation at ϕ_{end} is

$$N(\phi) \equiv \int_a^{a_e} d\ln a = \int_t^{t_e} H\,dt = \int_\phi^{\phi_e}\frac{H}{\dot{\phi}}\,d\phi = \int_\phi^{\phi_e}\frac{1}{\sqrt{2\epsilon_V}}\frac{|\mathrm{d}\phi|}{M_{\rm pl}} \approx \int_\phi^{\phi_e}\frac{1}{\sqrt{2\epsilon_V}}\frac{|\mathrm{d}\phi|}{M_{\rm pl}}\,. \tag{2.58}$$

To successfully address the horizon and flatness problems, the total number of inflationary e-folds must satisfy

$$N_{\rm tot} \equiv \ln \frac{a_{\rm end}}{a_{\rm start}} \gtrsim 60\,. \tag{2.59}$$

although the precise threshold depends on the energy scale of inflation and the details of the reheating temperature [13].

These are the conditions required to achieve a phase of accelerated expansion and to elegantly resolve the horizon and flatness problems. It is important to stress, however, that the microscopic origin of inflation remains unknown. Since inflation is thought to have occurred at extremely high energy scales, probably of order $\sim 10^{15}$GeV, any description of this epoch necessarily involves a significant extrapolation of the established laws of physics. In particular, the precise form of the inflationary potential is not known. Defining an inflationary model therefore amounts to specifying the action of the inflaton field. The dynamics of this field -from the time when the CMB fluctuations were generated until the end of inflation- are fully determined by the shape of the potential.

Non Slow-Roll Inflation

A large number of phenomenological models have been proposed with different theoretical motivations and observational predictions and, while the slow-roll approximation has long served as the cornerstone of inflationary model building, it is not a necessary condition for accelerated expansion. *Non-slow-roll (NSR)* scenarios explore regimes where the inflaton evolves rapidly, violating the standard slow-roll conditions yet still producing sufficient e-folds to solve the classical problems of the Big Bang and typically arise in models with steep potentials, non-canonical kinetic terms or attractor-like dynamics that stabilize the evolution despite large field velocities. By relaxing slow-roll constraints, such frameworks broaden the landscape of inflationary behaviour and lead to distinctive signatures in the primordial power spectrum, non-Gaussianities, reheating dynamics and even dark matter production. In particular, short phases of non-slow-roll evolution can amplify scalar curvature perturbations at small scales, potentially triggering the formation of primordial black holes [63–65] or enhance the primordial tensor spectrum. They may also explain possible anomalies in the CMB by leaving localized imprints in the scalar and tensor spectra.

So far, various models achieve these aims by introducing a short phase of inflationary non-attractor evolution. In one class of models, the first slow-roll parameter

$$\varepsilon \equiv -\frac{\dot{H}}{H^2} \tag{2.60}$$

remains small, while the absolute value of the second slow-roll parameter is large [66–68]. A well-studied realization of this idea is ultra-slow-roll inflation, characterized by $\varepsilon \simeq 0$, $\eta = -6$, naturally occurring near inflection points of the potential where $V_{,\phi} \simeq 0$.

Other scenarios, such as punctuated inflation with step-like features in the potential, lead to temporary violations of slow roll where ε briefly grows before relaxing back to small values [69–71],

producing potentially observable features at small scales that complement the near-perfect agreement between slow-roll single-field inflation and large-scale CMB and structure data. Altogether, the study of non-slow-roll phases provides a compelling extension of the inflationary paradigm, motivated both by theoretical consistency and by their rich phenomenological consequences.

An analytical framework for studying non-slow-roll inflation in a general setting is presented later in this work. In our approach, we address the inflationary problem by identifying common features in the scale-dependent properties of the fluctuation power spectrum. We focus on scenarios that include brief and transient phases of non–slow-roll evolution, without specifying the particular mechanism or model responsible for the departure from slow-roll.

Chapter 3

Cosmological perturbation theory

This thesis builds on the premise that quantum fluctuations during inflation may provide a mechanism for the generation of dark matter; fluctuations that become stretched across cosmic scales due to gravitational effects. This concept, revisited in references [16, 17, 58, 72, 73], finds compelling support in observational data, beautifully tying theoretical predictions to the fabric of our visible universe. In order to understand how such a mechanism could account for dark matter production, it is convenient to examine how the tiny anisotropies of the universe, combined with its accelerated expansion, can lead to efficient particle production.

It may sound astonishing that quantum effects, typically confined to the microscopic realm, can give rise to vast cosmic structures, like galaxies and clusters of galaxies. Indeed, in the early universe, these quantum fluctuations are amplified due to great energy scales and fleeting timescales, yet they remain small enough to act merely as gentle ripples atop the classical expansion. What changes everything is the extraordinary acceleration of the universe: these fluctuations are stretched by inflation to considerable sizes, far exceeding the Hubble horizon and, in doing so, they become "frozen," their amplitudes locked at non-zero values, poised to seed the intricate structure of the cosmos.
Therefore, inflation imprints the universe with its primordial irregularities precisely because the universe is quantum in nature, not classical. The vacuum of space indeed is anything but empty. While the accelerated expansion driven by a scalar field would, in a purely classical world, render the universe perfectly uniform, the quantum realm forbids such perfection: tiny residual fluctuations always persist in the scalar field. Remarkably, the size of these fluctuations is set entirely by quantum mechanics and is largely independent of the pre-inflationary state, making inflation an exceptionally predictive theory. In this sense, inflation provides us with "natural" initial conditions, which turn out to be the initial conditions that agree with the present observations.

In the following sections we address the topic of particle production in the very early universe. We explore a mechanism which is non-standard; namely the production of particles from the vacuum fluctuations during inflation [55, 72–75]. In order to do this, let us first analyse the quantum fluctuations of a generic massless scalar field during inflation. This will help develop a method for studying perturbations in an inflationary background.

3.1 Quantum Fluctuations of a Massless Scalar Field during Inflation

The quantum-mechanical fluctuations generated during inflation and their relation to cosmological perturbations can be investigated by looking at free fields in De Sitter space [13, 14]. An interesting property of what we are going to analyse is that the treatment of free fields in curved spacetime (and de Sitter space in particular) is similar to the one of a collections of harmonic oscillators with time-dependent frequencies.
It is also worth remarking that the fluctuations weren't deliberately built into the theory; rather, they emerge organically as a direct result of applying quantum mechanics to the inflationary framework.

Let us assume φ is a massless scalar field, which contributes negligibly to the overall energy density, and thus does not induce any back-reaction on the geometry. A field of this nature is commonly referred to as a spectator field.

We consider an unperturbed and spatially flat background spacetime metric which, in conformal time, reads:

$$ds^2 = a^2(\tau)(-d\tau^2 + \delta_{ij}dx^i dx^j). \tag{3.1}$$

The action of the massless, free scalar field φ in such a spacetime is:

$$S = -\frac{1}{2}\int d^4x\sqrt{-g}\, g^{\mu\nu}\partial_\mu\varphi\partial_\nu\varphi = -\frac{1}{2}\int d^4x\sqrt{-g}\ \partial_\mu\varphi\partial^\mu\varphi \tag{3.2}$$

with $g = \det(g_{\mu\nu}) = -a^8(\tau)$. Thus, explicitly:

$$S = \frac{1}{2}\int d\tau d^3x\ a^2\left[\varphi'^2 - (\nabla\varphi)^2\right]\ , \tag{3.3}$$

where we used the notation: $(...)' \equiv \partial_\tau(...)$.

In order to quantize the system, it is useful to define the *canonically normalized field* $v = a(\tau)\varphi$. Rescaling the field, the action becomes:

$$S = \frac{1}{2}\int d\tau\ d^3x\left[v'^2 - (\nabla v)^2 + \frac{a'^2}{a^2}v^2 - 2\frac{a'}{a}vv'\right]. \tag{3.4}$$

We manipulate the last two terms writing

$$\frac{a'^2}{a^2}v^2 - 2\frac{a'}{a}vv' = -\frac{d}{d\tau}\left(\frac{a'}{a}v^2\right) + \frac{a''}{a}v^2 \tag{3.5}$$

and, sending the boundary terms to vanish, we obtain:

$$S = \frac{1}{2}\int d\tau\ d^3x\left[v'^2 - (\nabla v)^2 + \frac{a''}{a}v^2\right]\ , \tag{3.6}$$

which effectively describes a scalar field in a FRW spacetime. The time dependence of the action is entirely due to the variable background gravitational field. Besides, the equation of motion which follows from Eq. 3.6 is:

$$v'' - \nabla^2 v - \frac{a''}{a} v = 0 \ . \tag{3.7}$$

We now Fourier expand the field v as

$$v(\tau, \mathbf{x}) = \int \frac{d^3k}{(2\pi)^3} \, v_k(\tau) \, e^{i\mathbf{k}\cdot\mathbf{x}} \tag{3.8}$$

and, inserting the Fourier expansion in Eq. 3.7, we obtain the e.o.m. for the k-mode $v_{\mathbf{k}}$:

$$v_{\mathbf{k}}'' + k^2 v_{\mathbf{k}} - \frac{a''}{a} v_{\mathbf{k}} = 0 \ . \tag{3.9}$$

Since Eq. 3.9 does not show a directional dependence of the wavevector $\mathbf{k}$, we drop the vector notation in the subscript: the mode functions $v_k(\tau)$ are identical for all Fourier modes with fixed magnitude $|\mathbf{k}|$. Then the resulting equation is

$$\boxed{v_k'' + \left(k^2 - \frac{a''}{a}\right) v_k = 0} \ , \tag{3.10}$$

which is referred to as *Mukhanov-Sasaki (MS) equation.* This equation shows an explicit time dependence in the coefficient of the term v_k. Being $a(\tau) = -\frac{1}{H\tau}$ in De Sitter space, it follows that

$$\frac{a''}{a} = \frac{2}{\tau^2} \ , \tag{3.11}$$

which encapsulates the contribution due to the expansion of the universe.

We observe that the resulting equation closely resembles that of a Klein-Gordon scalar field in flat space-time, with the only distinction arising from the time dependence encoded in the effective mass term $m_{eff}^2 \equiv \frac{a''}{a} = \frac{2}{\tau^2}$. In light of this, and given that

$$\tau = -\frac{1}{aH} \tag{3.12}$$

during inflation, MS equation is rewritten as:

$$v_k'' + \left(k^2 - 2(aH)^2\right) v_k = 0 \ . \tag{3.13}$$

It is really useful to study the behaviour of this equation on sub-Hubble and super-Hubble scales [14]. We can distinguish the two significant cases:

1) **Sub-Hubble scales:** $k \gg aH$

2) **Super-Hubble scales:** $k \ll aH$

1) In this first limit, the contribution given by aH can be neglected and the e.o.m. reduces to:

$$v_k'' + k^2 v_k \approx 0 \tag{3.14}$$

whose solution is a plane wave

$$v_k = \frac{e^{-ik\tau}}{\sqrt{2k}} \ . \tag{3.15}$$

This tells that, at early times, the effective mass of the field is negligible compared to the momentum of the relevant Fourier modes. In this regime, the wavelength is much smaller than the Hubble radius and then a flat spacetime is a good approximation. Besides, the dynamic simplifies to that of a simple *harmonic oscillator* in flat spacetime.
Consequently, the quantum fluctuations of the field can be described using the standard quantization procedure for a harmonic oscillator.

2) On Super-Hubble scales, the k^2 term is irrelevant compared to the effective mass. The equation of motion then simplifies to:

$$v_k'' - 2\frac{a''}{a} v_k \approx 0 \tag{3.16}$$

with solution:

$$v_k = B(k) a \ , \tag{3.17}$$

where $B(k)$ is integration constant.
Recalling the definition $v = a\varphi$, we find that:

$$\varphi_k = B(k) = const \qquad \text{at Super-Hubble scales.} \tag{3.18}$$

Therefore, when a mode's wavelength λ becomes comparable to the Hubble radius H^{-1}, a crucial transition occurs: the mode ceases to oscillate. This marks the moment when the fluctuation crosses the Hubble horizon. Beyond this point -on super-Hubble scales- the quantum fluctuation effectively "freezes in" and its amplitude becomes constant in time. Thus, we find that the quantum fluctuations of the field remain conserved once their wavelengths exceed the Hubble radius.

The value of the constant $B(k)$ can be determined by imposing continuity between the sub-Hubble and super-Hubble solutions at horizon crossing, where $k = aH = -\frac{1}{\tau}$:

$$|v_k| = \frac{1}{\sqrt{2k}} = |B(k)|a \quad \Longrightarrow \quad |B(k)| = \frac{1}{a\sqrt{2k}} = \frac{H}{\sqrt{2k^3}}. \tag{3.19}$$

So, on super-Hubble scales, the fluctuation of the field remains constant and is roughly given by

$$\varphi_k \simeq \frac{H}{\sqrt{2k^3}} \ . \tag{3.20}$$

3.1.1 Quantization

In the sub-Hubble limit, the quantization of the field v proceeds in direct analogy with the treatment of the quantum harmonic oscillator. We adopt the canonical formalism, from which the conjugate momentum to v can be readily identified as

$$\pi \equiv \frac{\partial \mathcal{L}}{\partial \dot{v}} = \dot{v} \ . \tag{3.21}$$

We promote the fields $v(\tau, \mathbf{x})$ and $\pi(\tau, \mathbf{x})$ to the operators $\hat{v}(\tau, \mathbf{x})$ and $\hat{\pi}(\tau, \mathbf{x})$ which satisfy the equal time commutation relations:

$$[\hat{v}(\tau, \mathbf{x}), \hat{\pi}(\tau, \mathbf{x}')] = i\delta(\mathbf{x} - \mathbf{x}') \tag{3.22}$$

$$[\hat{v}(\tau, \mathbf{x}), \hat{v}(\tau, \mathbf{x}')] = [\hat{\pi}(\tau, \mathbf{x}), \hat{\pi}(\tau, \mathbf{x}')] = 0 \tag{3.23}$$

with $\hbar = 1$. In Fourier space:

$$\begin{aligned}
[\hat{v}_{\mathbf{k}}(\tau), \hat{\pi}_{\mathbf{k}'}(\tau)] &= \int d^3x \int d^3x' \ [\hat{v}(\tau, \mathbf{x}), \hat{\pi}(\tau, \mathbf{x}')] \ e^{-i\mathbf{k}\cdot\mathbf{x}} e^{-i\mathbf{k}'\cdot\mathbf{x}'} \\
&= i \int d^3x \ e^{-i(\mathbf{k}+\mathbf{k}')\cdot\mathbf{x}} \\
&= i \ (2\pi)^3 \delta(\mathbf{k} + \mathbf{k}') \\
&\Downarrow \\
[\hat{v}_{\mathbf{k}}(\tau), \hat{\pi}_{\mathbf{k}'}(\tau)] &= i \ (2\pi)^3 \delta(\mathbf{k} + \mathbf{k}')
\end{aligned} \tag{3.24}$$

which implies that modes with different wavelengths commute.

Decomposing the pair of operators $\hat{v}$ and $\hat{\pi}$ in terms of a single time-independent, non-Hermitian operator $\hat{a}_{\mathbf{k}}$, the Fourier components $v_{\mathbf{k}}$ read:

$$\hat{v}_{\mathbf{k}}(\tau) = v_k(\tau) \, \hat{a}_{\mathbf{k}} + v_k^*(\tau) \, \hat{a}^\dagger_{-\mathbf{k}} \tag{3.25}$$

The field operator $\hat{v}_{\mathbf{k}}(\tau)$ is then expressed in terms of a complex mode function $v_k(\tau)$ and a time-independent, non-Hermitian operator $\hat{a}_{\mathbf{k}}$. The function $v_k(\tau)$ satisfies the classical equation of motion 3.10 and $v_k^*(\tau)$ denotes its complex conjugate. Similarly, $\hat{a}^\dagger_{\mathbf{k}}$ is the Hermitian conjugate of $\hat{a}_{\mathbf{k}}$. Alternatively:

$$\hat{v}(\tau, \mathbf{x}) = \int \frac{d^3\mathbf{k}}{(2\pi)^3} \left[v_k(\tau) \, \hat{a}_{\mathbf{k}} \, e^{i\mathbf{k}\cdot\mathbf{x}} + v_k^*(\tau) \, \hat{a}^\dagger_{\mathbf{k}} \, e^{-i\mathbf{k}\cdot\mathbf{x}} \right] . \tag{3.26}$$

Inserting 3.25 into 3.24 and recalling that $\hat{\pi}_{\mathbf{k}} = \partial_\tau \hat{v}_{\mathbf{k}}$:

$$\begin{aligned}
[\hat{v}_{\mathbf{k}}(\tau), \hat{\pi}_{\mathbf{k}'}(\tau)] &= [v_k(\tau) \, \hat{a}_{\mathbf{k}} + v_k^*(\tau) \, \hat{a}^\dagger_{-\mathbf{k}}, \ \partial_\tau (v_k(\tau) \, \hat{a}_{\mathbf{k}'} + v_k^*(\tau) \, \hat{a}^\dagger_{-\mathbf{k}'})] \\
&= [v_k(\tau) \, \hat{a}_{\mathbf{k}} + v_k^*(\tau) \, \hat{a}^\dagger_{-\mathbf{k}}, \ v_k'(\tau) \, \hat{a}_{\mathbf{k}'} + v_k'^*(\tau) \, \hat{a}^\dagger_{-\mathbf{k}'}] \qquad (3.27) \\
&= (v_k v_k'^* - v_k^* v_k')[\hat{a}_{\mathbf{k}}, \hat{a}^\dagger_{-\mathbf{k}'}] \\
&= i \ (2\pi)^3 \, \delta^3(\mathbf{k} + \mathbf{k}'). \qquad (3.28)
\end{aligned}$$

This holds if and only if we assume the following normalization of the mode functions:

$$v_k(\tau)\, v_k'^*(\tau) - v_k^*(\tau)\, v_k'(\tau) = i \ . \tag{3.29}$$

This normalization relation provides the first of two boundary conditions on the solutions to the Mukhanov equation 3.10.
However, applying this condition alone still leaves a one-parameter family of solutions for the mode functions. This reflects the *non-uniqueness of the vacuum.*
The second boundary condition, which fully determines the mode functions, is set by the choice of vacuum state.

At this stage, indeed, we have not yet uniquely determined the mode functions, and consequently, the vacuum state remains unfixed. Any transformation of the mode function v_k that preserves the solution $v_{\mathbf{k}}$ will induce a corresponding change in the creating operator, hence a change in the definition of the vacuum.
This ambiguity is not merely a technical artifact: it reflects a profound conceptual feature of quantum field theory in time-dependent or curved backgrounds. In the case of a simple harmonic oscillator with a time-dependent frequency $\omega(t)$ and analogously for quantum fields propagating in curved spacetime, there exists no unique prescription for selecting the mode functions v_k. As a result, the decomposition of the field v into annihilation and creation operators is inherently non-unique.
This is linked to the fact that, in flat spacetime, the presence of a global timelike Killing vector allows for a natural definition of positive frequency modes, which in turn leads to a canonical vacuum state -the Minkowski vacuum. However, in curved spacetime, such a global symmetry is generally not present anymore. The lack of a preferred time coordinate means that the notion of "positive frequency" becomes observer-dependent, and so does the vacuum.
Different choices of mode functions correspond to different quantization schemes, each yielding a distinct set of annihilation and creation operators. Consequently, each choice defines a different vacuum state. This leads to the striking result that the vacuum is not an absolute concept in curved spacetime, but rather a relative one, contingent upon the observer's frame and the specific mode decomposition employed.
Besides, this non-uniqueness has deep physical implications. For instance, it underlies phenomena such as particle creation in expanding universes and the Unruh effect, where different observers disagree on the particle content of a given quantum field.

3.1.2 Choice of the vacuum

Choosing a vacuum corresponds to specify the second boundary condition for v_k.
The choice of the vacuum is guided by physical considerations such as asymptotic behaviour in the early universe, but it remains a choice nonetheless, not a necessity dictated by the geometry.

The conventional choice is the Minkowski vacuum, defined with respect to a comoving observer in the asymptotic past $\tau \to -\infty$, when all comoving modes were back inside the Hubble scale and satisfied $k \gg aH$, i.e., were deeply sub-Hubble. In this limit, the curvature of spacetime is negligible and the field behaves as in flat space, justifying the use of the standard Minkowski vacuum as the initial condition. Furthermore, the e.o.m. 3.10 reduces to 3.14, which is the equation of a simple harmonic oscillator with time-independent frequency.
For this particular case we can find a specific solution v_k by choosing the vacuum as the eigenstate of $\hat{H}$ which minimizes the energy. This definition fixes the mode functions and determines the physical vacuum.

In order to find this preferred choice, let us consider the Hamiltonian of the system:

$$\hat{H} = -\hat{\mathcal{L}} + \hat{\pi}\hat{v}' \ , \tag{3.30}$$

which is:

$$\hat{H} = \frac{1}{2}\int d^3x \left[v'^2 + (\nabla v)^2 - \frac{a''}{a}v^2\right]. \tag{3.31}$$

Upon using the decomposition 3.26, each term in the integral can be expressed in terms of the creation and annihilation operators. The first piece reads:

$$\begin{aligned} I_1 = \ \frac{1}{2}\int d^3x\, v'^2(\mathbf{x},\tau) = \frac{1}{2}\int d^3x \int \frac{d^3k}{(2\pi)^{3/2}}\frac{d^3q}{(2\pi)^{3/2}}\Big[\ \hat{a}_{\mathbf{k}}\ \hat{a}_{\mathbf{q}}\ v'_{\mathbf{k}}\ v'_{\mathbf{q}}\ e^{i(\mathbf{k}+\mathbf{q})\cdot\mathbf{x}} + \\ + \hat{a}_{\mathbf{k}}\ \hat{a}^\dagger_{-\mathbf{q}}\ v'_{\mathbf{k}}\ v'^*_{\mathbf{q}}\ e^{i(\mathbf{k}-\mathbf{q})\cdot\mathbf{x}} + \hat{a}^\dagger_{-\mathbf{k}}\ \hat{a}_{\mathbf{q}}\ v'^*_{\mathbf{k}}\ v'_{\mathbf{q}}\ e^{-i(\mathbf{k}-\mathbf{q})\cdot\mathbf{x}} + \\ + \hat{a}^\dagger_{-\mathbf{k}}\ \hat{a}^\dagger_{-\mathbf{q}}\ v'^*_{\mathbf{k}}\ v'^*_{\mathbf{q}}\ e^{-i(\mathbf{k}+\mathbf{q})\cdot\mathbf{x}}\Big] \ . \end{aligned} \tag{3.32}$$

After integration over $\mathbf{x}$:

$$I_1 = \ \frac{1}{2}\int d^3k\Big[\ \hat{a}_{\mathbf{k}}\ \hat{a}_{-\mathbf{k}}\ v'_k\ v'_{-k} + \hat{a}_{\mathbf{k}}\ \hat{a}^\dagger_{-\mathbf{k}}\ v'_k\ v'^*_k + \hat{a}^\dagger_{-\mathbf{k}}\ \hat{a}_{\mathbf{k}}\ v'^*_k\ v'_k + \hat{a}^\dagger_{-\mathbf{k}}\ \hat{a}^\dagger_{\mathbf{k}}\ v'^*_k\ v'^*_{-k}\ \Big]. \tag{3.33}$$

Finally, using the commutation relations:

$$I_1 = \ \frac{1}{2}\int d^3k\ [\ \hat{a}_{\mathbf{k}}\ \hat{a}_{-\mathbf{k}}\ v'_k\ v'_{-k} + \hat{a}^\dagger_{\mathbf{k}}\ \hat{a}^\dagger_{-\mathbf{k}}\ v'^*_k\ v'^*_{-k} + 2\,\hat{a}^\dagger_{-\mathbf{k}}\ \hat{a}_{\mathbf{k}}\ |v'_k|^2 + \delta(0)|v'_k|^2]\ . \tag{3.34}$$

Applying the same procedure to the other two terms of the integral yields:

$$I_2 = \ \frac{1}{2}\int d^3x\,(\nabla v(\mathbf{x},\tau))^2 = \frac{1}{2}\int d^3k\ k^2\ [\ \hat{a}_{\mathbf{k}}\ \hat{a}_{-\mathbf{k}}\ v_k\ v_{-k} + \hat{a}^\dagger_{\mathbf{k}}\ \hat{a}^\dagger_{-\mathbf{k}}\ v^*_k\ v^*_{-k} + 2\,\hat{a}^\dagger_{-\mathbf{k}}\ \hat{a}_{\mathbf{k}}\ |v_k|^2 + \delta(0)|v_k|^2]\ ,$$

$$I_3 = \ -\frac{1}{2}\int d^3x\,\frac{a''}{a}v(\mathbf{x},\tau)^2 = -\frac{1}{2}\int d^3k\,\frac{a''}{a}\ [\ \hat{a}_{\mathbf{k}}\ \hat{a}_{-\mathbf{k}}\ v_k\ v_{-k} + \hat{a}^\dagger_{\mathbf{k}}\ \hat{a}^\dagger_{-\mathbf{k}}\ v^*_k\ v^*_{-k} + 2\,\hat{a}^\dagger_{-\mathbf{k}}\ \hat{a}_{\mathbf{k}}\ |v_k|^2 + \delta(0)|v_k|^2]\ .$$

Combining the three pieces, and defining the time-dependent frequency as

$$\omega_k(\tau) \equiv k^2 - \frac{a''}{a}, \tag{3.35}$$

we obtain:

$$\hat{H} = \frac{1}{2}\int d^3k \Big[\hat{a}_{\mathbf{k}}\hat{a}_{-\mathbf{k}}\Big(v_k'^2 + \omega_k(\tau)v_k^2\Big) + \hat{a}^\dagger_{\mathbf{k}}\hat{a}^\dagger_{-\mathbf{k}}\Big(v_k'^{*2} + \omega_k(\tau)v_k^{*2}\Big) + \Big(2\hat{a}^\dagger_{\mathbf{k}}\hat{a}_{\mathbf{k}} + \delta(0)\Big)\Big(|v_k'|^2 + \omega_k(\tau)|v_k|^2\Big)\Big]$$
$$= \frac{1}{2}\int d^3k \Big[\hat{a}_{\mathbf{k}}\hat{a}_{-\mathbf{k}}\ F_k^* + \hat{a}^\dagger_{\mathbf{k}}\hat{a}^\dagger_{-\mathbf{k}}\ F_k + \Big(2\hat{a}^\dagger_{\mathbf{k}}\hat{a}_{\mathbf{k}} + \delta(0)\Big)\ E_k\Big] \tag{3.36}$$

where

$$F_k^*(\tau) = v_k'^2 + \omega_k^2(\tau)v_k^2\ , \tag{3.37}$$
$$E_k(\tau) = |v_k'|^2 + \omega_k^2(\tau)|v_k|^2. \tag{3.38}$$

Since the frequency $\omega_k(\tau) = k^2 - \frac{a''}{a}$ depends only on the magnitude $k = |\mathbf{k}|$, the evolution of the mode functions is isotropic and independent of the direction of $\mathbf{k}$. However, the constant operators $\hat{a}_{\mathbf{k}}$ and $\hat{a}^\dagger_{\mathbf{k}}$, which encode the initial conditions, may retain directional dependence, thereby introducing anisotropies into the initial quantum state.

To evaluate the vacuum expectation value of the Hamiltonian, we compute:

$${}_v\langle 0|\hat{H}|0\rangle_v = \frac{\delta(0)}{2}\int d^3k\, E_k(\tau)\ , \tag{3.39}$$

where the $\delta(0)$ is an artefact of integrating over an infinite volume. In order for $|0\rangle_v$ to represent the true vacuum state, the quantity E_k must be minimized. This requirement determines the specific form of the mode functions v_k.
In order to find the configuration which minimizes the vacuum, we write:

$$v_k(\tau) = r_k(\tau)e^{i\theta_k} \tag{3.40}$$

and then

$$v_k'(\tau) = r_k'(\tau)e^{i\theta_k} - \frac{i}{2r_k}e^{i\theta_k}\ , \tag{3.41}$$

since it is a solution of Eq. 3.10. Substituting in the first boundary condition, Eq. 3.29:

$$r_k e^{i\theta_k}\left(r_k' e^{-i\theta_k} - i r_k\theta_k' e^{-i\theta_k}\right) - r_k e^{-i\theta_k}\left(r_k' e^{i\theta_k} + i r_k\theta_k' e^{i\theta_k}\right) = i\ . \tag{3.42}$$

Thus:

$$-2i\, r_k^2\ \theta_k' = i \quad \Rightarrow \quad \theta_k' = -\frac{1}{2r_k^2}\ . \tag{3.43}$$

Moreover, substituting in the expression for E_k:

$$E_k = |v_k'|^2 + k^2|v_k|^2 = \left(r_k' - \frac{i}{2r_k}\right)\left(r_k' + \frac{i}{2r_k}\right) + k^2 r_k^2\ . \tag{3.44}$$

Straightforwardly, this becomes:

$$E_k = r_k^2 + \frac{1}{4r_k^2} + k^2 r_k^2 \tag{3.45}$$

and now, minimizing E_k, we find:

$$\begin{cases} \frac{dE_k}{dr'_k} = 2r'_k \iff r'_k = 0 \\ \frac{dE_k}{dr_k} = -\frac{1}{2r_k^3} + 2k^2 r_k = 0 \iff r_k = \frac{1}{\sqrt{2k}} \end{cases} \tag{3.46}$$

Hence, from the previous expression,

$$\theta_k = -\int d\tau \ \frac{1}{2r_k} = -\int d\tau \ k = -k\tau + c \ . \tag{3.47}$$

We have thus determined that the quantities

$$r_k = \frac{1}{\sqrt{2k}} \quad , \quad \theta_k = -k\tau \tag{3.48}$$

correspond to the configuration that minimizes the energy. From this result, we finally obtain the second initial condition:

$$\boxed{\lim_{\tau \to -\infty} v_k = \frac{1}{\sqrt{2k}} e^{-ik\tau}} \ , \tag{3.49}$$

which uniquely specifies the vacuum by requiring $|0\rangle_v$ to be the minimum energy state and, together with 3.29, completely fixes the mode functions on all scales.

It can be easily proved that the most general solution of eq. 3.10 is:

$$v_k(\tau) = c_1 \left(1 - \frac{i}{k\tau}\right) \frac{e^{-ik\tau}}{\sqrt{2k}} + c_2 \left(1 + \frac{i}{k\tau}\right) \frac{e^{ik\tau}}{\sqrt{2k}} \ , \tag{3.50}$$

where the coefficients c_1 and c_2 encapsulate the non-uniqueness of the mode functions.

Inserting the general solution (3.50) into the normalization condition for the mode functions

$$v_k v'^*_k - v'_k v^*_k = i, \tag{3.51}$$

implies the constraint:

$$|c_1|^2 - |c_2|^2 = 1 \ . \tag{3.52}$$

At this stage, basing on what we outlined before, the mode function $v_k(\tau)$ remains still undetermined up to a one-parameter family of solutions. This is equivalent to say that a redefinition of $v_k(\tau)$ can be compensated by a corresponding transformation of the operator $\hat{a}_{\mathbf{k}}$, leaving the field operator $\hat{v}_{\mathbf{k}}(\tau)$ invariant.

However, the coefficients can be determined by enforcing the second boundary condition, which requires the vacuum to asymptotically approach an instantaneous minimum-energy state in the far past:

$$v_k = \frac{1}{\sqrt{2k}} e^{-ik\tau} \qquad \text{as} \ \ \tau \to -\infty \ . \tag{3.53}$$

The quantization condition, combined with the subhorizon limit, uniquely fixes $c_1 = 1$ and $c_2 = 0$.
This exclusively determines:

$$\boxed{v_k = \frac{1}{\sqrt{2k}}\Big(1 - \frac{i}{k\tau}\Big)e^{-ik\tau}} \tag{3.54}$$

as the function that ensures the state annihilated by $\hat{a}_{\mathbf{k}}$ is identified with the oscillator's ground state.
The unique mode functions of the previous expression are known as the *Bunch-Davies mode functions*, and they describe the unique solution to the equations of motion in de Sitter space that instantaneously minimizes the energy.

3.1.3 Power Spectrum of a Massless scalar in Quasi-de Sitter

Once the mode functions v_k have been determined, they can be employed to compute the power spectrum, a fundamental quantity for characterizing the statistical features of cosmological perturbations.

Consider a generic field $f(x,t)$, which can be expanded in Fourier space as:

$$f(\mathbf{x},t) = \int \frac{d^3k}{(2\pi)^3}\, e^{i\mathbf{k}\cdot\mathbf{x}}\, f_{\mathbf{k}}(t) \tag{3.55}$$

The power spectrum is defined through the two-point correlation function in momentum space:

$$\langle 0|f_{\mathbf{k}_1} f_{\mathbf{k}_2}|0\rangle \equiv (2\pi)^3\delta^{(3)}(\mathbf{k}_1 + \mathbf{k}_2)|f_{\mathbf{k}}|^2 \tag{3.56}$$

where $|0\rangle$ denotes the vacuum state of the quantum field. This leads to

$$\left\langle 0\left|f^2(\mathbf{x},t)\right|0\right\rangle = \int \frac{d^3k}{(2\pi)^3}\, f_{\mathbf{k}} f_{-\mathbf{k}} = \int \frac{d^3k}{(2\pi)^3}\,|f_{\mathbf{k}}|^2 = \int \frac{dk}{k}\,\mathcal{P}_f(k)\ , \tag{3.57}$$

which gives the definition of the power spectrum $\mathcal{P}_f(k)$ [14] associated with the field $f(\mathbf{x},t)$:

$$\boxed{\mathcal{P}_f(k) = \frac{k^3}{2\pi^2}|f_k|^2}\ . \tag{3.58}$$

In our specific case, we defined the field $\hat{v}_{\mathbf{k}}$ as $\hat{v}_{\mathbf{k}} = a(\tau)\hat{\varphi}_{\mathbf{k}}$. We now proceed to compute the power spectrum associated with the field $\hat{\varphi}_{\mathbf{k}}$. Starting from the Bunch-Davies mode functions:

$$v_k(\tau) = \frac{e^{-ik\tau}}{\sqrt{2k}}\left(1 - \frac{i}{k\tau}\right), \tag{3.59}$$

the two-point correlation function in Fourier space is given by:

$$\langle \hat{\varphi}_{\mathbf{k}}(\tau)\hat{\varphi}_{\mathbf{k}'}(\tau)\rangle = (2\pi)^3\delta^{(3)}(\mathbf{k}+\mathbf{k}')\frac{|v_{\mathbf{k}}(\tau)|^2}{a^2} = (2\pi)^3\delta^{(3)}(\mathbf{k}+\mathbf{k}')\frac{H^2}{2k^3}\left(1+k^2\tau^2\right). \tag{3.60}$$

In the superhorizon regime, where $|k\tau| \ll 1$, the expression simplifies to a constant:

$$\langle \hat{\varphi}_{\mathbf{k}}(\tau)\hat{\varphi}_{\mathbf{k}'}(\tau)\rangle \to (2\pi)^3\delta^{(3)}(\mathbf{k}+\mathbf{k}')\ \frac{H^2}{2k^3}\ , \tag{3.61}$$

which equivalently corresponds to the dimensionless power spectrum:

$$\Delta^2_{\varphi} = \left(\frac{H}{2\pi}\right)^2\ . \tag{3.62}$$

Therefore, in the limit $|k\tau| \ll 1$, corresponding to modes well outside the horizon, the power spectrum of the rescaled field $\hat{\varphi}_{\mathbf{k}}$ approaches a constant value. This behaviour has profound physical implications. As inflation proceeds, modes with comoving wavenumber k exit the horizon when $k = aH$. Once outside, their physical wavelength exceeds the causal horizon, and their dynamics effectively freeze. The amplitude of the fluctuations becomes insensitive to local physics and remains constant.
The constancy of $\Delta^2_{\varphi}(k)$ implies that all modes have the same amplitude at horizon exit, regardless of scale. This is the essence of *scale invariance*, a key prediction of inflationary cosmology. It is consistent with observations of the cosmic microwave background, which show nearly uniform fluctuations across a wide range of scales.
Besides, in the super-horizon regime, the evolution of perturbations is governed by the background geometry (quasi-de Sitter), which is homogeneous and isotropic. As a result, the fluctuations settle into a universal amplitude which characterize all the modes.

3.1.4 Adiabatic and Isocurvature fluctuations

In the following sections, we will show how a massive vector field produced during primordial expansion can serve as a robust and well-motivated dark matter candidate. Before proceeding, it's important to underline that, for such a candidate to serve as a viable and interesting proposal, its power spectrum must be consistent with the observed structures distribution of the universe. This requires consistency with the constraints derived from the CMB and, simultaneously, the reproduction of statistical properties of the universe. Such information is encoded in the primordial density perturbations generated in the early universe, which can be classified into two distinct contributions.
In this section, we provide a brief overview of these two types of primordial fluctuations and examine the constraints they impose on viable dark matter candidates, setting the stage for understanding how a massive vector field can satisfy these cosmological requirements.

Primordial density perturbations in the early universe can be classified into two distinct types: *adiabatic* and *isocurvature* fluctuations. Adiabatic fluctuations correspond to variations in the

total energy density, affecting all matter and radiation components uniformly. In such regions, the relative fractions of dark matter, baryons and radiation remain constant, so the overall composition of the universe is preserved even as the total density varies. In contrast, isocurvature fluctuations involve changes in the relative abundances of different components while keeping the total energy density unchanged. In this case, some constituents become locally more or less abundant, producing a distinct primordial imprint on the universe that affects the relative composition rather than the overall density.

The presence of these two types of perturbations is directly reflected in the anisotropy patterns of the cosmic microwave background. On large scales, observations indicate that isocurvature fluctuations contribute at most approximately 1–10% of the total primordial perturbations. This corresponds to an amplitude of less than 10^{-10} for the isocurvature power spectrum on these scales. However, on smaller scales, where nonlinear processes can erase or modify primordial information, observational constraints are far weaker and the strict bounds from the CMB no longer apply. As a result, the behaviour of perturbations on sub-CMB scales remains largely unconstrained, leaving room for additional effects.

Therefore, for the vector boson to be a compelling dark matter candidate, it must reproduce the observed matter power spectrum of the universe. In particular, it should not generate large isocurvature perturbations on long wavelengths -a common challenge for light bosonic fields. Remarkably, the massive vector naturally avoids this problem.
Furthermore, it must exhibit adiabatic, nearly scale-invariant fluctuations on cosmological scales, consistent with observations. As we will show, these conditions are indeed satisfied, making the massive vector a robust and observationally consistent dark matter candidate.

Chapter 4

The Origin of Dark Matter

Dark matter is one of the most fascinating and enigmatic components of the universe [10, 11, 22, 27, 76, 77]. Accounting for approximately 85% of the total matter content, its presence is inferred from a wide range of astrophysical and cosmological observations, including galactic rotation curves, gravitational lensing, the dynamics of galaxy clusters and the anisotropies in the cosmic microwave background. The rotation curves, in particular, represent the most direct evidence for dark matter on galactic scales. These curves plot the circular velocities of stars and gas against their distance from the galactic centre, revealing a striking discrepancy with the expectations from visible matter alone. Together with the bounds on the abundance of light chemical elements from Big Bang Nucleosynthesis, which constrain the amount of baryonic matter, all these observations strongly point to the need for a clustering component of non-baryonic origin.
This component must not interact strongly with photons and dominates the matter content of the universe. Despite its gravitational influence being well established, the fundamental nature of dark matter remains unknown.

This is one of the oldest unsolved problems in cosmology, dating back to the 1930s, and at the same time one of the best measured. The first clear evidence for dark matter emerged in the 1970s [78]. Today, the case for its existence comes from precise measurements across a wide range of scales, from sub-galactic and galactic environments, to galaxy clusters and up to the large-scale structure (LSS) of the universe. Across a wide range of astrophysical systems we observe dynamical anomalies that cannot be accounted for by standard matter only. This component, which is believed to be responsible for the "missing" mass in our universe, is then the main ingredient for all the structures we have in our universe [21, 22].

Currently, the concordance model of cosmology, the ΛCDM model, has accumulated a remarkable number of observational successes, despite the fact that, as the observations and simulations of the small non-linear scales and galactic scales improve, a number of challenges have emerged for this coarse grained description from ΛCDM.
Within this framework, the Cold Dark Matter (CDM) paradigm arose from large-scale observations, describing the component responsible for cosmic structure formation through gravitational clustering. In the CDM model, dark matter is treated as a perfect fluid: it must be massive, sufficiently cold (non-relativistic at the epoch of structure formation) and collisionless, in order to account for the observational data on large, linear scales. This coarse-grained description of CDM has been extremely successful in reproducing observations across the CMB, LSS, galaxy clusters

and the general properties of galaxies.

This allows for the creation of a plethora of possible models of DM. Those models recover the large scale properties of CDM, but invoke very different objects and phenomena to play the role of DM, as can be seen in the following, not to scale, picture:

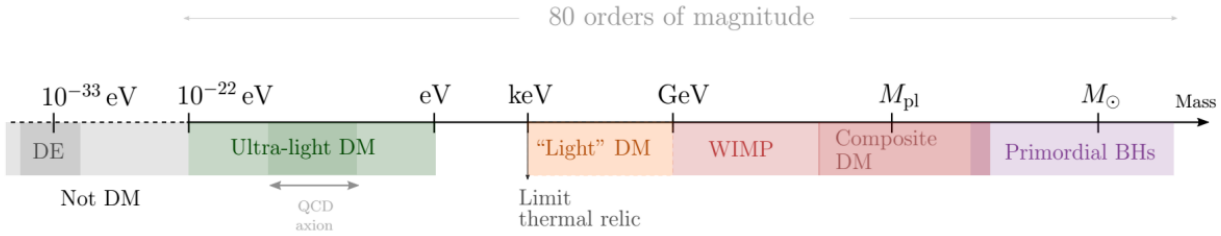

Figure 4.1: Figure taken from [21]. A very wide range of dark matter models has been proposed, with DM represented by different phenomena, spanning from new particle candidates to primordial black holes.

This figure illustrates the wide variety of broad classes of dark matter models, each of which can encompass many specific realizations. The range extends over more than 80 orders of magnitude, covering very different hypotheses for DM: from new elementary particles, to composite objects and even astrophysical-scale primordial black holes. This highlights that, despite the hydrodynamical properties of dark matter on large scales are now known with high precision, its underlying microphysical nature remains elusive.

Historically, the weakly interacting massive particle (WIMP) has been the dominant candidate for dark matter [79]. Dark matter was assumed to be composed of non-relativistic, weakly interacting particles that decoupled from the thermal bath in the early universe. Traditional production mechanisms, such as thermal freeze-out or freeze-in, rely on interactions within a hot, radiation-dominated background. However, these scenarios face increasing tension with observational constraints and null results from direct detection experiments. Another accredited candidate that comes from extensions of the standard model of particle physics is the QCD axion [80], first introduced to address the strong CP problem of quantum chromodynamics (QCD).
Although we have these very well motivated candidates from particle physics, we still have no conclusive evidence for electroweak or other non-gravitational interactions for dark matter. All the knowledge we have about dark matter is gravitational.

In recent years, a diverse array of alternative candidates has garnered increasing attention. Among these, ultra-light dark matter [21] has emerged as a particularly compelling possibility, offering novel phenomenology and distinct cosmological signatures. The central idea is that the wave-like nature of dark matter on galactic scales gives rise to non-CDM behaviour, leading to a rich and distinct phenomenology on those scales. On large scales, however, DM still behaves like CDM, albeit with different initial conditions for ULDM compared to CDM, thereby preserving the well-established observational successes of the standard paradigm. There exist multiple realizations of this small-scale non-CDM phenomenology. Depending on how ULDM is modelled, it can give rise to different condensate structures and, consequently, to distinct astrophysical signatures.

An alternative and theoretically intriguing possibility is that dark matter was produced during the inflationary epoch itself [17, 58, 81, 82]. Inflation, a period of accelerated expansion in the early universe, not only resolves several classical problems of cosmology but also provides a natural framework for generating primordial perturbations. In this context, dark matter may arise from quantum fluctuations of spectator fields, non-minimally coupled scalars or other degrees of freedom that are excited by the inflationary dynamics.

4.1 Ultra-light Dark Matter

A significant effort has been devoted to developing a wide array of theoretical models and experimental strategies aimed at identifying the true nature of dark matter. These models exhibit considerable diversity and complexity, yet it is often useful to classify them according to the mass of the proposed dark matter candidate, which spans an extraordinary range; from approximately $10^{-22}\,\mathrm{eV}$ to $\sim 10\,M_\odot$. Despite decades of investigation, no non-gravitational interaction of dark matter has been conclusively observed [22].

The term *ultralight dark matter* encompasses a broad class of candidates with masses in the range $10^{-24}\,\mathrm{eV} \lesssim m \lesssim \mathrm{eV}$. Notable examples include the QCD axion [80], the dark photon [83] and light scalar fields arising from compactified extra dimensions in string theory. These models differ significantly in their couplings, both within the dark sector and to Standard Model particles. However, a common feature among them is that their low mass leads to a high occupation number per de Broglie wavelength in galactic environments. For $m \lesssim \mathrm{eV}$, this occupation number typically exceeds unity, implying -via the Pauli exclusion principle-, that all viable ultralight dark matter candidates must be bosonic.

The sub-region of parameter space with masses on the order of $\lesssim 10^{-19}$ eV is commonly referred to as *fuzzy dark matter* [22, 84]. In this mass regime, dark matter exhibits wave-like behaviour on astrophysical scales, leading to distinctive phenomenology in structure formation and galactic dynamics. A commonly studied scenario assumes that the entire dark matter content is composed of a minimally coupled classical field. This simple yet compelling model is phenomenologically attractive, as it is fully characterized by a single parameter: the field *mass*. Despite its minimalistic formulation, it gives rise to a rich phenomenology, yielding constraints from a broad spectrum of astrophysical observables.
Indeed, just by assuming the the existence of a single ultralight field which constitutes all the dark matter, a variety of effects and constraints can influence distinct domains of astrophysical and cosmological relevance, such as primordial power spectrum of density fluctuations, the present day halo mass function, the scales at which we would expect to observe fluctuations in the Lyman-alpha forest.

So, *why consider particles with such extremely small masses?* This regime is interesting not only due to its theoretical motivation within particle physics, but also because particles of ultra-light

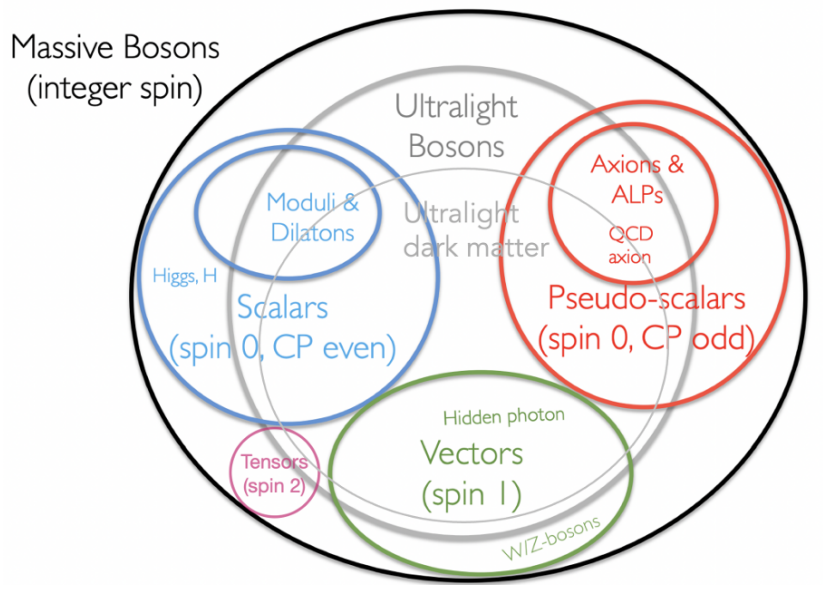

Figure 4.2: Bosonic fields with non-zero mass that may constitute the ultra-light dark matter. Adapted from [85].

mass exhibit exceptionally large de Broglie wavelengths. The de Broglie wavelength is defined as:

$$\lambda_{\mathrm{dB}} \equiv \frac{2\pi\hbar}{mv}, \tag{4.1}$$

which, for typical galactic velocities, evaluates to:

$$\lambda_{\mathrm{dB}} \sim 0.48 \text{ kpc} \left(\frac{10^{-22} \text{ eV}}{m}\right) \left(\frac{250 \text{ km/s}}{v}\right), \tag{4.2}$$

where v denotes the non-relativistic velocity of the particle, or more specifically, the velocity dispersion of the galactic halo. Here, $\hbar = h/2\pi$ is the reduced Planck constant.
In the context of ultra-light dark matter (ULDM), this implies that the de Broglie wavelength can reach astrophysical scales. For instance, when $m \sim 10^{-23}$ eV, the wavelength is on the order of kiloparsecs for a Milky Way-like halo. Another relevant aspect of ULDM is related to its production: due to its extremely low mass, this component could not have remained in thermal equilibrium with the primordial plasma at late times. If it had, it would be relativistic today, which is ruled out by observational constraints.

As illustrated in [21] and [22], a wide range of particle candidates could potentially account for ultra-light dark matter. Any bosonic field with an ultra-light mass that can be produced in sufficient abundance throughout the universe may serve as a viable microphysical description of this component. These candidates include: the QCD axion, axion-like particles, massive scalar fields, vector or higher-spin bosonic fields.
Each of these possibilities offers distinct theoretical motivations and phenomenological implications.

4.2 Primordial Black Holes

In this section, the topic of primordial black holes (PBHs) will be briefly addressed.
Although primordial black holes are not the central focus of this work, they bear relevance to the results presented, as it will discussed in Section 6.5. For completeness, it is useful to briefly review their key properties and the mechanisms by which they may be formed in the early universe.

Multiple lines of observational evidence -such as galaxy rotation curves, large-scale structure formation and the dynamics of the Bullet Cluster-strongly suggest that the majority of gravitationally bound matter in the universe is non-baryonic. This unseen component is commonly referred to as *dark matter*. An intriguing and economical explanation that might account for DM density in our universe is a scenario where DM is made of compact objects, such as primordial black holes. PBHs would represent a unique class of dark matter candidates in that they do not require the introduction of new fundamental particles. Instead, PBHs can form within the first second after the Big Bang through the gravitational collapse of overdense regions seeded by early-universe fluctuations.

Initial ideas in this direction emerged from the realization that primordial black holes (PBHs) could form through the gravitational collapse of over-dense inhomogeneities in the early universe. By the mid-1970s, it was further recognized that primordial black holes (PBHs) might contribute to the dark matter (DM) density and serve as seeds for the supermassive black holes (BHs) populating our universe. Interest in PBHs grew even further following the first detection of gravitational waves (GWs) from merging black holes.

There is still no clear direction or agreement on how primordial black holes could arise. They are expected to form well before the end of the radiation-dominated era (i.e. prior to matter-radiation equality). Once formed, they behave as cold and collisionless matter, making them a compelling dark matter candidate -provided their masses are sufficiently large, $M_{\rm PBH} \gtrsim 10^{15}$ g $\simeq 10^{-18} M_\odot$, to ensure a lifetime comparable to the age of the universe.

A natural and compelling origin for the perturbations leading to PBH formation lies in the quantum fluctuations generated during inflation, which are stretched outside the horizon in much the same way as those responsible for the anisotropies of the cosmic microwave background (CMB). However, while CMB observations are explained by relatively small scalar perturbations, the formation of PBHs requires overdense regions with amplitudes several orders of magnitude larger on much smaller scales ($k_{\rm PBH} \gg k_{\rm CMB}$, corresponding to the late stages of inflation). Since CMB data favours a red-tilted power spectrum on large scales, PBH production typically demands either a blue-tilted spectrum or specific features in the power spectrum localized at the scales associated with PBH formation (see [86–88] for reviews).

In this context, producing PBHs requires modifications to the standard slow-roll inflationary picture. In particular, brief periods of non-attractor dynamics, corresponding to departures from slow-roll evolution, can significantly amplify scalar fluctuations on small scales [89, 90]. Two broad approaches are commonly considered: (*i*) generating substantial scale dependence in the curvature perturbation after horizon crossing, thereby boosting the small-scale spectrum; or (*ii*) introducing mechanisms that already imprint strong scale dependence at the time of horizon exit.

Consequently, producing a sufficient abundance of PBHs necessitates non-standard initial conditions that amplify small-scale perturbations well beyond the nearly scale-invariant spectrum predicted by conventional inflationary models. Such enhancement typically arises from modifications to the inflationary dynamics, which can lead to a localized increase in the power spectrum at small scales. These scenarios will be reviewed in Sections 6.5and 6.5.1, in relation to the results presented in this work.

Chapter 5

Vector Fields in the Early Universe

Inflation is one of the most elegant and powerful paradigms in modern cosmology for describing the very early universe: a brief epoch of accelerated expansion that reshapes our understanding of the universe. It provides a coherent theoretical framework to address fundamental puzzles of standard cosmology that plagued the standard Big Bang model, such as the horizon problem and the flatness problem. Beyond solving these puzzles, it not only solves the traditional problems of cosmology, but also provides a natural way to explain the large-scale structures of our universe, by generating the primordial density fluctuations that seeded galaxies and cosmic structure, through quantum fluctuations stretched to cosmic scales.
The very mechanism that drives inflation seeds the universe with the primordial inhomogeneities that evolve into galaxies, clusters and the cosmic web. It's a profound synthesis of quantum mechanics and general relativity, where the smallest scales give rise to the largest structures.

However, while inflation is widely accepted as the origin of structures in the universe, the nature and origin of dark matter is still unknown. Cosmological measurements show that the observed growth of structure in our universe requires its existence.

Traditionally, the origin of dark matter is considered to be independent of the inflationary dynamics. While it is reasonable to consider these two sectors as decoupled, it is nonetheless tempting to ask whether inflation -a theory that so elegantly accounts for the origin of cosmic structure- might also serve as the source of the dark matter essential for the growth of the structures in the universe [15]. In fact, particles can be produced from vacuum fluctuations during inflation [16, 17, 58, 72, 73]. Thus, inflation naturally provides a mechanism for generating a cosmological abundance of particles: as the universe transitions from the inflationary phase to the subsequent radiation- or matter-dominated era, quantum field modes that were initially in their vacuum state become excited due to the rapidly changing spacetime background. This process, known as gravitational particle production, arises from the non-adiabatic evolution of the metric and can lead to the creation of particles even in the absence of direct couplings. Remarkably, this mechanism is capable not only of contributing to the reheating of the universe, but also of sourcing the matter content itself, offering a unified framework in which both the thermal history and the origin of dark matter may be addressed within the inflationary paradigm.

The earliest attempts to link dark matter production to inflation focused on a massive scalar field produced via quantum fluctuations. In particular, it was noted that a scalar field with mass $m \ll H_I$, where H_I is the Hubble parameter during inflation, would be naturally and coherently

populated through inflationary quantum fluctuations (see, e.g., [17, 58, 82]). These fluctuations yield a nearly scale-invariant power spectrum and, for sufficiently light fields, such as axions or axion-like particles, the resulting energy density could, in principle, account for the observed dark matter abundance.

This mechanism is theoretically appealing due to its minimal assumptions and natural embedding in inflationary dynamics. However, it faces a critical observational challenge. The fluctuations of such a light scalar field are uncorrelated with the inflaton perturbations and thus manifest as *isocurvature* modes in the primordial power spectrum. These isocurvature perturbations evolve differently from adiabatic ones and leave distinct imprints on the cosmic microwave background, particularly in the temperature anisotropies and polarization spectra. Observations from the *Planck* satellite place stringent upper bounds on the amplitude of isocurvature modes, requiring them to be subdominant compared to adiabatic perturbations. But, for a scalar field to account for the full dark matter abundance, the associated isocurvature fluctuations would typically exceed these bounds unless the inflationary scale H_I is unnaturally low, which conflicts with other inflationary observables such as the tensor-to-scalar ratio.

Therefore, while scalar field production during inflation offers an elegant route to generating dark matter, the unavoidable presence of isocurvature perturbations renders this scenario incompatible with CMB observations.

Given these well-established results for scalar (and tensor) perturbations, it is natural to ask: what about *vector fields?* Interestingly, unlike scalars and tensors, the power spectrum of massive vector fields produced during inflation is not flat. As we will see in Section 5.40, their spectrum behaves quite differently: it is peaked around a characteristic scale k_*, which corresponds to a cosmologically small wavelength. The isocurvature power spectrum falls off at long wavelengths (low k), reaching levels that are effectively unobservable, for which we have no constraints at present days. So, unlike the case for scalars, the spectrum of density inhomogeneities produced by this mechanism matches with those observed in the CMB.

5.0.1 Compatibility with CMB Constraints

At first glance, the difference in the spectra of scalar (or tensor) and vector perturbations may appear surprising. After all, the production of these particles during inflation is governed entirely by gravitational dynamics. One might expect, based on the equivalence principle, that all bosonic degrees of freedom would acquire identical spectra. Indeed, for sub-horizon modes, the energy densities of scalar and vector fields evolve in the same way.

However, the behavior of super-horizon modes reveals a crucial distinction: the energy density of vector bosons evolves differently from that of scalars. As we shall see, during inflation, the primordial spectrum of the longitudinal vector mode A_L grows as k^2, in sharp contrast to the

scale-invariant spectrum of the scalar mode φ. This scale dependence, together with the subsequent evolution during radiation domination, gives rise to a momentum-dependent spectrum that increases toward small scales and develops a pronounced peak whose position and amplitude are determined by the vector mass. Since longitudinal vector perturbations behave as isocurvature modes, their amplitude is strongly suppressed at the large scales probed by the CMB, and therefore they remain well within current observational bounds. Significant power only appears at much smaller wavelengths, which are not yet accessible to experiment. Consequently, the presence of a peak in the spectrum of longitudinal vector modes does *not* lead to any conflict with CMB data; rather, it reflects the fact that isocurvature power is negligible on large scales.

The discrepancy between the scalar and vector power spectra does not violate the equivalence principle either, which is inherently a local statement and thus only constrains the evolution of sub-horizon fluctuations. The distinct evolution of super-horizon modes is precisely why inflation efficiently generates massless scalars and tensors (i.e., gravitational waves), but does not source massless vectors. At the same time, this behaviour implies that isocurvature perturbations are not problematic for massive vector bosons generated during inflation and they then represent a **viable dark matter candidate**.

5.1 Ultra-light vector bosons as dark matter candidates

We investigate the inflationary production of ultra-light vector bosons. Such bosons can naturally emerge in extensions of the Standard Model [10, 11]. Their interactions with Standard Model particles may be extremely weak, which prevents them from thermalizing with the primordial plasma in the early universe. As a result, a population of these vector bosons generated during inflation could survive until late times, making their cosmological abundance potentially significant. We demonstrate that ultra-light vector bosons are indeed produced during inflation. While their initial spectrum resembles that of scalar and tensor modes, its subsequent evolution during cosmological expansion differs markedly, leading to distinct observational implications.

Remarkably, this mechanism requires no additional terms in the Lagrangian -such as explicit couplings to the Standard Model. The mere existence of a massive vector boson is sufficient, if we have an accelerated expansion of the universe: the combined presence of inflation and an ultra-light massive vector boson is enough to account for the abundance and the key properties of dark matter.

5.2 A Massive Vector in the Expanding Universe

We demonstrate that ultra-light vector bosons are naturally produced during inflation. Although their initial spectrum closely resembles that of scalar and tensor modes, a key distinction arises in their subsequent evolution: the spectrum of vector bosons undergoes a different transformation during cosmological expansion. This difference enables inflationary production of such vector fields to account for the entirety of the observed dark matter density.

A massive vector field possesses three degrees of freedom: two transverse modes and one longitudinal mode. During inflation, the transverse modes -being approximately conformal, akin to massless vectors- are only weakly produced. In contrast, the longitudinal mode is generated copiously. It is this *longitudinal component* that naturally emerges as a viable dark matter candidate [15, 91].
In this way, quantum fluctuations during inflation naturally give rise to a relic population of massive vector bosons, with their abundance governed exclusively by two parameters: the Hubble scale H_I during inflation and the mass M of the vector field.

Much like the case for scalars that we have already addressed, the analysis involves decomposing the vector field into spatial Fourier modes. These modes begin deep inside the horizon and are stretched to super-horizon scales as inflation progresses, effectively populating the spectrum. Later, during the radiation-dominated era, the modes re-enter the horizon. To accurately determine the present-day abundance and spectral distribution of these particles, one must carefully follow their evolution across both sub-horizon and super-horizon regimes.

To achieve this, let us consider a Friedman universe with the metric:

$$ds^2 = a^2(\tau)\left[-d\tau^2 + \delta_{ij}\, dx^i dx^j\right], \tag{5.1}$$

so a spatially flat, homogeneous and isotropic background metric [1].
The dynamic of a massless vector field is governed by the action:

$$S = -\frac{1}{4}\int d^4x\,\sqrt{-g}\,F_{\mu\nu}F^{\mu\nu} = -\frac{1}{4}\int d^4x\,\sqrt{-g}\,F_{\mu\rho}F_{\nu\sigma}g^{\mu\nu}g^{\rho\sigma}\,, \tag{5.2}$$

where the field strength tensor is $F_{\mu\nu} = \partial_\mu A_\nu - \partial_\nu A_\mu$.
This action is invariant under a confromal transformation $g_{\mu\nu} \to \Omega^2 g_{\mu\nu}$. This property ensures that the conformal structure of the theory is preserved and, consequently, the conformal vacuum remains unaffected in such a spacetime.

To generate and enhance quantum fluctuations during inflation, it becomes necessary to endow the electromagnetic field with a non-zero mass thanks to which it is possible to break conformal

[1] The above line element neglects the scalar metric fluctuations, under the assumption that they provide subdominant contributions to the dynamics of the longitudinal vector modes. This assumption is justified by the fact that such scalar perturbations are not amplified by the mechanism to be discussed next. Consequently, we are assuming that the longitudinal vector fluctuations are non-adiabatic.

invariance [2]. Such a system would carry three degree of freedom -two transversal components and a longitudinal one. The latter breaks conformal invariance and is the key point of this model. Therefore, let us focus on the action:

$$S = \int d^4x \sqrt{-g} \left[-\frac{1}{4} F_{\mu\nu} F^{\mu\nu} - \frac{M^2}{2} A_\mu A^\mu \right] \tag{5.3}$$

for a massive vector field in a flat, homogenous and isotropic spacetime. The quantity M^2 is a mass parameter that can depend on spacetime coordinates -for example, through its coupling to dynamical fields active during inflation, such as the inflaton. We assume that the vector field A_μ has no homogeneous background value and instead behaves as a perturbation propagating on the cosmological background. We also assume the mass to be a Stueckelberg mass; for an Abelian gauge boson, such a mass term is simply a parameter in the Lagrangian and is technically natural.

The transversal and the longitudinal components behave differently under a conformal transformation. As outlined, the transverse modes are approximately conformal, much like massless vectors, and then their production is suppressed during inflation. On the other hand, the longitudinal mode is copiously produced since it is the the only one who breaks conformal invariance. Thus, the longitudinal mode of a massive vector boson sourced by inflation becomes the dark matter of the universe [15].

For our future analysis, it is convenient to decompose the spatial part of the vector potential into its transverse and longitudinal components, as follows:

$$A_i = A_i^{\mathrm{T}} + \partial_i \varphi \tag{5.4}$$

where the transverse vector component satisfies the condition $\partial_i A_i^{\mathrm{T}} = 0$ and φ is the scalar (longitudinal) degree of freedom. Consequently, the vector field A_μ decomposition takes the form:

$$A_\mu(x) = \big(A_0(x),\, \partial_i \varphi(x) + A_i^T(x) \big) \ . \tag{5.5}$$

Following the procedure outlined in Appendix A, the action 5.3 can be reformulated in terms of the components as:

$$S = \frac{1}{2} \int d^4x \left[A_i^{\mathrm{T}\prime} A_i^{\mathrm{T}\prime} + A_i^{\mathrm{T}} \Delta A_i^{\mathrm{T}} + 2 A_0 \, \Delta\varphi' - A_0 \, \Delta A_0 - \varphi' \, \Delta\varphi' + M^2 a^2 \Big(A_0^2 + \varphi \, \Delta\varphi - A_i^{\mathrm{T}} A_i^{\mathrm{T}} \Big) \right] \ . \tag{5.6}$$

The variation of this action with respect to A_0 gives:

$$-\Delta A_0 + \Delta\varphi' + M^2 a^2 A_0 = 0 \ . \tag{5.7}$$

The temporal component A_0 appears in the action without time derivatives; therefore, it is a non dynamical auxiliary field. Fourier transforming the e.o.m., we find an algebraic equation in this variable, allowing A_0 to be expressed in terms of φ, without introducing a new dynamical degree of freedom. Thus, the A_0 component is a constrained field whose evolution is governed by the

[2]The breaking of conformal invariance could be achieved also by requiring the electromagnetic field effective coupling to be time-dependent during inflation [92].

dynamics of the component φ, referred to as the *longitudinal scalar component.*
Taking the Fourier transform of the fields

$$\varphi(\mathbf{x},\tau) = \int \frac{d^3k}{(2\pi)^{3/2}}\,\varphi_{\mathbf{k}}(\tau)\,e^{i\mathbf{k}\cdot\mathbf{x}}\ , \quad A_0(\mathbf{x},\tau) = \int \frac{d^3k}{(2\pi)^{3/2}}\,A_{0\mathbf{k}}(\tau)\,e^{i\mathbf{k}\cdot\mathbf{x}}\ , \tag{5.8}$$

we obtain:

$$A_{0\mathbf{k}} = \frac{k^2}{k^2+M^2a^2}\,\varphi'_{\mathbf{k}}\ . \tag{5.9}$$

In the following, we restrict our attention to the scalar sector, characterized by the fields A_0 and φ. In Fourier space, the physical longitudinal component of the vector field takes the form:

$$A_{L\mathbf{k}}(\tau) = ik\,\varphi_{\mathbf{k}}(\tau). \tag{5.10}$$

Substituting into action 5.6 the expansions 5.8, focusing only on the scalar modes and using 5.9 to express A_0 in terms of φ, the action reads

$$S = \int d\tau\,d^3k\,\frac{k^2a^2(\tau)}{2}\left[\frac{M^2}{k^2+M^2a^2(\tau)}\,\varphi'_{\mathbf{k}}\,\varphi'_{-\mathbf{k}} - M^2\,\varphi_{\mathbf{k}}\,\varphi_{-\mathbf{k}}\right]. \tag{5.11}$$

The non-canonical kinetic structure of the scalar variable φ is due to the procedure of integrating out the auxiliary field A_0. The corresponding equation of motion is:

$$\varphi''_{\mathbf{k}} + \frac{k^2}{k^2+a^2M^2}\,2aH\varphi'_{\mathbf{k}} + \left(k^2+M^2a^2\right)\,\varphi_{\mathbf{k}} = 0\ . \tag{5.12}$$

To bring the kinetic term into canonical form, we define the canonically normalized field:

$$\pi_{\mathbf{k}} \equiv \frac{kMa}{\sqrt{k^2+a^2M^2}}\,\varphi_{\mathbf{k}}\ , \tag{5.13}$$

so that the canonically normalized action is:

$$S = \frac{1}{2}\int d\tau\,d^3k\left[\pi'_{\mathbf{k}}\,\pi'_{-\mathbf{k}} - \left(k^2+a^2M^2+\frac{3k^2M^2a'^2}{(k^2+a^2M^2)^2} - \frac{k^2}{k^2+a^2M^2}\frac{a''}{a}\right)\pi_{\mathbf{k}}\,\pi_{-\mathbf{k}}\right]\ , \tag{5.14}$$

where the term in parentheses acts as an effective time-dependent mass squared and a boundary term has been subtracted to eliminate single time derivatives, ensuring the action is in canonical form.

5.3 Evolution of the longitudinal modes through the expansion of the Universe: the dynamics of A_L

We proceed by deriving the solutions to the evolution equations across different regimes -namely, inflation and radiation domination. Our analysis reveals that the longitudinal modes of a vector

field are a compelling dark matter candidate, with their phenomenological features governed by the vector mass M.

5.3.1 Evolution during Inflation

To analyze the dynamics of $\varphi_{\mathbf{k}}$ or, equivalently, of A_L during inflation, we begin by noting that, owing to the hierarchy $M \ll H_I$, all modes initially evolve in the relativistic regime $k \gg aM$ and remain in this regime until after horizon crossing. In this limit, the dynamics of the longitudinal mode effectively reduces to that of a massless scalar field, apart from an overall (and crucial) rescaling.

In order to see this, let's work in standard slow-roll inflation, driven by an additional field independent of the vector sector under consideration. We suppose that, at early times,

$$M \ll H_I \tag{5.15}$$

and, for wavelengths within the Hubble radius, $\lambda \ll H_I^{-1}$:

$$aH_I \ll k, \tag{5.16}$$

i.e., we are working in the relativistic limit, where the physical momentum of the mode is much larger than its mass. By doing this, we are considering modes with wavelengths much smaller than the Hubble radius.
In relation 5.16, k is the comoving wavenumber, a is the scale factor, and H_I is the Hubble parameter during inflation, which is constant assuming a de Sitter expansion during this epoch.
We can conclude that in the highly relativistic limit, the longitudinal mode is equivalent to a massless scalar and when the wavelength of the fluctuation is within the horizon, the fluctuation oscillates.

In this regime, the a^2M^2 term can be dropped from the field redefinition 5.13 and $\pi_{\mathbf{k}}$ can be approximated as:

$$\pi_{\mathbf{k}} \simeq aM\varphi_{\mathbf{k}} \ . \tag{5.17}$$

Correspondingly, the canonical action 5.14 is well approximated by setting $M = 0$ in the equation. In doing so, the standard action of a free massless scalar field in de Sitter is obtained. This confirms that the vector longitudinal component of the vector field behaves as a standard real massless scalar field in the expanding universe.

In fact, in the $k \gg aH_I$ limit, we can drop M^2 contribute and the equation of motion is approximately

$$\varphi_{\mathbf{k}}'' + 2aH\,\varphi_{\mathbf{k}}' + k^2\varphi_{\mathbf{k}} \simeq 0 \ . \tag{5.18}$$

Upon the field redefinition 5.17, then:

$$\varphi_{\mathbf{k}} = \frac{\pi_{\mathbf{k}}}{aM}, \qquad \varphi_{\mathbf{k}}' = \frac{\pi_{\mathbf{k}}'}{aM} - \frac{a'}{a^2}\frac{\pi_{\mathbf{k}}}{M}, \qquad \varphi_{\mathbf{k}}'' = \frac{\pi_{\mathbf{k}}''}{aM} - 2\frac{a'}{a^2}\frac{\pi_{\mathbf{k}}'}{M} + \left(2\frac{(a')^2}{a^3} - \frac{a''}{a^2}\right)\frac{\pi_{\mathbf{k}}}{M} \tag{5.19}$$

and, plugging these expressions into the e.o.m, multiplying the entire expression by aM and recalling that the conformal Hubble parameter is $H = \frac{1}{a}\frac{a'}{a}$, we find:

$$\pi_{\mathbf{k}}'' - 2\frac{a'}{a}\,\pi_{\mathbf{k}}' + \left(2\frac{(a')^2}{a^2} - \frac{a''}{a}\right)\pi_{\mathbf{k}} + 2\frac{a'}{a}\,\pi_{\mathbf{k}}' - 2\frac{(a')^2}{a^2}\,\pi_{\mathbf{k}} + k^2\,\pi_{\mathbf{k}} = 0. \tag{5.20}$$

The terms proportional to $\pi_{\mathbf{k}}'$ and to $\left(\frac{a'}{a}\right)^2\pi_{\mathbf{k}}$ cancel and we are left with:

$$\pi_{\mathbf{k}}'' + \left(k^2 - \frac{a''(\tau)}{a(\tau)}\right)\pi_{\mathbf{k}} = 0\ . \tag{5.21}$$

During inflation one has $a''/a = 2/\tau^2$; consequently, the solution of Eq. 5.20, matching the Bunch–Davies vacuum deep inside the horizon ($-k\tau \gg 1$), is

$$\pi_{\mathbf{k}} = \frac{aH_I}{\sqrt{2k^3}}\left(1 - \frac{ik}{aH_I}\right)e^{\frac{ik}{aH_I}}. \tag{5.22}$$

Inverting the field redefinition (Eq. 5.17) by writing $\varphi = \left(\frac{\pi}{aM}\right)$, the solution for the longitudinal mode in the relativistic regime becomes

$$\varphi_{\mathbf{k}} = \varphi_{\mathbf{k}}^{(0)}\left(1 - \frac{ik}{aH_I}\right)e^{\frac{ik}{aH_I}}, \tag{5.23}$$

where we have defined the k-dependent super-horizon amplitude as

$$\varphi_{\mathbf{k}}^{(0)} = \frac{1}{\sqrt{2k^3}}\,\frac{H_I}{M}\ . \tag{5.24}$$

Finally, by invoking the relation 5.10, which links the longitudinal mode to the underlying scalar dynamics, we are now in a position to explicitly determine the behavior of $A_{L\mathbf{k}}$. We find:

$$A_{L\mathbf{k}} = A_{L\mathbf{k}}^{(0)}\left(1 - \frac{ik}{aH_I}\right)e^{\frac{ik}{aH_I}}\ . \tag{5.25}$$

Shortly after horizon exit, all modes rapidly settle into a constant amplitude, as given by 5.24, regardless of whether a particular mode subsequently becomes non-relativistic. Consequently, longitudinal modes freeze out efficiently on super-horizon scales and asymptotically approach a fixed amplitude determined by

$$|A_{L\mathbf{k}}| \xrightarrow{\tau\to\ 0} \frac{1}{\sqrt{2k}}\left(\frac{H_I}{M}\right) \qquad\qquad |A_{L\mathbf{k}}'| \xrightarrow{\tau\to\ 0} 0 \tag{5.26}$$

If M is small enough, the condition $aM \ll k$ remains valid throughout the inflationary period, across all scales relevant to our analysis, applying both in the sub-horizon regime ($k \gg aH_I$) already discussed and in the super-horizon regime ($k \ll aH_I$). The super-horizon limit indeed can be expressed by the inequality:

$$\frac{M}{H_I} \ll \frac{k}{aH_I} \ll 1\ . \tag{5.27}$$

As a consequence, even at super-horizon scales, the a^2M^2 term in the equation of motion can be safely neglected, yielding a dynamical behaviour that closely mirrors that of a massless scalar field. This regime corresponds to a frozen kinetic energy regime. Indeed, in this regime, the equation of motion simplifies to

$$\varphi_{\mathbf{k}}'' + 2aH\,\varphi_{\mathbf{k}}' \simeq 0\,. \tag{5.28}$$

During quasi–de Sitter expansion we have $a(\tau) \simeq -1/(H\tau)$, implying $aH = -1/\tau$. Thus the mode equation becomes

$$\varphi_{\mathbf{k}}'' - \frac{2}{\tau}\,\varphi_{\mathbf{k}}' \simeq 0\,, \tag{5.29}$$

whose solution is

$$\varphi_{\mathbf{k}}(\tau) = C_1 + C_2\,\tau^3\,. \tag{5.30}$$

Since $a \propto (-\tau)^{-1}$,we can rewrite the solution as

$$\varphi_{\mathbf{k}}(\tau) = C_1 + C_2\,a^{-3}\,. \tag{5.31}$$

Therefore, once the mode is outside the horizon, its amplitude consists of a constant mode and a decaying mode. The decaying contribution quickly vanishes, leaving only the constant piece. As a consequence, the fluctuation's amplitude becomes effectively fixed in time: it "freezes" until the mode re-enters the horizon during later cosmological epochs.
Since when the wavelength stretches beyond the Hubble horizon, causal communication across the mode is lost: different parts of the fluctuation cannot interact.

We may thus outline the following scenario: consider a fluctuation whose initial physical wavelength $\lambda \sim a/k$ lies well within the Hubble radius. On sub-horizon scales, modes with $k \gg aH$ undergo rapid oscillations and the mass term can play a significant role -unless $M \ll H_I$, in which case the mass contribution remains negligible compared to the expansion rate. As cosmic expansion proceeds, the wavelength stretches and eventually approaches the horizon scale. Once the mode crosses outside the Hubble radius, its oscillations are suppressed due to the dominance of Hubble friction and, if $M \ll H_I$, the field behaves as if it were massless and its Compton wavelength becomes much larger than the Hubble radius; the fluctuation then effectively freezes, retaining its amplitude until re-entry.
In the two regimes under consideration, the dynamics of the longitudinal component of the field are equivalent to those of a massless scalar field.
This behavior is observed both on sub-horizon and super-horizon scales during inflation and corresponds respectively to the pale blue region marked as "De Sitter Vacuum fluctuations" and to the "Frozen Kinetic Energy" region in Figure 5.2. See also Figure 5.1 for a detailed explanation of the various regimes.
Accordingly, we conclude that the massless scalar approximation remains valid throughout the entire inflationary epoch.

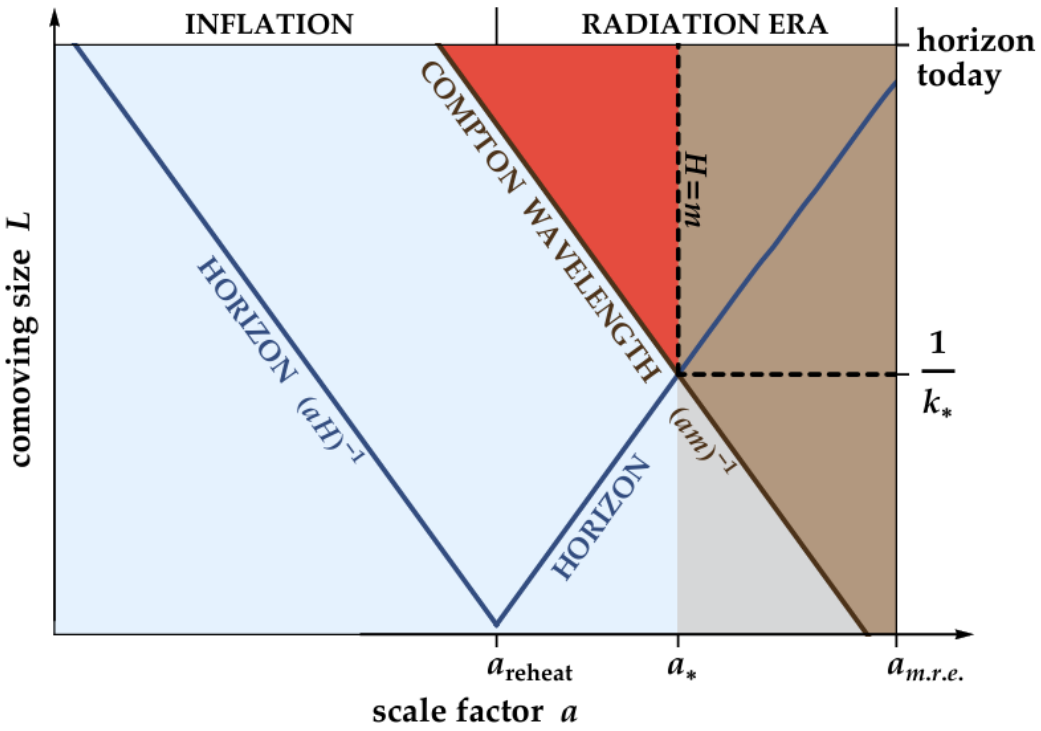

Figure 5.1: The diagram illustrates how cosmological length scales evolve and how the longitudinal mode of a vector field behaves across different regimes. The curve labelled horizon represents the comoving Hubble radius $\frac{1}{aH}$, which contracts during inflation and expands after reheating. The curve labeled Compton wavelength corresponds to the comoving Compton wavelength of the vector field, given by $\frac{1}{am}$. Vector field modes, characterized by a fixed comoving wavevector k, propagate along straight trajectories from left to right. In the pale blue region, where the condition $k \ll M$ holds, the modes are relativistic. In the pale brown region, where Hubble dumping becomes negligible ($H \ll M$), the longitudinal mode behaves like a free massive scalar field. Between these two regimes lies the red triangular zone, where the longitudinal mode exhibits novel dynamics not reducible to any scalar behavior. Modes that pass through the tip of this region reenter the horizon precisely as they transition to non-relativistic motion, defining a characteristic scale k_*. Adapted from [15].

5.3.2 Evolution during Radiation Domination

During the radiation-dominated universe (RDU), the dynamics of the longitudinal mode exhibit considerable richness and complexity.

The problem of determining the post-inflationary dynamical evolution of the modes has been addressed and analytically solved in [15], where it was demonstrated that, after the end of inflation, different regimes can be identified for the description of the modes. The way in which the mode redshifts during RD era does depend on the wavelength of the mode itself and therefore, equivalently, on the scale of horizon exit. In particular, three distinct regimes were found

to characterize the modes evolution during this epoch: a Hubble-damped, non-relativistic regime (referred to as the "vector regime" in Fig. 5.2), a super-horizon relativistic regime and a late-time non-relativistic regime.

In the sub-horizon relativistic regime, the mass contribution is negligible, the mode behaves as radiation and its energy density evolves as a^{-4}, while in the late-time non-relativistic approximation, the energy density redshifts as a^{-3}, behaving as matter. Particular attention must be given to the vector regime, which is something new with respect to the standard massless scalar dynamics: in this case, the solution contains a term which grows with a, which might naively be expected to dominate. However, this regime is preceded by a long period of super-horizon relativistic evolution, during which the field becomes effectively constant. To maintain continuity with this prior regime, the linear growth does not occur; the solution remains approximately constant. As a result, in the vector regime the energy density redshifts as a^{-2}.

Interestingly, this behaviour contrasts with that of massive scalar modes, whose energy density in a comparable regime would contribute with a constant value.

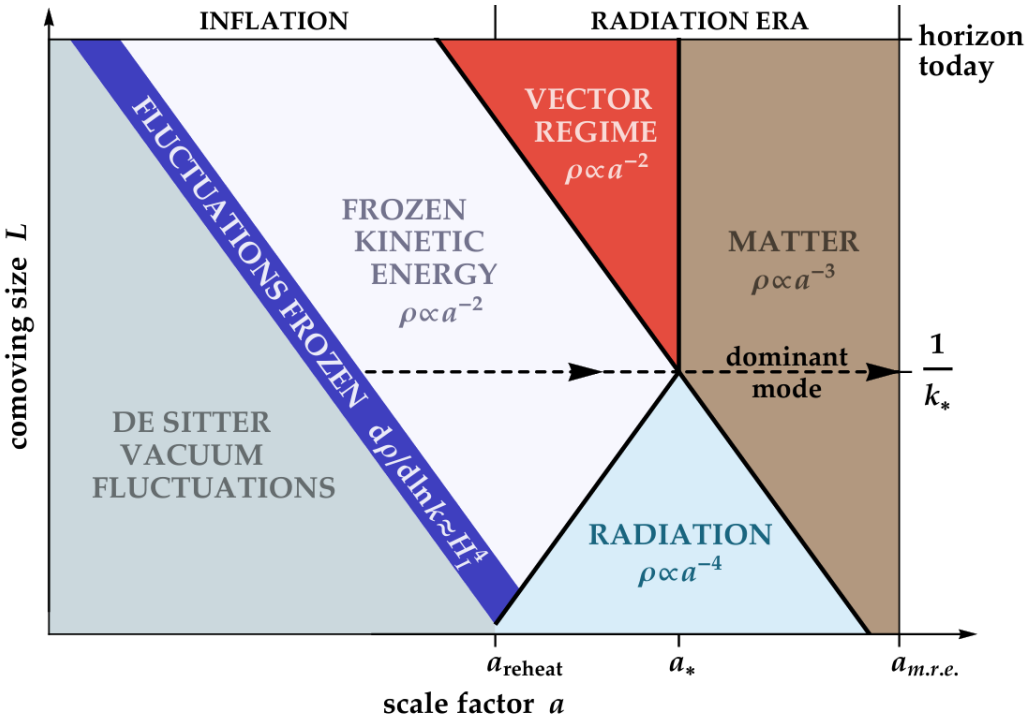

Figure 5.2: From [15]. Outside the region marked as the "Vector regime" (red triangle), the energy density evolves identically to that of a massive scalar field. Within this regime, however, the behaviour differs: while the scalar energy would remain constant, the vector energy redshifts as a^{-2}. This additional damping suppresses large-scale isocurvature perturbations, enabling the resulting vector population to constitute the dark matter. The abundance is mainly set by modes of comoving size $1 \sim 1/k_*$, highlighted by the dashed line.

The treatment carried out in reference [15] provides valuable insight, though it is approximate;

a more thorough and precise analysis requires a numerical approach. Specifically, to accurately track the evolution of the mode from inflation through to the deep RDU phase, one must account for the transitions between different cosmological epochs. This can be achieved by introducing a dimensionless quantity $\mathcal{T}$, which serves as a *transfer function* encoding the full time evolution of the longitudinal mode across these regimes. This approach has been developed in [34] and thoroughly used in [93, 94].

For this purpose, we follow the cosmological evolution during radiation domination of the transfer function. Therefore we write

$$\varphi_{\mathbf{k}}(\tau) = T_L(k\tau)\, \varphi^{(0)}_{\mathbf{k}}(\tau) \ , \tag{5.32}$$

where we give the initial condition $\varphi^{(0)}_{\mathbf{k}}(\tau)$ in terms of the value of the longitudinal mode at the onset of inflation. By combining this with the transfer function, one obtains the evolution of the mode after its re-entry into the horizon. This approach, as will be demonstrated, enables the derivation of the power spectrum associated with the longitudinal component of the vector field in the post-inflationary epoch.

To determine accurate initial conditions for the transfer function at the beginning of RDU, the evolution of $\mathcal{T}$ for a given mode k must be studied from the time of its horizon crossing until the end of inflation. The numerical procedure used to carry out this analysis is explicitly described in [34] and we will reproduce the core points in the following. With this method we can successfully determinate the initial conditions for the transfer function at the beginning of the radiation-dominated universe.

We introduce a set of quantities that will prove useful in the subsequent analysis and in the following sections:

$$\begin{aligned} &- \ k_* \equiv a_* M \\ &- \ x \equiv k\tau \\ &- \ y \equiv \frac{x}{x_*} = \frac{a}{a_*} \\ &- \ x_* \equiv k\tau_* = \frac{k}{k_*} \end{aligned} \tag{5.33}$$

These are suggested to facilitate the numerical analysis, in consistency with the conventions of [34, 93]. In the first definition, k_* is the wave number that re-enters the horizon at the time when the co-moving Hubble horizon is equal to the Compton horizon, as set by the bare mass

$$(a_* M)^{-1} \ = \ (a_* H_*)^{-1} \ = \ \tau_* \quad \Longrightarrow \quad \tau_* \equiv \ k_*^{-1} \ = \ \tfrac{1}{a_* M} \ .$$

In the third one we used the fact that $a \propto \tau$ during RD.
Inserting the *transfer function* into the equation of motion 5.12 of the longitudinal mode, we obtain the evolution equation for $\mathcal{T}$:

$$k^2 \ T''(x) + k \ \frac{2 \ k^2 a H}{k^2 + a^2 M^2} \ T'(x) + \left(k^2 + a^2 M^2\right) \ T(x) = 0 \ . \tag{5.34}$$

Dividing by k^2 and recalling that, in this era, $aH = \frac{1}{\tau}$, we ultimately find that the transfer function obeys the following evolution equation during RD:

$$T''(x) + \frac{2}{x}\Big(1 + \frac{a^2M^2}{k^2}\Big)^{-1} T'(x) + \Big(1 + \frac{a^2M^2}{k^2}\Big)\, T(x) = 0 \ . \tag{5.35}$$

Here, the parameter M denotes the mass of the vector field during the radiation-dominated (RD) era, the Hubble rate decreases relative to its inflationary value H_I and, as anticipated previously, a_* is the value of the scale factor at which the Hubble rate becomes equal to the vector mass, i.e.:

$$H_* \equiv H(a_*) = M \ . \tag{5.36}$$

In terms of the new variables, Eq. 5.35 reads:

$$\frac{d^2T}{dy^2} + \frac{2}{y}\left(1 + \frac{y^2}{x_*^2}\right)^{-1} \frac{dT}{dy} + \Big(x_*^2 + y^2\Big)T(y) = 0 \ . \tag{5.37}$$

The evolution equation for for the transfer functions $\mathcal{T}$ during RD has analytical solutions for in the regimes of small and large y. These solutions can be conveniently approximated by considering the two regimes $x_* \ll 1$ and $x_* \gg 1$ [95]. For an extended description of the method, see Appendix B.

Both the analytical and numerical approach are graphically synthesized in Fig.

5.2. After the end of inflation, the subsequent redshifting of the energy density evolves differently for distinct modes and at different epochs, as illustrated. In particular, if $k \gg aM$, the mode behaves relativistically and redshifts as radiation; if $k \ll aM$ the mode behaves as matter and redshifts as a^{-3}. Thus, within the pale-blue and brown regions of the figure, the energy density of vector and scalar modes redshifts in an identical manner. This behaviour is expected, since in these domains the effective action of the vector reduces to that of a scalar field (up to field redefinitions).

By contrast, in the red region of Fig. 5.2, the energy density of vector modes redshifts as a^2, whereas for scalar modes it would remain constant. Geometrically, one can infer from this plot that the modes experiencing the least redshifting are those with the characteristic wavenumber k_*. Modes with longer wavelengths (towards the upper part of the figure) undergo additional redshifting in the vector regime, causing their final energy to scale as k^2 at small k. Conversely, shorter-wavelength modes (towards the lower part of the figure) redshift rapidly while behaving as radiation, leading their final energy density to fall off as k^{-1} at large k.

This behaviour stands in sharp contrast to that of scalars. For scalar modes, the energy density remains constant throughout the red region. Consequently, all modes with momentum below k_* carry the same power, leading to isocurvature perturbations at length scales directly accessible to the CMB.

As a result, we expect the power spectrum of vectors to be different from the scalr one and to exhibit a pronounced peak, centred around the characteristic wavenumber k_*. This is exactly what we will outline in the following sections.

5.4 The Power Spectrum at the End of Inflation

For light scalar fields, the spectrum of fluctuations produced by inflation is flat (or nearly at) over a large range of wavelengths.
Instead, the longitudinal modes are generated with a power spectrum that deviates from scale invariance, whereas the transverse modes remain suppressed. We find, in particular, that the longitudinal modes of a canonically coupled massive vector are produced with a peaked spectrum. If the vector field is stable on cosmological timescales, the produced abundance survives as cold relic matter in the late universe, manifesting as a coherently oscillating condensate of the field.

The peak occurs at an intermediate scale: it is much smaller than the present horizon of the observable universe, yet considerably larger than the usual ultraviolet cut-off associated with inflationary perturbations. Consequently, the resulting power spectrum is suppressed at the largest wavelengths, in stark contrast to the flat spectrum of light scalar and tensor perturbations.

The departure from scale invariance in the spectrum originates from a fundamental difference in the behaviour of scalar and vector fields in the early universe. For scalar fields, the energy density in non-relativistic modes remains effectively constant when the Hubble parameter exceeds the field mass. In contrast, the energy density of a vector field redshifts as a^{-2} in the same regime. This difference arises from the fact that the norm of a vector field intrinsically involves the spacetime metric and thus the scale factor. Simply raising or lowering the index of the field introduces a dependence on the background geometry, which is absent in the scalar case [15].

It is a well-established result that, for a free, real, massless and canonically normalized scalar field, the Fourier modes that cross the inflationary horizon evolve into classical field fluctuations. Initially emerging as small-scale vacuum fluctuations, these modes experience an amplification in amplitude as they are stretched beyond the horizon, at which point their quantum nature effectively freezes and they behave classically.

Using the expression 5.24 and the definition of the power spectrum given in Section 3.1.3, we understand that the super-horizon power spectra of the field φ is:

$$\mathcal{P}_{\varphi}^{(0)} = \frac{1}{4\pi^2}\Big(\frac{H_I}{M}\Big)^2. \tag{5.38}$$

From which, by recalling the expansion of A_L in Eq. 5.10, we find that the power spectrum of the longitudinal mode A_L at the end of inflation is:

$$\mathcal{P}_{\varphi}^{(0)} = \frac{1}{4\pi^2}\Big(\frac{H_I}{M}\Big)^2 \quad \Rightarrow \quad \mathcal{P}_{A_L}^{(0)} = \frac{k^2}{4\pi^2}\Big(\frac{H_I}{M}\Big)^2 , \tag{5.39}$$

where the suffix (0) has been added to indicate that these quantities are constant, and they provide initial conditions for the mode evolution during the radiation dominated era.

Therefore, as it is evident from Eq. 5.39, the primordial spectrum of the longitudinal scalar field φ exhibits scale invariance, with its amplitude governed by the vector mass and the Hubble parameter during inflation. In contrast, the longitudinal component of the vector field A_L features a spectrum that grows proportionally to k^2 throughout the inflationary epoch, as expected from

the relation 5.10. Thus we learn, as already shown in [15], that the power spectrum at the end of inflation is suppressed at large scales while it increases as k^2 towards small scales (large k).

5.5 The Power Spectrum during Radiation Domination

Once the modes exit the horizon during inflation, they evolve as coherent classical field modes. When they re-enter the horizon, they behave differently basing on the wave-umber k. This is shown thanks to analytical approximations in [15] and it is resumed in Fig. 5.2. At the same time, the different behaviour is captured also by the transfer function we defined in the previous section.

Making use of the above-mentioned transfer function, the power spectrum of the longitudinal mode can be expressed directly in terms of it, since the transfer function encapsulates the full evolution of the mode throughout the radiation-dominated era. Consequently, at sufficiently late times, the power spectrum takes the form

$$\mathcal{P}_{A_L} = |\mathcal{P}^{(0)}_{A_L}||T_L(k\tau)| = \Big(\frac{k_*}{2\pi}\frac{H_I}{M}\Big)^2\Big(\frac{k}{k_*}\Big)^2|T_L(k\tau)| \tag{5.40}$$

in terms of the transfer function T_L and the scale k_* already introduced [93].

This is evaluated numerically by solving the differential equation 5.37 for T_L and integrating for a set of different values $x_* = k/k_*$ -corresponding to different comoving momenta normalized to the pivot momentum k_*. For each integration, the initial conditions

$$T(y_{\rm in}) = 1, \qquad \left.\frac{dT}{dy}\right|_{y_{\rm in}} = 0 \ ,$$

are imposed, with $y_{\rm in} \equiv a_{\rm in}/a_* \equiv \sqrt{M/H_I}$.
Since during radiation domination $H \propto t^{-1}M \propto a^{-2}$, the choice

$$y_{\rm in} \equiv \sqrt{\frac{M}{H_I}}$$

corresponds to

$$H_{\rm in} = H_*\left(\frac{a_*}{a_{\rm in}}\right)^2 = H_I \ .$$

In other words, the variable y takes the value $y_{\rm in}$ at the onset of radiation domination, which in this computation is assumed to occur immediately after the end of inflation.
The result is then evaluated at a sufficiently late time,

$$y_f = \frac{a_f}{a_*} \sim e^4,$$

when the longitudinal spectrum stabilizes its shape as a function of frequency [93].

The resulting normalized spectrum is:

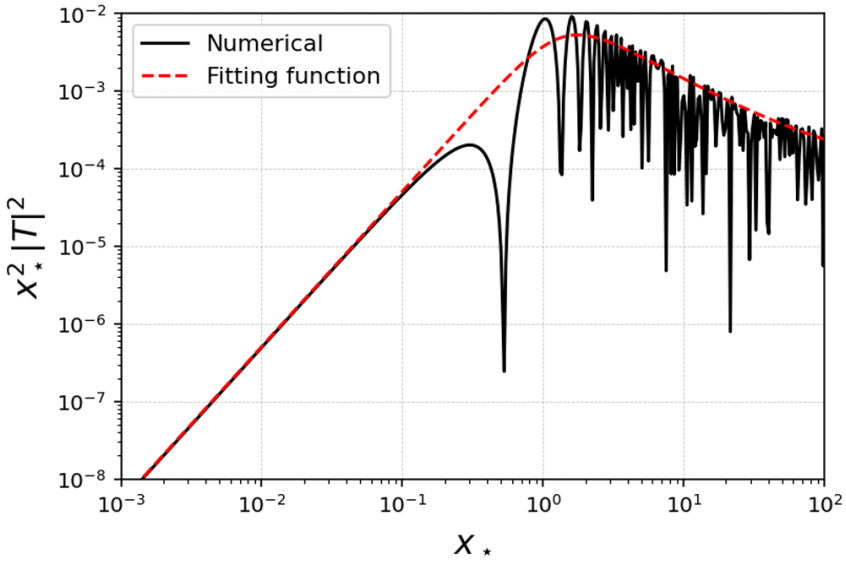

Figure 5.3: From [93]. Primordial power spectrum of the longitudinal modes of a massive vector field, purely generated by inflationary fluctuations. The spectrum is normalized versus $\frac{(k_\star H_I)^2}{(2\pi M)^2}$, evaluated at time $y_{fin} = 55$, while $y_{in} = 10^{-3}$. In red dashed the analytical fitting function from the same reference.

Notice that the spectrum changes slope around $x_* = 1$, i.e., for scales $k \sim k_*$, and thus shows some characteristic and unique features: a pronounced peak located at an intermediate momentum $k_* = a_* M$, which corresponds to the physical scale re-entering the horizon at the epoch when $H(a_*) = M$.

We can outline its specific features: from large scales toward smaller ones, the spectrum rises proportionally to k^2 . This growth originates from the inflationary initial conditions. This scaling reflects the fact that long-wavelength modes remain mostly outside the horizon and evolve with an approximately constant transfer function. In contrast, modes with wavelengths smaller than this characteristic scale (i.e., $k \gtrsim k_*$), undergo sub-horizon evolution and their amplitudes decay. At late times, this causes their power amplitude to decrease and the spectrum approximately goes as k^{-1}.

It is worth emphasizing that this peaked spectrum emerges without any fine-tuning of parameters. This peaked structure implies that the power in long-wavelength fluctuations of the vector energy density -those probed by the CMB- is strongly suppressed. On the contrary, this production mechanism does predict significant power at short wavelengths, but such scales have not yet been experimentally explored.
More specifically, an important consequence of the long-wavelength suppression is the absence of isocurvature modes on cosmological scales, which would be visible in the CMB and are ruled out by observations. Such isocurvature modes are dangerous if the dark matter candidate is a scalar, since there is no suppression and this results in large parts of parameter space being typically

ruled out. However, the vector naturally avoids these observational constraints.
On the contrary, in the case of scalars, whose energy density remains constant, all modes with comoving momenta smaller than k contribute equally, yielding an isocurvature spectrum precisely at the cosmological scales investigated through the CMB.

Certainly, for a light vector to qualify as a viable dark matter candidate, it must reproduce the well-established, nearly scale-invariant and adiabatic spectrum of density perturbations on cosmological scales, characterized by fluctuations of order 10^{-5}. Interestingly, the vector field naturally inherits this spectrum without the need for additional assumptions.

This feature can be understood through the *Separate Universe* picture [96, 97]: since the relevant vector dynamics occurs at sub-horizon scales, while the observed adiabatic modes correspond to wavelengths much larger than the horizon at that time, each region of the universe can be regarded as evolving independently, as if it were a homogeneous universe. In this description, the long-wavelength inflaton perturbations act solely as a shift in the local scale factor or cosmic clock. Such a shift affects the energy density of vector dark matter in exactly the same way as it influences any other dark matter candidate, such as a thermally produced relic. Consequently, the vector density fluctuations automatically track the adiabatic pattern imprinted by inflation.

Therefore, inflationary fluctuations of a light vector field not only generate the required dark matter abundance but also ensure consistency with the observed adiabatic perturbation spectrum, providing a compelling and novel production mechanism.

5.6 Abundance of the Longitudinal Vector Mode

We now consolidate the preceding results to compute the final abundance of longitudinal vector modes. Remarkably, these modes can account for the totality of dark matter across a wide range of vector masses. The resulting dark matter abundance depends only on the mass M of the vector field, rendering the scenario both minimal and predictive.

The computation of the energy density ρ_{A_L} stored in the longitudinal component of the massive vector field serves as a useful first application of the analytic expressions derived in the preceding sections. The quantity ρ_{A_L} is obtained from the time component of the energy-momentum tensor associated with the vector field, and is given by [15]:

$$\rho_{A_L} = \frac{M^2}{2a^2} \int d\ln k \left[\frac{\mathcal{P}_{(\partial_\tau A_L)}}{k^2 + a^2 M^2} + \mathcal{P}_{A_L} \right] , \tag{5.41}$$

with M the vector mass during radiation domination [3]. By substituting expression 5.40 for the primordial spectrum of longitudinal vector modes during RD into 5.41, the integral takes the

[3]In order to account for the variety of possible physical scenarios, the abundance could be defined with a multiplicative factor σ_0 [93]. This parameter effectively keeps track of generalizations of the baseline model proposed in [15]. In our following discussion, σ_0 would encode the impact of a non–slow-roll phase on the final abundance. For the time being, however, we set $\sigma_0 = 1$ and restrict ourselves to the standard case.

explicit form:

$$\rho_{A_L} = \frac{M^2}{2a^2}\int d\ln k\,\left[\frac{1}{k^2+a^2M^2}\Big(\frac{k_* H_I}{2\pi M}\Big)^2\Big(\frac{k}{k_*}\Big)^2|\partial_\tau T|^2 + \Big(\frac{k_* H_I}{2\pi M}\Big)^2\Big(\frac{k}{k_*}\Big)^2|T|^2\right]$$
$$= \frac{1}{2a^2}\Big(\frac{H_I\ k_*}{2\pi}\Big)^2\frac{a_*}{a}\left[\int d\ln k\,\left(\frac{k^2\,a}{k_*^2\ a_*\ (k^2+a^2M^2)}|\partial_\tau T|^2 + \frac{k^2\ a}{k_*^2\ a_*}|T|^2\right)\right]\ . \tag{5.42}$$

Let us now focus on the dimensionless integral enclosed in the square brackets of equation 5.42:

$$\mathcal{I}_\rho = \int d\ln k\,\left[\frac{k^2\,a}{a_\star\,k_\star^2(k^2+a^2M^2)}|\partial_\tau T|^2 + \frac{a\,k^2}{a_\star\,k_\star^2}|T|^2\right]\ . \tag{5.43}$$

By recalling the definitions: $y = \frac{x}{x_*} = \frac{a}{a_*}$ and $x_* = \frac{k}{k_*}$, the resulting expression in the new time coordinate is

$$\mathcal{I}_\rho(y) = \ y\int d\ln x_*\,\left[\frac{x_*^2}{x_*^2+y^2}|\partial_y T|^2 + x_*^2|T|^2\right]\ . \tag{5.44}$$

The integral is evaluated at late times, $y = y_{\rm end}$, employing the analytical transfer functions derived earlier. Following the analysis of [93], we choose a sufficiently large $y_{\rm end}$, in order to ensure that the subsequent integration acquires a stable, convergent value.
Furthermore, guided and motivated by the discussion in Appendix B regarding the two regimes of the analytic transfer function solutions, we find convenient to split the integral into two distinct domains: $y < 1$ and $y > 1$. Thus,

$$\mathcal{I}_\rho(y_{\rm end}) = y_{\rm end}\int_0^1 \frac{dx_\star}{x_\star}\ \left[\frac{x_\star^2}{x_\star^2+y_{\rm end}^2}|\partial_y T^{(A)}_{\rm late}|^2 + x_\star^2|T^{(A)}_{\rm late}|^2\right]$$
$$+\ y_{\rm end}\int_1^{y_{\rm end}} \frac{dx_\star}{x_\star}\ \left[\frac{x_\star^2}{x_\star^2+y_{\rm end}^2}|\partial_y T^{(B)}_{\rm late}|^2 + x_\star^2|T^{(B)}_{\rm late}|^2\right]\ . \tag{5.45}$$

The integral appearing in the first line of Eq. 6.58 is easily numerically integrated by taking the large $y_{\rm end}$ limit directly within the integrand. The resulting result yields a value of 0.475883.
Turning to the second integral in Eq. 6.58, we note that the parameter $y_{\rm end}$ enters both the integration extreme and the integrand itself. To simplify the analysis, we perform a change of variable from x_* to $z \equiv x_*/y_{\rm end}$. In terms of z, the lower limit becomes $\frac{1}{y_{\rm end}}$, which is small and can be safely approximated by zero.

Following this rescaling, the integrand contains terms that oscillate rapidly over the interval $0 \le z \le 1$ and are suppressed by inverse powers of $y_{\rm end}$. These contributions effectively average out and can be neglected. Aside from these oscillatory terms, the integrand features a ratio of polynomials in x_*, which, upon integration, yields a value of 1.025 in the large $y_{\rm end}$ limit.

Summing the two contributions, we obtain:

$$\mathcal{I}_\rho\ =\ 1.50088\ \simeq\ \frac{3}{2}\,, \tag{5.46}$$

a number of order one. We then find the following expression for the present-day energy density of longitudinal vector modes:

$$\rho_{A_L}\ =\ \frac{3}{2}\frac{H_I^2\ k_*^2}{8\pi^2}\frac{a_*}{a^3} \tag{5.47}$$

Combining this result with the definition of H_* and recalling that $k_* = a_* M$, Eq. 5.47 can be rewritten as:

$$\rho_{A_L} = \frac{3}{2} \frac{H_I^2 \, M^2}{8\pi^2} \frac{a_*^3}{a^3} \, . \tag{5.48}$$

We evaluate this relation at matter-radiation equality, taking into account that, during radiation domination:

$$\frac{a_{\rm eq}}{a_*} = \left(\frac{t_{\rm eq}}{t_*}\right)^{1/2} = \left(\frac{H_*}{H_{\rm eq}}\right)^{1/2} = \frac{M^{1/2}}{H_{\rm eq}^{1/2}} \, . \tag{5.49}$$

This gives

$$\rho_{A_L} = \frac{3}{2} \, \frac{H_I^2 \, M^2}{8\pi^2} \, \left(\frac{H_{\rm eq}}{M}\right)^{3/2} . \tag{5.50}$$

Besides, the present-day dark matter energy density can be accurately approximated by the expression:

$$H = H_{\rm eq} \, , \quad \rho_{\rm DM} = \frac{3 H_{\rm eq}^2 M_{Pl}^2}{2} \tag{5.51}$$

Thus, using the value $H_{\rm eq} = 3 \times 10^{-28}$ eV, that we obtain from:

$$H_{\rm eq} = \frac{H_{\rm eq}}{H_0} H_0 = \left(\frac{t_0}{t_{\rm eq}}\right) H_0 = \left(\frac{a_0}{a_{\rm eq}}\right)^{3/2} H_0 \simeq 3400^{3/2} \times 1.43 \times 10^{-33} \, {\rm eV} \simeq 2.8 \times 10^{-28} \, {\rm eV} \, , \tag{5.52}$$

we compute the ratio of the two abundances and we get:

$$\frac{\rho_{A_L}}{\rho_{\rm DM}} = \left(\frac{M}{0.6 \times 10^{-6} \, {\rm eV}}\right)^{1/2} \left(\frac{H_I}{10^{14} \, {\rm GeV}}\right)^2 \, , \tag{5.53}$$

which provides the ratio of the energy density of the longitudinal vector A_L versus the dark matter energy density today.
Therefore, in order to make up the measured dark matter abundance we need a condition on the *mass* of the vector and the *Hubble scale* of inflation. The current bound on the scale of inflation is $H_I \lesssim 10^{14} \, {\rm GeV}$ and places a lower limit on the vector mass required for this mechanism to account for the entire dark matter abundance. Choosing the scale $H_I \sim 10^{14} \, {\rm GeV}$, a vector mass of the order $m \sim 10^{-6}$ eV, would account for the totality of dark matter present in the universe: the abundance of the longitudinal vector component is equal to the observed dark matter. Conversely, for vector boson masses lying below this range, the production mechanism still operates but yields a subdominant contribution to the total dark matter content.

This result highlights a striking feature of the model: without requiring additional fine-tuning or couplings beyond gravitational interactions, inflation itself provides a natural and robust mechanism for the generation of a cosmological abundance for any massive vector boson, which would correspond to the correct relic abundance of dark matter. Moreover, the framework naturally accommodates both dominant and subdominant dark matter components, depending in particular on the mass scale of the vector field.

Chapter 6

Ultralight Dark Matter from Non-Slow-Roll Inflation

Having established that the inflationary epoch offers a natural stage for the production of dark matter, we now seek to refine the framework and to improve the existing estimates. In [15] and in the previous sections, it has been demonstrated that the longitudinal component of a massive vector field is as a promising dark matter candidate. To reproduce the observed dark matter density today, however, the required vector mass M appears to be of the order $M \sim 10^{-6}$ eV and this does not correspond to any known particle, nor to any established mass scale in particle physics which could represent a viable dark matter candidate. This motivates the question of whether modifications of the initial conditions could yield a mass compatible with well-motivated dark matter frameworks. Our aim, in particular, is to embed this mechanism within the *dark photon* scenario, showing that, upon suitably altering the conditions, one can obtain an ultralight dark matter candidate with a mass of order 10^{-19} eV or smaller. Furthermore, we consider the possibility of mixed scenarios where dark matter coexists with primordial black holes.

An intriguing aspect of dark matter composed of longitudinal modes of a massive vector field, is its broad testability across different experimental fronts. From a particle physics perspective, dark photons can interact with the Standard Model via milli-charged couplings [83], allowing for a variety of laboratory and collider constraints. The cosmological evolution of dark photons also exhibits distinctive features and they can leave observable imprints in environments such as black hole surroundings or through the formation of cosmic strings. Furthermore, they may be detectable through precision instruments such as accelerometers, or via gravitational wave observatories or through gravitational waves in the LISA frequency band. These signals are sourced at second order in cosmological perturbations by the amplified longitudinal vector modes [83].

The central idea of our proposal is to supplement the standard inflationary picture with a brief phase of *non–slow-roll (NRS)* evolution [98]. Specifically, we investigate how such a transient departure from slow-roll affects dark matter generation, how it can be consistently modelled and what physical motivations justify this extension. Our generalization of the minimal setup introduced in [15] will allow for the production of dark matter candidates with extremely small masses, thereby broadening the phenomenological landscape and opening the way to new connections between inflation and particle physics.

Such brief NSR era should last few e-folds but gives rise to important differences with respect to the slow-roll base case, leaving distinct imprints in the small-scale regions of the spectrum.

As anticipated in the discussion on SR inflation, there are several mechanisms by which one can introduce a temporary deviation from the slow-roll regime. In our scenario, this is achieved through a *rapid variation of the vector mass*. We analyze how such a modification alters the inflationary dynamics and we find that the resulting framework has profound phenomenological implications: it naturally accommodates viable ultralight vector dark matter candidates, providing a concrete realization of *ultralight spin-1 dark matter*. Moreover, this mechanism offers a compelling generalization of previous results on the maximal amplification of adiabatic fluctuations during inflationary phases with transient non–slow-roll evolution. Taken together, these insights highlight a rich interplay between inflation, dark matter and primordial black holes, and point to promising new directions for early-universe cosmology.

6.1 The setup

Generalizing the formalism developed in Section 5.2 to a dark matter candidate with mass $M(\tau)$, it is possible to present a cosmological scenario involving a massive vector field whose mass evolves dynamically during inflation. We propose to work with a variable mass, which undergoes a rapid variation over a brief interval during inflation, to then stabilize to a constant value by when inflation ends. As a consequence, the system exhibits distinctive features, which characterize and shape our results. The scenario we are going to introduce in this chapter, allows for a new mechanism to produce ultralight dark matter in the form of vector bosons during inflation, in such a way that the longitudinal vector dark matter abundance and its properties are controlled by the vector mass scale and its time variation during inflation.
We argue that this mechanism provides a compelling framework for generating dark matter in the form of the longitudinal mode of a massive dark vector field, using ideas borrowed from physics of primordial black hole formation and with interesting phenomenological ramifications.

Let us start from a setup similar to the one previously introduced in 5.2. We work with a spatially flat, homogeneous and isotropic Friedmann–Robertson–Walker (FRW) metric.

To investigate how the introduction of a non-slow-roll phase can yield a viable dark matter candidate -in particular, a dark photon- we begin by generalizing the action through the inclusion of a time-dependent mass term in a cosmological setting:

$$S = \int d^4x \sqrt{-g} \left[-\frac{1}{4} F_{\mu\nu} F^{\mu\nu} - \frac{M(\tau)^2}{2} A_\mu A^\mu \right] , \tag{6.1}$$

where $F_{\mu\nu} = \partial_\mu A_\nu - \partial_\nu A_\mu$ as before, and where the mass parameter $M(\tau)$ now acquires a time dependence through

$$M^2(\tau) = \frac{m^2 \, J^2(\tau)}{a^2(\tau)} , \tag{6.2}$$

with m denoting a constant mass scale corresponding to the physical vector mass at the end of inflation τ_R. The dimensionless function $J(\tau)$ depends on conformal time. For convenience, we impose the condition

$$J(\tau_R) = a(\tau_R) \ , \tag{6.3}$$

ensuring

$$M(\tau_R) = m \ . \tag{6.4}$$

The non-zero vector mass explicitly breaks an Abelian gauge symmetry, thereby rendering the longitudinal mode of the vector field physical and dynamical. A natural motivation for the time dependence of $J(\tau)$ arises if it originates from a coupling to the inflaton field, whose dynamics during inflation control the evolution of the effective vector mass.

The time dependence of M^2 can therefore be generated through couplings to dynamical fields active during inflation. In particular, we are guided by scenarios in which the inflaton's velocity undergoes a rapid and transient variation-, as for example happens in ultra–slow-roll inflation [68, 99, 100] or constant-roll models [101–103]. Such abrupt departures from standard slow-roll behaviour are expected to manifest as short-lived, sharp features in the function $J(\tau)$. For the purpose of our analysis, however, we need not commit to a specific inflationary framework; it is sufficient to assume that the mass undergoes a rapid variation. In this sense, our arguments remain general and can be applied across a broad class of models.

We further assume that the vector field A_μ has no homogeneous background component and instead appears only as a perturbation propagating on the cosmological background. Its decomposition takes the schematic form of expression 5.5 and, in what follows, we neglect fluctuations of the metric, assuming that their contributions do not spoil the early universe amplification mechanism.

Basing on these considerations, the central problem we need to address is the analysis of vector fluctuations when $J(\tau)$ exhibits a rapid transition during inflation. Successfully doing so, allows us to broaden the parameter space of the longitudinal vector dark matter model [15], thereby accommodating light dark matter candidates with potentially rich phenomenological implications.

With the considerations we outlined, the action 6.1 of the vector field minimally coupled with gravity explicitly reads:

$$S = \int d\tau \, d^3x \, a^2(\tau) \left[-\frac{1}{4} F_{\mu\nu} F^{\mu\nu} - \frac{m^2 J^2(\tau)}{2a^2(\tau)} A_\mu A^\mu \right] \ . \tag{6.5}$$

Making use of the decomposition of A_μ, the gauge field splits into two distinct components: transverse vector modes and a scalar longitudinal mode. In the remainder of this analysis, we concentrate just on the scalar sector, governed by the fields A_0 and φ.
We follow the same steps as in Section 5.2 for the case of a general longitudinal mode: we move to Fourier space, where the *physical* longitudinal mode of the vector field can be expressed as

$$A_{L\,\mathbf{k}}(\tau) = ik \, \varphi_{\mathbf{k}}(\tau) \, , \tag{6.6}$$

as in Eq. 5.10.
We then solve the equation of motion for the nondynamical component A_0, which yields the following relation in Fourier space:

$$A_{0\,\mathbf{k}}(\tau) = \frac{k^2}{k^2 + m^2 J^2(\tau)} \, \varphi'_{\mathbf{k}}(\tau) = \frac{-ik}{k^2 + m^2 J^2(\tau)} \, A'_{L\,\mathbf{k}}(\tau) \, . \tag{6.7}$$

This expression generalizes the result 5.9 obtained previously, with the important difference that the time dependence is now encoded in the dimensionless function $J(\tau)$.
We substitute the relation 6.7 back into 6.1 and we obtain the effective quadratic action for the longitudinal scalar mode $\varphi_{\mathbf{k}}$:

$$S = \int d\tau\, d^3k\, \frac{k^2 J^2(\tau)}{2} \left[\frac{m^2}{k^2 + m^2 J^2(\tau)}\, \varphi'_{\mathbf{k}}(\tau)\varphi'_{-\mathbf{k}}(\tau) - m^2\, \varphi_{\mathbf{k}}(\tau)\varphi_{-\mathbf{k}}(\tau) \right] . \tag{6.8}$$

To bring the kinetic term into canonical form, we define the canonically normalized field:

$$\pi_{\mathbf{k}}(\tau) \equiv \frac{kmJ(\tau)}{\sqrt{k^2 + m^2 J^2(\tau)}}\, \varphi_{\mathbf{k}}(\tau)\, . \tag{6.9}$$

In terms of $\pi_{\mathbf{k}}$, the quadratic action becomes:

$$S = \frac{1}{2} \int d\tau\, d^3k \left[\pi'_{\mathbf{k}}\, \pi'_{-\mathbf{k}} - \left(k^2 + m^2 J^2 + \frac{3k^2 m^2 J'^2}{(k^2 + m^2 J^2)^2} - \frac{k^2}{k^2 + m^2 J^2}\, \frac{J''}{J} \right) \pi_{\mathbf{k}}\, \pi_{-\mathbf{k}} \right] , \tag{6.10}$$

which constitutes the starting point for our discussion.

Throughout this section we assume a quasi-de Sitter background with scale factor

$$a(\tau) = -\frac{1}{H_I \tau}\, . \tag{6.11}$$

Besides, we work under the hypothesis that the physical vector mass at the end of inflation is much smaller than the Hubble scale during inflation, $m \ll H_I$, where m is the constant mass parameter defined in Eq. 6.2 and H_I denotes the inflationary Hubble rate, taken to be approximately constant. We assume that this condition remains valid over the full duration of the accelerated expansion epoch. These considerations translate into the following hierarchy of scales:

- On sub-horizon scales, the physical momentum satisfies:

$$\frac{k}{aH_I} \gg 1 \gg \frac{Jm}{aH_I}\ ; \tag{6.12}$$

- On super-horizon scales the ordering becomes:

$$\frac{Jm}{aH_I} \ll \frac{k}{aH_I} \ll 1\ . \tag{6.13}$$

Under these conditions, the leading contributions to the action 6.10 simplify considerably. In particular, the equation of motion for the canonically normalized scalar field $\pi_{\mathbf{k}}$ takes the form

$$\pi''_{\mathbf{k}}(\tau) + \left(k^2 - \frac{J''(\tau)}{J(\tau)} \right) \pi_{\mathbf{k}}(\tau) = 0 \tag{6.14}$$

and, since $Jm \ll k$ throughout inflation, both on sub-horizon and super-horizon scales, $\pi_{\mathbf{k}} \simeq m\, J(\tau)\, \varphi_{\mathbf{k}}$, and the power spectrum of the original scalar mode φ can be related to that of the canonically normalized mode π simply by

$$\mathcal{P}_{\varphi} = \frac{\mathcal{P}_{\pi}}{m^2 J^2(\tau)}\,. \tag{6.15}$$

To understand how the introduction of a non-slow-roll phase affects the phenomenology of our system, we need to determine the spectrum $\mathcal{P}_{\pi}$. In the following, we adopt the approach developed in [104] and we analytically solve the mode evolution equations in different regimes - inflation and radiation domination- in order to account the differences with respect to the SR case encountered in previous sections and to demonstrate that vector longitudinal modes can constitute an interesting dark matter candidate, whose properties depend on the vector mass m and on the characteristics of the time-dependent function $J(\tau)$.
In particular, we show that the introduction of a non-slow-roll phase significantly alters the k-dependence of the power spectrum. This modification has direct implications for the production of dark matter during inflation.
Interestingly, this is not the full story. We also find that the enhancement of the power spectrum bears a striking resemblance to the maximal k^4 amplification typically encountered in primordial black hole scenarios. This parallel naturally leads us to consider possible correlations between the two dark matter candidates.

6.2 A brief, transient departure from Slow-Roll Conditions

The introduction of a non-slow-roll phase during inflation offers an appealing possibility to achieve an enhancement of the power spectrum. Studying the spectrum of cosmological fluctuations in single-field inflation models with brief and transient departures from slow-roll conditions provides a valuable opportunity to explore new phenomenological effects triggered by this departure.

The motivation for considering a non-slow-roll phase primarily comes from models of primordial black hole formation [86–88], where a significant amplification of the curvature perturbation amplitude is required. Specifically, producing PBHs demands an increase in the power spectrum amplitude by approximately seven orders of magnitude from large to small scales [89, 90]. This dramatic growth cannot be achieved within the standard slow-roll framework of single-field inflation, necessitating a temporary violation of slow-roll conditions. Such a strong enhancement in the scalar curvature power spectrum can push perturbations beyond the threshold for PBH formation. Consequently, the breakdown of slow-roll makes the analysis of fluctuation dynamics more complex but also opens the door to discovering novel effects in the inflationary power spectrum.
In addition, there is another important outcome: the non-slow-roll phase can enhance the primordial gravitational wave spectrum at high frequencies, potentially bringing it within the reach of gravitational wave detectors.

In such scenario, the evolution of fluctuations becomes analytically challenging because the usual slow-roll approximation is no longer valid.
In order to address the problem of studying the power spectrum associated with the field when we introduce a non–slow-roll phase, we can rely on the analytical, model-independent method developed in [104]. To this end, we introduce the ratio $\Delta\tau/\tau_1$ as the parameter quantifying the duration of the non–slow-roll epoch relative to a reference timescale. This ratio is small, allowing us to expand the evolution equations of the fluctuations in a Taylor series around it. Starting from this expansion, we will solve the equations at first order in $\Delta\tau/\tau_1$. In this way, we will derive the properties of the corresponding spectrum of fluctuations in scenarios where the amplitude is significantly enhanced toward small scales.

In the definition of $\Delta\tau/\tau_1$, the quantity $\Delta\tau$ is the duration of the non–slow-roll phase,

$$\Delta\tau \equiv |\tau_1 - \tau_2| \,, \tag{6.16}$$

with τ_1 and τ_2 denoting the start and end of the NSR phase, respectively, while τ_1 is the reference timescale we consider, much larger than the transient phase, which we suppose to be particularly brief.
The other key quantity, specific to the model under consideration, is $J(\tau)$, which we refer to as the pump field (following [104]) and which characterizes the dynamics of the fluctuations.
In a regime of slow-roll single-field inflation, the pump field would have the generic profile

$$J(\tau) = -\frac{c_0}{H_0\tau} \,, \tag{6.17}$$

where c_0 denotes a (nearly) constant parameter depending on the system under study. With such a pump field, the evolution equation can be solved exactly in the pure de Sitter limit of slow-roll inflation.

During the brief non-slow-roll epoch, however, the pump field is not described by the simple profile of Eq. 6.17. In this phase we do not expect an attractor regime of inflation and the would-be decaying mode can become temporarily relevant, thereby affecting the features of the power spectrum.
In our case, we parametrize the pump field as depending on a function $\omega(\tau)$. More in detail, we assume that the time-dependent vector mass profile of Eq. 6.2 is encoded in the function

$$J(\tau) = a(\tau)\,\sqrt{\omega(\tau)} \,. \tag{6.18}$$

In the ultra–slow-roll model, $\omega(\tau) \propto \tau^6$ [104], while in the case of slow-roll inflation, $\omega(\tau)$ is nearly constant. In the case under study, $\omega(\tau)$ encapsulates the (possibly rapid) time dependence of the physics governing the vector mass during the inflationary epoch. As we explained, such a situation can arise, for example, when the vector mass depends on the inflaton velocity, which may vary abruptly over a brief interval in a non-slow-roll phase.
More generally, assuming inflation occurs in the conformal time interval $\tau \leq \tau_R$ (τ_R being the epoch of the instantaneous reheating), we take

$$\omega(\tau) = \begin{cases} \omega(\tau_1) = \text{const.} & \text{for } \tau < \tau_1 \,, \\ \text{smooth but rapidly varying} & \text{for } \tau_1 < \tau < \tau_2 \,, \\ 1 & \text{for } \tau_2 < \tau_R \,, \end{cases} \tag{6.19}$$

with the transition interval satisfying $|\tau_1 - \tau_2|/|\tau_1| \ll 1$. The conformal time τ_1 denotes the moment when the inflationary system first leaves the slow-roll phase and enters the non–slow-roll era. We focus on scenarios where the duration of the non–slow-roll period is much shorter than the characteristic timescales of the system, which we take to be of order $|\tau_1|$ [1].
This assumption is quantified by the inequality

$$\frac{|\Delta\tau|}{|\tau_1|} \ll 1\,. \tag{6.20}$$

With this profile we intend to model a non-slowroll phase treated as nearly instantaneous for analytical tractability, which makes the inflaton velocity rapidly evolve affecting the vector mass.

The remaining technical task is to solve Eq. 6.14. To this end, we adopt the following perturbative Ansatz [104]

$$\pi_{\mathbf{k}}(\tau) = \frac{e^{-ik\tau}\, a(\tau)\sqrt{\omega(\tau)}H_I}{\sqrt{2k^3}}\Big[1 + ik\tau + (ik\tau)^2 A_{(2)}(\tau) + (ik\tau)^3 A_{(3)}(\tau) + \dots\Big]\,, \tag{6.21}$$

which has the property to match to the standard de Sitter mode function when the functions $A_{(n)} = 0$. The functions $A_{(n)}(\tau)$ account for corrections arising from the time dependence of $\omega(\tau)$. An arbitrary reference scale τ_0 can be introduced to make the series dimensionless, though the final results are independent of this choice.
We choose this Ansatz since the dimensionless functions $A_{(n)}$ are taken such that they vanish for $\tau \leq \tau_1$, while they encapsulate the corrections to the field during the NSR phase. This ensures that, at early times, the solution reduces to the general de Sitter solution and that, later in the expansion, it takes in account the effects of the non-slow-roll phase during $\Delta\tau$.

Plugging the Ansatz into Eq. 6.14, we find the following system of differential equations in the time coordinate, valid for each power of $k \geq 2$ (the prime indicates derivative along time). We aim to solve it order by order in powers of k:

$$\text{For } n = 2 \qquad \left[\frac{\omega(\tau)}{\tau^2}\tau_0^2 A'_{(2)}(\tau)\right]' = \frac{\omega'(\tau)}{\tau}\,, \tag{6.22}$$

$$\text{For } n > 2 \qquad \left[\frac{\omega(\tau)}{\tau^2}\left(\tau_0 A'_{(n)}(\tau) - A_{(n-1)}(\tau)\right)\right]' = \frac{\omega(\tau)A'_{(n-1)}(\tau)}{\tau^2}\,. \tag{6.23}$$

A formal solution of A_2 in 6.22 is:

$$\tau_0^2 A_{(2)}(\tau) = \int_{-\infty}^{\tau} d\tau_a \frac{\tau_a^2}{\omega(\tau_a)}\left(\int_{-\infty}^{\tau_a} d\tau_b \frac{\omega'(\tau_b)}{\tau_b}\right) \tag{6.24}$$

[1] We are considering a single phase of non slow-roll expansion. We point out that is also possible to consider situations with multiple non-slow-roll epochs and with intermediate phases of slow-roll expansion in between. In [104] it has been shown that, if this is the case, the behaviour of the spectrum during phases of non-slow-roll evolution might have a "memory" of what occurs prior to these phases, and such memory can be stored in the slope of the spectrum.

while a solution of 6.23 is given by:

$$\tau_0 A_{(n)}(\tau) = \int_{-\infty}^{\tau} d\tau_a \, A_{(n-1)}(\tau_a) + \int_{-\infty}^{\tau} d\tau_a \, \frac{\tau_a^2}{\omega(\tau_a)} \left(\int_{-\infty}^{\tau_a} d\tau_b \, \frac{\omega(\tau_b) A'_{(n-1)}(\tau_b)}{\tau_b^2} \right) , \tag{6.25}$$

where the extremes of integration are chosen to satisfy $A_{(n)}(\tau) = 0$ as $\tau \leq \tau_1$. With this, we determined the most general formal solutions for the functions $A_{(n)}$, in analogy with what has been done in [104].

We can now expressly calculate the functions $A_{(n)}$, solving the equations at leading order in $\Delta\tau/\tau_1$. Having required $\Delta\tau$ to be small we Taylor expand $A_{(2)}$ $(n \geq 2)$:

$$A_{(2)}(\tau_2) \, = \, A_{(2)}(\tau_1) + A^{\mathbf{1}}_{(2)}(\tau_1)\Delta\tau + \frac{1}{2} A^{\mathbf{2}}_{(2)}(\tau_1)\Delta\tau^2 + \dots \tag{6.26}$$

where the upper index in boldface indicates the order of derivative. It is clear that $A_{(2)}(\tau_1) = 0$. Then inserting in 6.24 and arresting at first order, we get

$$\tau_0^2 \, A^{\mathbf{1}}_{(2)}(\tau_1) \, = \tau_0^2 \, A_{(2)}(\tau_2) \, = \, \frac{\tau^2}{\omega(\tau)} \int_{-\infty}^{\tau} d\tau_a \, \frac{\omega'(\tau_a)}{\tau_a} \qquad \Rightarrow \qquad A^{\mathbf{1}}_{(2)}(\tau_1) \, = \, 0 \, , \tag{6.27}$$

since $\omega' = 0$ for $\tau < \tau_1$. Thus, the first derivative vanishes. On the other hand, the second derivative has a non-vanishing contribution:

$$\tau_0^2 \, A^{\mathbf{2}}_{(2)}(\tau_1) \, = \, \tau \frac{\omega'(\tau)}{\omega(\tau)} \Big|_{\tau=\tau_1} = \, \frac{d \, \ln \omega(\tau)}{d \ln \tau} \Big|_{\tau=\tau_1} . \tag{6.28}$$

Identifying the last quantity with the parameter α,

$$\alpha \equiv \, \frac{d \, \ln \omega(\tau)}{d \ln \tau} \Big|_{\tau=\tau_1} \tag{6.29}$$

we therefore find:

$$\tau_0^2 A^2_{(2)}(\tau_1) = \left[\partial_\tau \left(\frac{\tau^2}{\omega(\tau)} \right) \int_{-\infty}^{\tau} d\tau_a \, \frac{\omega'(\tau_a)}{\tau_a} \right] + \frac{\tau}{\omega(\tau)} \omega'(\tau) \quad \Rightarrow \quad \tau_0^2 A^2_{(2)}(\tau_1) = \frac{\tau_1 \omega'(\tau_1)}{\omega(\tau_1)} \tag{6.30}$$

which implies that

$$A_{(2)}(\tau_2) \, \simeq \, \frac{\alpha}{2} \frac{\Delta\tau^2}{\tau_0^2} \tag{6.31}$$

is the leading contribution to the Taylor series in an expansion in $\Delta\tau/\tau_0$.
Proceeding recursively for each $A_{(n)}$, one finds that the first non-zero derivative of $A_{(n)}$ evaluated at $\tau = \tau_1$ is the n-th, with

$$\tau_0^n \, A^{\mathbf{n}}_{(n)}(\tau_1) = 2 \, \tau_0^{n-1} \, A^{\mathbf{n-1}}_{(n-1)}(\tau_1) \, = \, 2^{n-2} \, \alpha \, . \tag{6.32}$$

This indicates that for each n, the leading order in the corresponding Taylor expansion is

$$A_{(n)}(\tau_2) \, \simeq \, \frac{2^{n-2}}{n!} \, \alpha \, \frac{\Delta\tau^n}{\tau_0^n} \, , \qquad \text{for any } n \geq 2. \tag{6.33}$$

Thus, we solved the system of equations order by order in n, determining, for each n, the leading-order contribution to the functions $A_{(n)}$ in a Taylor expansion in the small parameter $\Delta\tau/\tau_0$. The solutions depend on the duration $\Delta\tau$ of the non-slow-roll era and on the parameter α which characterizes the slope of the pump field.

The parameter α is a dimensionless quantity which represents the logarithmic rate of change of $\omega(\tau)$ at the transition. Since $d\ln\tau = -d\ln a(\tau)$ during inflation, a positive α corresponds to a negative rate of change for the vector mass $M(\tau)$ during inflation: the vector mass rapidly decreases during the non-slow-roll epoch.

We can now insert these results into the expression for the mode function $\pi_{\mathbf{k}}$ and evaluate it at any time τ within the interval $\tau_1 \leq \tau \leq \tau_2$, during which the slow-roll conditions are violated. As a concrete example, we consider the limit of the end of the non-slow-roll phase $\tau \to \tau_2$. We obtain:

$$\begin{aligned}\pi_{\mathbf{k}}(\tau) &= \frac{e^{-ik\tau}\, a(\tau)\sqrt{\omega(\tau)}H_I}{\sqrt{2k^3}} \left[1 + ik\tau_2 - \frac{\alpha}{4} - \frac{i}{2}k\alpha\Delta\tau + \frac{\alpha}{4}\sum_{n=0}^{\infty}\frac{(2ik)^n}{n!}\Delta\tau^n\right] \\ &= \frac{e^{-ik\tau}\, a(\tau)\sqrt{\omega(\tau)}H_I}{\sqrt{2k^3}} \left[(1 + ik\tau_2) - \frac{\alpha}{4}\left(1 + 2ik\Delta\tau - e^{2ik\Delta\tau}\right)\right] \ . \end{aligned} \tag{6.34}$$

This provides the analytic expression for the mode function at the end of the non-slow-roll phase and describes how the field $\pi_{\mathbf{k}}$ evolves after a brief period of slow-roll violation [2]. As previously discussed, the result depends on two key parameters: α, which characterizes the slope of the pump field and condenses in a single quantity any deviation with respect to de Sitter and $\Delta\tau$, representing the duration of the non-slow-roll phase.

For $\tau \leq \tau_2$, the mode function $\pi_{\mathbf{k}}(\tau)$ is given by the solution in Eq. 6.34. Having found the solution during the non-slow-roll phase, the mode function obtained can be connected at the transition time τ_2 to the final, slow-roll phase of inflation, spanning the interval from $\tau = \tau_2$ to $\tau = 0$. For $\tau \geq \tau_2$, the pump field $J(\tau)$ takes on its pure de Sitter form and the corresponding general solution for the mode function is given by

$$\pi_{\mathbf{k}}(\tau) = -\frac{i}{\sqrt{2k^3}}\frac{H_0}{c_0}\left[C_1(1 + ik\tau)e^{-ik\tau} + C_2(1 - ik\tau)e^{ik\tau}\right] . \tag{6.35}$$

We match the solutions and and their derivatives through *Israel matching conditions* at the transition time τ_2 and we find that the two coefficients $C_{1,2}$ must satisfy

$$C_1(k) = 1 + \alpha\ \frac{1 - e^{2ik\Delta\tau_A} - 2ik\Delta\tau_A(1 + 2ik\Delta\tau_B)}{8k^2\Delta\tau_B^2}\ , \tag{6.36}$$

$$C_2(k) = -\alpha\ \frac{e^{2ik\Delta\tau_B}}{8k^2\Delta\tau_B^2}\left(1 - 2ik(\Delta\tau_A + \Delta\tau_B) - e^{2ik\Delta\tau_A}(1 - 2ik\Delta\tau_B)\right)\ . \tag{6.37}$$

[2] It is important to note that this approach involves truncating the Taylor expansions at the leading non-zero term. While this is justified under certain conditions, it does not guarantee accuracy in all scenarios: the perturbative scheme we adopted remains valid when the non-slow-roll interval $\Delta\tau$ is sufficiently short and suitable conditions are met. However, in models where $\Delta\tau$ is not small, higher-order corrections may become significant, particularly if enhanced by large coefficients. In this work, we assume a regime where this perturbative method is reliable and the truncation is well justified.

with $\Delta\tau_A = \tau_2 - \tau_1$ and $\Delta\tau_B = 0 - \tau_2$ which is the duration of the final de Sitter phase.
The transition moment may also coincide with the end of inflation, though this is not necessarily the case. Additional phases of non-slow-roll evolution may also follow.

Let us now examine the effects of the NSR phase on the power spectrum of the fluctuations. Although brief, the NSR period significantly influences the system's phenomenology, introducing new features into its dynamics. These phenomenological differences are illustrated in Fig. 6.1, which highlights the impact of including an NSR phase during inflation.

For our purposes, let us recall the definition 3.58 of the power spectrum associated with our mode functions at the end of inflation:

$$\mathcal{P}_f(k) = \frac{k^3}{2\pi^2}|f_k|^2 \tag{6.38}$$

It is convenient to define the ratio:

$$\Pi_k(\tau) \equiv \frac{\mathcal{P}_k(\tau)}{\mathcal{P}_{k\to 0}(\tau)}\,, \tag{6.39}$$

which corresponds to the dimensionless ratio between the power spectra evaluated evaluated respectively at scale k and at very large scales $k \to 0$: this ratio goes to 1 for $k \to 0$, and makes more manifest the small-scale growth of the spectrum in scenarios with transient violation of slow-roll conditions.
At the end of inflation, when $\tau = 0$ it simply results

$$\Pi_k(\tau = 0) = |C_1(k) + C_2(k)|^2 \ . \tag{6.40}$$

Matching the solutions in the slow-roll (SR) and non-slow-roll (NSR) regimes at τ_2 using Israel junction conditions and substituting the values of $C_{1,2}$, we find that the spectrum of fluctuations exhibits distinctive features as a result of the slow-roll violation. These features are illustrated in the plot 6.1, for a specific choice of the NSR parameters.

We observe that the power spectrum initially follows the expected scaling $\propto (k/k_1)^2$, consistent with the behaviour of fluctuations deep in the slow-roll regime [15]. After this, we encounter the first key difference compared to the slow-roll case: the rise proportional to k^2 is followed by a pronounced dip, whose position and depth provide important information about the scale at which the spectrum starts to strongly deviate from the amplitude and scale dependence predicted in single-field slow-roll inflation.
Right after the dip, there is a sharp rise in power, and the spectrum begins to steadily increase as k grows. In this interval, the spectrum scales as $(k/k_1)^6$, peaking near the momentum scale $k \simeq k_1$, corresponding to modes that exited the horizon during the NSR phase.

The central parameter of the NSR epoch is α. Indeed, it controls the total growth of the spectrum: if we aim to gain several orders of magnitude in the amplitude of the spectrum with respect to its large-scale value, we need to choose a large value for the parameter α. Moreover, both the position and the depth of the dip also depend on it [104].
For even smaller scales ($k \gg k_1$), the growth rate of the spectrum gradually settles back to an average $(k/k_1)^2$ scaling. Strong oscillatory features at small scales result from the sudden transition

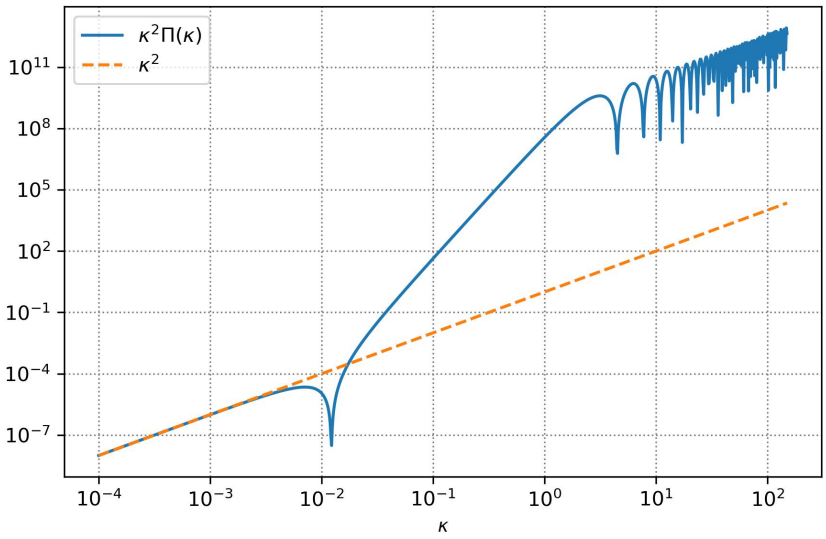

Figure 6.1: This plot displays the dimensionless power spectrum $\Pi(\kappa)$ of the longitudinal component of the vector field during inflation, plotted as a function of the dimensionless scale $\kappa = k/k_1$, where k_1 is the characteristic momentum defined in Eq. 6.42. The goal is to highlight the infrared modifications to the spectrum induced by a brief phase of non-slow-roll (NSR) evolution. The blue curve shows the resulting profile of the power spectrum for a representative value $\Pi_0 = 10^4$ (see the relation 6.44 for its definition), clearly exhibiting deviations from the standard slow-roll behavior at intermediate and small scales. Π_0 parameterizes the net growth of the power spectrum across scales during the NSR evolution. For comparison, the dashed orange line represents the baseline scaling $\propto \kappa^2$, corresponding to the case without NSR effects (i.e., $\Pi_0 = 0$). This comparison emphasizes how the NSR phase enhances the spectrum and introduces nontrivial scale dependence, especially in the infrared regime.

between the NSR and the final slow-roll phase; smoother transitions would likely suppress these oscillations.

Notably, the resulting spectrum exhibits characteristics reminiscent of models that enhance curvature perturbations for primordial black hole formation (see [105] for a comprehensive review). In particular, the time-dependent vector mass during the NSR phase injects energy into the longitudinal modes, triggering a rapid growth in the spectrum over an intermediate range of scales. The shift from a k^2 to a k^6 scaling in the infrared mirrors the maximal fourth-order enhancement seen in PBH scenarios [18, 20, 89, 90] , where such growth emerges from an initially nearly scale-invariant spectrum. Similarly, in our context, the spectrum can attain a maximal increase of four powers in momentum relative to the standard slow-roll case.

The intermediate $(k/k_1)^6$ growth phase is particularly significant for determining the final dark matter abundance sourced by longitudinal vector modes. Its presence introduces new parameters into the model, thereby expanding the phenomenologically relevant parameter space and opening potential connections with observable signatures, including those in gravitational wave physics.

6.2.1 Large α limit

In an idealized yet insightful limit, originally motivated by techniques introduced by 't Hooft [106], the analytical expressions simplify considerably. In order to see this, we have to turn out the attention on the slope parameter α. In many relevant scenarios, it temporarily exceeds unity during a brief stage of inflation. To gain analytical control over such dynamics, we can consider the regime where $\alpha \gg 1$, treating $1/\alpha$ as a small expansion parameter in a controlled perturbative framework [107]. This approach allows for significant simplification of the equations, enabling also to derive explicit analytic expressions for the two-point correlation functions of the perturbations.

The limit of large α we intend to explore exhibits an interesting analogy with the large-N limit of SU(N) QCD, as originally proposed by 't Hooft [106]. In that context, a $1/N$ expansion offers valuable insights into its dynamics. The large-N limit, taken alongside $g \to 0$ -with g the QCD coupling constant and N the number of colors- and helding $g^2 N$ finite, simplifies the theory while preserving key physical properties.
Similarly, in our scenario, it is useful to consider the limit of vanishing e-folds of NSR expansion $\Delta N_{\rm NSR} \to 0$ and to take the limit $\alpha \to \infty$, while keeping their product fixed. This combination controls the enhancement of the power spectrum across scales. In this regime, expanding in $1/\alpha$ leads to significant simplifications, allowing for analytic control over the n-point correlation functions.
In order to exploit this limit to our advantage, we consider the quantity $\Delta\tau/\tau_1$ to be infinitesimal, and simultaneously take the parameter α to be very large. This limiting procedure, as previously discussed, allows us to analytically capture the scale dependence of the power spectrum in a significantly simplified manner.
The time scale τ_1 denotes the moment at which the non-slow-roll phase occurs and serves as a reference for characterizing the onset of deviation from slow-roll dynamics.
Besides, it has a physical interpretation in terms of a (small) number $\Delta N_{\rm NSR}$ of e-folds of NSR evolution. Indeed:

$$\Delta N_{\rm NSR} = \ln\left(\frac{a(\tau_2)}{a(\tau_1)}\right) = \ln\left(\frac{\tau_1}{\tau_2}\right) = \ln\left(\frac{1}{1-\frac{\Delta\tau}{\tau_1}}\right) \simeq \frac{\Delta\tau}{\tau_1}, \tag{6.41}$$

where in the last equality we expanded for small $\frac{\Delta\tau}{\tau_1}$.

In order to work with this, we also define the pivot scale

$$k_1 = H_I a(\tau_1) = -\frac{1}{\tau_1}\ , \tag{6.42}$$

corresponding to the comoving wavenumber of modes leaving the horizon at the onset of the brief non-slow-roll era. We then express our formulas in terms of the dimensionless momentum scale:

$$\kappa \equiv k\tau_1 = \frac{k}{k_1}. \tag{6.43}$$

The expressions we use simplify with this notation, as we can easily identify modes with $\kappa \sim 1$ which cross the horizon at epochs corresponding to the NSR phase. From a physical perspective, this limiting regime permits the realization of a sufficient enhancement of the power spectrum, as

demonstrated in [107]. In particular, since we are operating within the domain $\Delta\tau/\tau_1 \ll 1$, the realization of such an enhancement necessitates a large value of α during the NSR phase. This amplification acquires particular significance in scenarios aimed at generating a substantial abundance of dark matter through primordial black hole formation, wherein a pronounced increase of the spectrum at small scales is required.

Under these conditions, the expression for the dimensionless power spectrum 6.39 simplifies considerably. Thus, we take the simultaneous limits:

$$\alpha \to \infty\,, \qquad \frac{|\tau_1 - \tau_2|}{|\tau_1|} \to 0\,, \qquad \text{keeping} \quad \frac{\alpha|\tau_1 - \tau_2|}{|\tau_1|} \equiv 2\Pi_0 \quad \text{finite}\,. \tag{6.44}$$

where Π_0 parameterizes the net growth of the power spectrum across scales. A value $\Pi_0 = 0$ corresponds to no enhancement.

Expanding in $1/\alpha$ at fixed Π_0, one finds, at leading order:

$$\Pi(\kappa) = 1 - 4\kappa\Pi_0 \cos\kappa\, j_1(\kappa) + 4\kappa^2\Pi_0^2\, j_1^2(\kappa)\,. \tag{6.45}$$

The function $j_1(\kappa)$ is the spherical Bessel function of the first kind:

$$j_1(\kappa) = \frac{\sin\kappa}{\kappa^2} - \frac{\cos\kappa}{\kappa}\,. \tag{6.46}$$

The dimensionless function Π_0 encodes the imprint of the non-slowroll phase, which -as explained above- we assume is making the vector mass changing rapidly during a small time interval.

Restoring all dimensionful quantities, we finally obtain the expression for the power spectrum of the longitudinal mode of the vector field after the non-slow-roll phase. The result reads:

$$\mathcal{P}^{(0)}_{A_L}(k) \;=\; \frac{H_I^2\, k^2}{4\pi^2 m^2}\,\Pi(\kappa) = \frac{H_I^2\, k^2}{4\pi^2 m^2}\,\Pi\left(\frac{k}{k_1}\right)\,. \tag{6.47}$$

This expression is the resulting power spectrum for the longitudinal mode of the vector field, when evaluated at the end of inflation, after a brief phase of non-slow-roll inflation during which the field mass $M(\tau)$ changed its value accordingly to 6.19. The function $\Pi(k)$ encapsulates both universal features of the spectrum -such as its infrared limit and the presence of a characteristic enhancement at small scales- as well as model-dependent details encoded in the duration and slope of the NSR phase. In particular, as discussed, the total amplification is governed by the combination $\Pi_0 \simeq \frac{\alpha\ \Delta\tau/\tau_1}{2}$, controlling the transition to NSR regime. This setup allows us to capture the key features of the power spectrum arising from a sudden, localized departure from slow-roll, controlled by the amplitude Π_0 and the scale k_1.

6.3 Evolution during Radiation Domination

During the radiation-dominated (RD) epoch that follows inflation, the large-scale longitudinal component of the vector field, A_L, re-enters the horizon and subsequently evolves. The behavior of this mode depends sensitively on its comoving momentum k. As we have already seen in Section 5.3.2, at a generic time $\tau \geq \tau_R$ within RD, the power spectrum of A_L is determined by a transfer function $\mathcal{T}(k\tau)$ and takes the form

$$\mathcal{P}_{A_L}(\tau, k) \;=\; \left|T(k\tau)\right|^2 \mathcal{P}^{(0)}_{A_L}(k)\,, \tag{6.48}$$

where $\mathcal{P}^{(0)}_{A_L}(k)$ denotes the primordial spectrum evaluated at the end of inflation, now incorporating the effects of the mass-varying phase, while $\mathcal{T}$ corresponds to the transfer function introduced in Section 5.3.2.

In the standard slow-roll framework of [15], the spectrum exhibits a turnover at a characteristic comoving scale $k_* \sim a_* M$, with M the vector mass and a_* the scale factor at the epoch defined by $H = M$. Our objective here is to explore how the presence of a transient non-slow-roll phase during inflation modifies this baseline prediction, with particular emphasis on the resulting deformation of the spectrum shape, as illustrated in Fig. 6.1.

For notational clarity, it is convenient to work again with the variables defined in 5.3.2. However, unlike before, we now have two distinct reference scales:

– τ_1, the time at which the non-slow-roll phase of inflation begins,

– τ_*, the time at which $H_* = m$, corresponding to the vector mass scale at the end of the NSR phase, which occurs during the radiation-dominated period.

It is then useful to define the following ratio:

$$\sigma = \frac{k_*}{k_1} = \frac{a_* H_*}{a_1 H_I} = \frac{a_*}{a(\tau_1)} \frac{m}{H_I}. \tag{6.49}$$

To explore the physical implications of the relevant scales, we first recall that the comoving momentum

$$k_1 = a(\tau_1) H_I = -\frac{1}{\tau_1} \tag{6.50}$$

marks the onset of the non-slow-roll phase during inflation. In contrast,

$$k_* = a_* m \tag{6.51}$$

defines the physical momentum at which the vector mass becomes dynamically relevant during radiation domination. Thus, σ measures the relative size of the two physical scales in the problem: the momentum scale k_1 associated with the onset of the non-slow-roll phase of inflation and the scale $k_\star$ where the vector mass effects become relevant in the radiation era.
In other words, σ quantifies how much the universe expands between these two events and how the characteristic momentum scales are separated. Thus, σ encodes the hierarchy between inflationary dynamics and post-inflationary vector physics, and it plays a central role in determining the evolution of the modes. This is made evident by the following illustrative cases:

Denoting by a_R the scale factor at the end of inflation, we have

$$\frac{a_R}{a_1} = e^{N_1}, \quad \text{with } N_1 \text{ the number of } e\text{-folds between } \tau_1 \text{ and the end of inflation,} \tag{6.52}$$

$$\frac{a_*}{a_R} = \frac{\tau_*}{\tau_R} = \left(\frac{H_I}{H_*}\right)^{1/2} = \left(\frac{H_I}{m}\right)^{1/2}. \tag{6.53}$$

Combining these expressions gives

$$\sigma = e^{N_1} \left(\frac{m}{H_I}\right)^{1/2}. \tag{6.54}$$

To illustrate typical values of σ, consider two examples:

- For $N_1 = 30$ e-folds before the end of inflation, $m = 10^{-19}$ eV and $H_I = 10^{14}$ GeV, we find $e^{30} \sim 10^{13}$ and $(m/H_I)^{1/2} \sim 10^{-21}$, giving $\sigma \sim 10^{-8}$, a negligible value.
- For $N_1 = 49$ e-folds before the end of inflation, $m = 10^{-19}$ eV, and $H_I = 10^{10}$ GeV, we obtain $e^{49} \sim 10^{21.2}$ and $(m/H_I)^{1/2} \sim 10^{-19}$, yielding $\sigma \sim 10^{2.2}$, a significantly large value.

Hence, depending on the inflationary history and the vector mass scale m, the parameter σ can vary over many orders of magnitude.

We can now re-express the power spectrum of Eq.6.48 using the dimensionless variable $x_* = k/k_*$, yielding

$$\mathcal{P}_{A_L}(x_*) = \left(\frac{H_I a_*}{2\pi}\right)^2 \left[x_*^2\, \Pi(\sigma x_*)\, |T_L(x_*)|^2\right], \tag{6.55}$$

where $\Pi(\sigma x_*)$ is defined in Eq.6.45 and explicitly is

$$\Pi(\sigma x_*) = 1 - 4\ \sigma x_* \cos(\sigma x_*) j_1(\sigma x_*)\Pi_0 + 4\ \sigma^2 x_*^2 j_1^2(\sigma x_*)\Pi_0^2\ , \tag{6.56}$$

showing its dependence on the parameters σ and Π_0, which contain the information on the NSR phase. The combination appearing in square brackets of Eq.6.55 is displayed in three panels of Fig. 6.2 and, notably, does not depend on m or H_I.

Besides clearly illustrating the effects of the non-slow-roll phase on the dip and subsequent rise of the spectrum, the plots also reveal a nontrivial interplay between the modification of the inflationary spectrum by $\Pi(\sigma x_*)$ and the influence of the transfer function $|T_L(x_*)|^2$. For sufficiently large Π_0, for instance $\Pi_0 = 10^4$ (a choice motivated by the applications discussed in Sections 6.4 and 6.5), the longitudinal spectrum develops a pronounced peak followed by a turnover whose position depends on the model parameters. Near this peak, the amplitude is substantially larger than in the slow-roll case ($\Pi_0 = 0$), indicating that the non-slow-roll phase efficiently amplifies the production of longitudinal vector modes. As discussed previously, deviations from slow-roll dynamics enhance the infrared part of the spectrum, accelerating its growth toward the peak.
The turnover scale appears to be particularly sensitive to the value of σ.

- When $\sigma \sim 1$, the turnover is close to the canonical scale $k \sim k_* = a_* m$, as in the standard slow-roll picture (Fig. 6.2, upper left panel);

- For $\sigma \ll 1$, however, the turnover shifts to much smaller scales ($k \gg k_*$), concentrating power at high k (Fig. 6.2, upper right panel);

- Conversely, when $\sigma \gg 1$, the turnover remains near $k \sim k_*$, but the spectrum grows more steeply at small k (Fig. 6.2, lower panel), suggesting that the contribution of short-wavelength modes can be significantly enhanced.

Overall, the plots in Fig. 6.2 clearly illustrate the dependence of the spectrum (6.55) on the parameters m, Π_0, and σ, pointing to a rich phenomenology that we explore in the following.

This behaviour distinguishes the scenario from others -such as models with nonstandard post-inflationary histories [26, 27] -where the spectral modifications occur primarily *after* the peak.

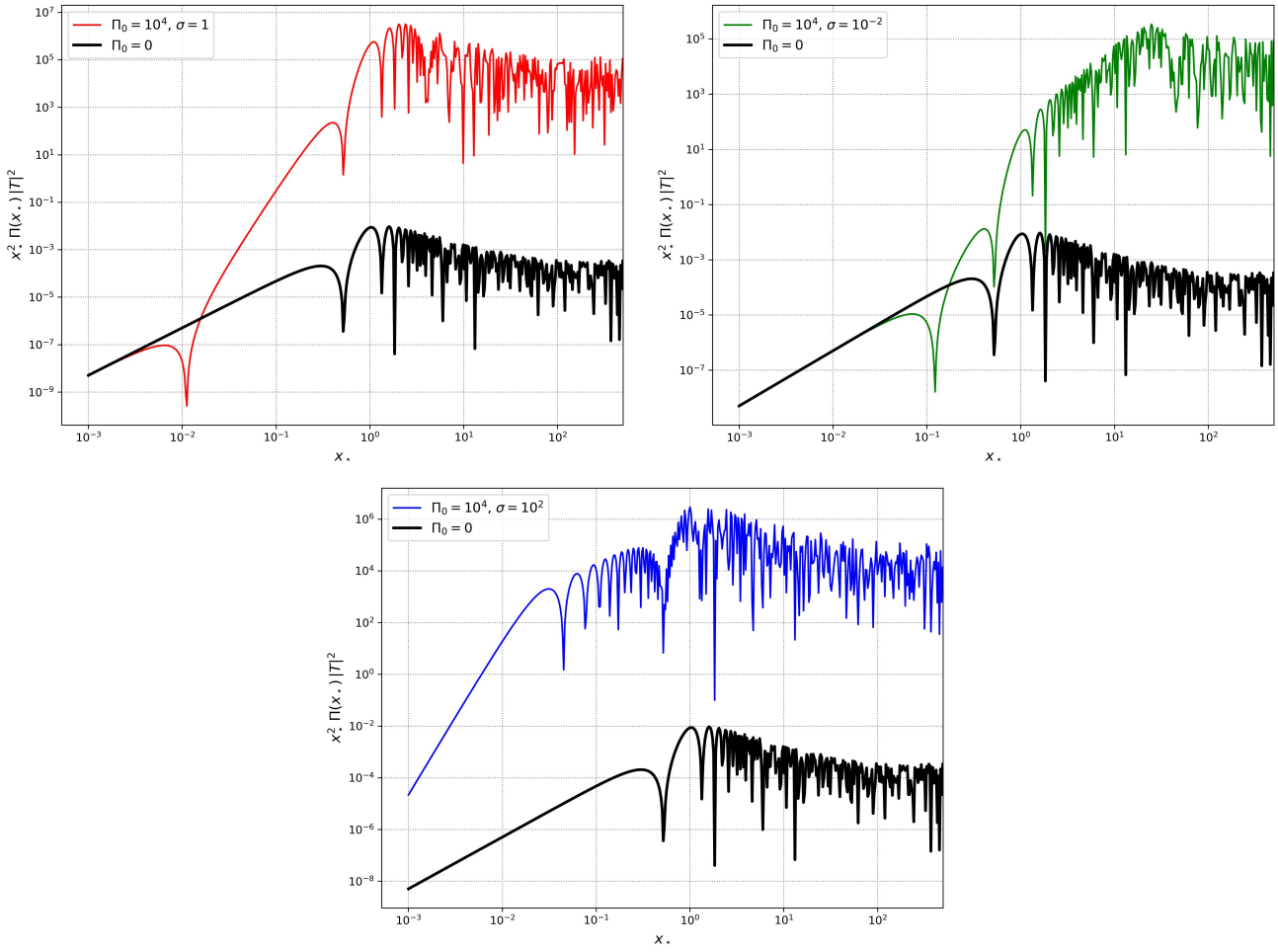

Figure 6.2: This series of plots shows the power spectrum $\mathcal{P}_{A_L}$ of the vector longitudinal mode, both during inflation and the radiation-dominated era, as a function of scale. The emphasis is on illustrating the impact in the infrared part of the spectrum of effects controlling a brief period of non-slowroll evolution during inflation. (See the main text for definitions of the parameters and further discussion.) The colored curves show the evolution of $\mathcal{P}_{A_L}$ during radiation domination for various values of the parameters Π_0 and σ, compared to the black line representing the standard profile in the absence of non-slowroll effects. Note that changes in the parameter σ affect both the position and shape of the spectral peak.

6.4 Longitudinal Energy Density and Dark Matter Abundance

Our goal is to investigate whether the longitudinal vector mode A_L can account for some or all of the dark matter observed in the universe. To this end, we calculate its present-day energy density relative to the measured dark matter abundance. We then analyze how this fraction varies across the parameter space of the model, paying particular attention to the influence of the non-slow-roll phase of inflation on determining the final dark matter density.

By using the same considerations presented in Section 5.6, we obtain that the energy density stored in the longitudinal vector modes is given by

$$\rho_{A_L} = \frac{1}{2a^2}\frac{a_*}{a}\left(\frac{k_* H_I}{2\pi}\right)^2 \left[\int d\ln k \left(\frac{k^2}{k_*^2(k^2+a^2m^2)}\frac{a}{a_*}|\partial_\tau T|^2 + \frac{k^2}{k_*^2}\frac{a}{a_*}|T|^2\right)\Pi(k\tau_1)\right] , \tag{6.57}$$

where the explicit oscillatory structure in the last factor $\Pi(k\tau_1)$ of the integrand arises from the non-slowroll transition at time τ_1 and correspondingly introduces a physical scale $k_1 = a(\tau_1)H_I$.

Computing the integral

We adopt a similar procedure to the one outlined in Section 5.6 to evaluate the integral that determines the dark matter abundance contributed by our vector boson of mass m. To do so, we express the integral in terms of the variables x_* and y and compute it at late times, $y_{\rm end}$, corresponding to a period well within radiation domination. This allows us to average over the rapid oscillations of the modes. The integral is then naturally split into two regions: $x_* < 1$ and $x_* > 1$, which correspond, respectively, to modes outside and inside the Hubble radius during radiation domination. Thus, the integral we need to evaluate is:

$$\begin{aligned}\mathcal{I}_\rho(y_{\rm end}) = y_{\rm end}\int_0^1 \frac{dx_*}{x_*}\left(\frac{x_*^2}{x_*^2+y_{\rm end}^2}|\partial_y T^{(A)}_{\rm late}|^2 + x_*^2|T^{(A)}_{\rm late}|^2\right)\Pi(\sigma x_*) \\ + y_{\rm end}\int_1^{y_{\rm end}} \frac{dx_*}{x_*}\left(\frac{x_*^2}{x_*^2+y_{\rm end}^2}|\partial_y T^{(B)}_{\rm late}|^2 + x_*^2|T^{(B)}_{\rm late}|^2\right)\Pi(\sigma x_*)\,.\end{aligned} \tag{6.58}$$

Each line of Eq.6.58 depends on the different solutions for the analytic transfer functions which apply in different regimes of y (see Appendix B for a description of the solutions).
In this case, the integral includes the modulation function, defined in Eq.6.45, which depends on the spherical Bessel function. It consists of three distinct contributions:

$$\Pi(\sigma x_*) = 1 - 4\ \sigma x_* \cos(\sigma x_*) j_1(\sigma x_*)\Pi_0 + 4\ \sigma^2 x_*^2 j_1^2(\sigma x_*)\Pi_0^2\,. \tag{6.59}$$

Of course, when $\Pi_0 = 0$, the integral of Eq. 5.47 is recovered. However, for non-zero Π_0, additional non-trivial contributions arise, characterized by oscillatory functions. To handle these terms efficiently, it is necessary to distinguish between the two integration regimes, allowing us to exploit the oscillatory nature of $\Pi(\sigma x_*)$ to our advantage.

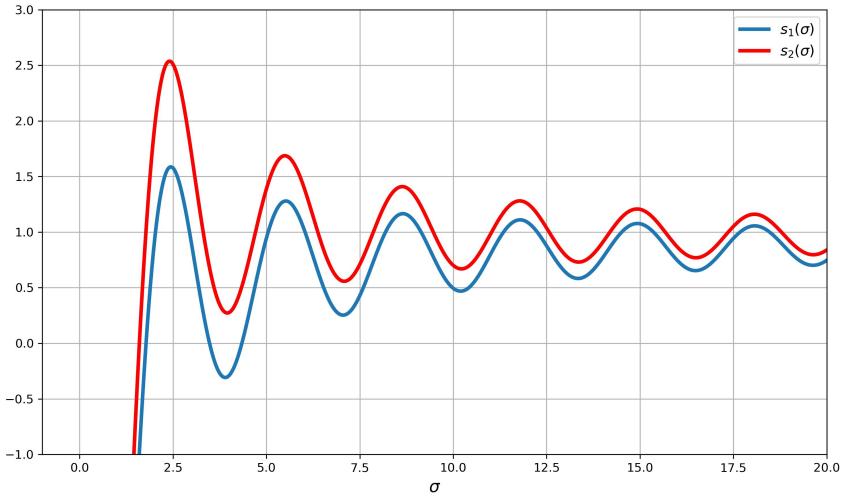

Figure 6.3: The functions $s_{1,2}(\sigma)$ defined in Eq. 6.60 exhibit oscillatory behavior, yet both converge to the same asymptotic value at large σ.

We first consider the contribution from the initial part of Eq. 6.58, which we denote by $\mathcal{I}^{(1)}$. In the limit of large $y_{\rm end}$, this term can be evaluated straightforwardly, giving

$$\mathcal{I}^{(1)} = 0.475883 + s_1(\sigma)\,\Pi_0 + s_2(\sigma)\,\Pi_0^2\,. \tag{6.60}$$

The functions $s_1(\sigma)$ and $s_2(\sigma)$ are lengthy and are reported in Appendix C. It is sufficient to note that both vanish as $\sigma \to 0$ and approach a common asymptotic value of approximately 0.95 for large σ, as shown in Fig. 6.3.

Next, we examine the second contribution of Eq. 6.58, which we denote $\mathcal{I}^{(2)}$. We rescale the integration variable via $z \equiv x_*/y_{\rm end}$. This transforms the lower limit $1/y_{\rm end}$ into a value sufficiently small to be approximated as zero. Moreover, the resulting integrand contains terms that oscillate rapidly over $0 \le z \le 1$, but these oscillations are suppressed by factors of $1/y_{\rm end}$ and average out to negligible contributions. After neglecting these terms, the remaining integral can be evaluated exactly, yielding

$$\mathcal{I}^{(2)} = 1.025\left[1 + 2\Pi_0 + \left(2 + \frac{0.685}{\sigma^2}\right)\Pi_0^2\right]\,. \tag{6.61}$$

We now collect the results obtained so far. The total integral in Eq. 6.58 is the sum of the two contributions previously evaluated,

$$\mathcal{I}_\rho = \mathcal{I}^{(1)} + \mathcal{I}^{(2)}\,, \tag{6.62}$$

and depends on both σ and Π_0.
In the limit of large σ, the expression for $\mathcal{I}_\rho$ simplifies considerably:

$$\mathcal{I}_\rho \simeq \frac{3}{2}\left(1 + 2\Pi_0 + 2\Pi_0^2\right)\,, \qquad \text{for large } \sigma\,. \tag{6.63}$$

The corresponding energy density of the longitudinal vector modes, which redshifts like matter, is

$$\rho_{A_L} = \frac{1}{2}\frac{a_*^3}{a^3}\left(\frac{mH_I}{2\pi}\right)^2 \mathcal{I}_\rho\,. \tag{6.64}$$

Evaluating this at matter-radiation equality and comparing with the total dark matter density as done in Section 5.6 [108],

$$\rho_{\rm DM} = \frac{3}{2} H_{\rm eq}^2 M_{\rm Pl}^2 \,, \quad H_{\rm eq} = 2.8 \times 10^{-28}\,{\rm eV}\,, \tag{6.65}$$

one obtains, in the large-σ regime, the ratio:

$$\frac{\rho_{A_L}}{\rho_{\rm DM}} = \frac{m^{1/2}}{3H_{\rm eq}^{1/2}} \left(\frac{H_I}{2\pi M_{\rm Pl}}\right)^2 \mathcal{I}_\rho \simeq \left(1 + 2\Pi_0 + 2\Pi_0^2\right) \left(\frac{m}{0.6 \times 10^{-6}\,{\rm eV}}\right)^{1/2} \left(\frac{H_I}{10^{14}\,{\rm GeV}}\right)^2 . \tag{6.66}$$

Hence, Eq. 6.66 provides a direct link between the energy density of longitudinal vector modes, ρ_{A_L}, and the observed dark matter density, $\rho_{\rm DM}$. This expression demonstrates a rich dependence on the model parameters; some important features are worth highlighting:

- **Dependence on the vector mass m:** The abundance scales as $m^{1/2}$, indicating that lighter vector masses require a higher inflationary Hubble scale or larger Π_0 to achieve the same contribution to the dark matter density. This scaling also emphasizes that the longitudinal modes behave as cold dark matter, redshifting as a^{-3} after production.
- **Role of the inflationary scale H_I:** The dependence on H_I^2 characterizes the efficiently of the mechanism at generating dark matter.
- **Impact of non-slow-roll dynamics (Π_0):** The factor $(1 + 2\Pi_0 + 2\Pi_0^2)$ captures the enhancement due to deviations from slow-roll during inflation. For $\Pi_0 \sim \mathcal{O}(1)$ or larger, the longitudinal mode production can be significantly amplified, showing that the inflationary dynamics have a direct effect on the final dark matter abundance.

Furthermore, Eq. 6.66 allows one to scan different combinations of (m, H_I, Π_0) to match the observed dark matter density. This highlights the flexibility of the model and provides guidance for identifying viable regions where the longitudinal vector could constitute all or part of the dark matter.

For instance:

- The combination $m = 1.5 \times 10^{-21}\,{\rm eV}$, $\quad H_I = 10^{14}\,{\rm GeV}$ and $\Pi_0^2 = 10^7$, reproduces the observed dark matter abundance;
- Alternatively, with $H_I = 5 \times 10^{13}\,{\rm GeV}$ while keeping the other parameters fixed, the longitudinal vector constitutes roughly 25% of the total dark matter.

Overall, then, Eq. 6.66 encapsulates the interplay between particle physics parameters and inflationary dynamics, providing a quantitative framework for assessing the feasibility of longitudinal vectors as dark matter candidates.

To conclude this section, we introduce a quantity that offers a detailed perspective on the distribution of energy density of the longitudinal vector mode across different momentum scales. We define the differential contribution, normalized to the total dark matter density, as

$$\frac{1}{\rho_{\rm DM}} \frac{d\rho_{A_L}}{d\ln k} \,. \tag{6.67}$$

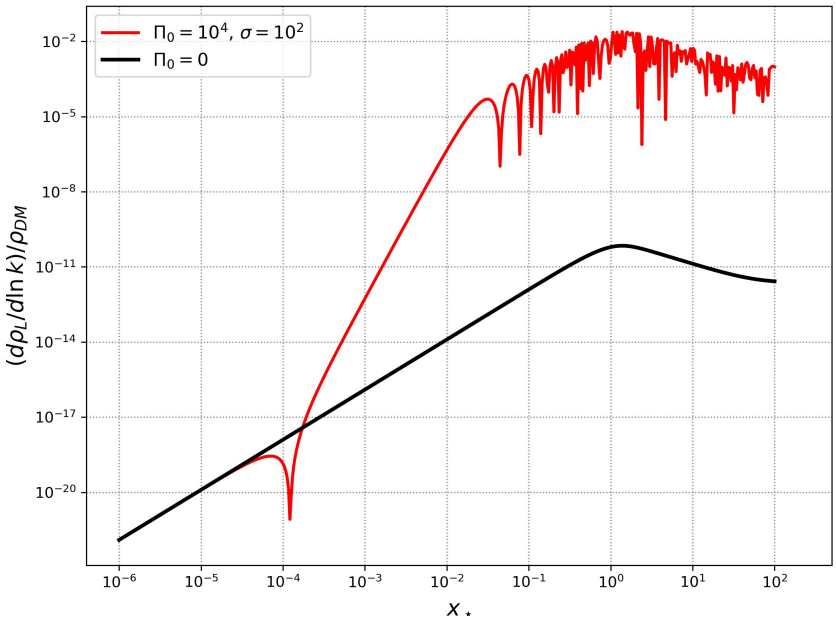

Figure 6.4: Differential energy density 6.67 as a function of momentum scale, shown for a representative vector mass $m = 1.5 \times 10^{-19}\,\mathrm{eV}$ and an inflationary Hubble scale $H_I = 10^{14}\,\mathrm{GeV}$. The parameters σ and Π_0, which characterize the non-slow-roll dynamics during inflation, play a key role in enhancing the peak amplitude.

This function quantifies the energy density contributed per logarithmic interval of momentum. Integrating it over the full range of momenta reproduces the total density ratio presented in Eq. 6.66. Before integration, however, it provides valuable insight into the relative importance of different modes and highlights scale-dependent features of the production process.

Fig. 6.4 illustrates this distribution. It is evident that the short non-slow-roll phase during inflation has a pronounced impact on the infrared portion of the spectrum, precisely in the region where the energy density grows. This modification indicates that the departure from slow-roll dynamics selectively amplifies certain momentum modes, leaving a distinct imprint on the shape of the spectrum.

6.5 Phenomenological implications

The mechanism for generating longitudinal vector dark matter during inflation, as outlined in the previous sections, leads to a number of distinctive outcomes.

First, the resulting spectrum of longitudinal modes is highly suppressed on cosmological scales, thereby remaining consistent with constraints from cosmic microwave background measurements. At the same time, the spectrum grows toward smaller scales, with a pronounced peak whose amplitude and position are controlled by the underlying parameters: the vector mass m and the quantities σ and Π_0 that encode the short departure from slow-roll dynamics. The low-

momentum region of the spectrum is particularly sensitive to this non-slow-roll phase, which leaves a characteristic imprint on its shape.

A noteworthy feature of this scenario is that it enables the efficient inflationary production of ultralight vector dark matter, with masses as small as $m \lesssim 10^{-19}\,\mathrm{eV}$, while still producing an energy density compatible with the observed dark matter abundance. Such ultralight dark matter candidates are phenomenologically attractive: their wave-like nature modifies the clustering of matter on small scales, providing a potential avenue to address tensions in conventional cold dark matter cosmology. Several recent analyses [109, 110] place bounds on the mass of generic ultralight dark matter if it accounts for the entire dark matter component and extensive reviews are available in [22, 51]. In the case where the dark matter takes the form of a dark photon, kinetic mixing with Standard Model particles introduces additional phenomenological opportunities, as discussed in [83]. From this perspective, our framework provides a novel route for producing ultralight dark matter directly from the dynamics of inflation.

Furthermore, the transition from a k^2 to a k^6 scaling in the infrared part of the spectrum is reminiscent of the maximal fourth-order enhancement identified in primordial black hole scenarios [18, 20], where it emerges from an initially nearly scale-invariant spectrum. Analogously, in our case we find that the spectrum can increase by at most four powers of momentum relative to its slow-roll behavior.

Beyond the direct abundance, the relation 6.66 has implications for experimental searches and cosmological observables. For example, ultralight masses $m \lesssim 10^{-21}\,\mathrm{eV}$ could give rise to observable features in structure formation or in the stochastic gravitational wave background.
In fact, the departure from slow-roll dynamics during inflation not only enhances the spectrum of longitudinal vector modes, but also has important implications for gravitational wave production. In particular, the amplification of these modes is expected to substantially increase the resulting gravitational wave background, potentially bringing its amplitude within the reach of forthcoming observational facilities.

In order to probe effects of spacetime deformations associated with vector degrees of freedom, is it possible to use stochastic gravitation wave backgrounds (SGWB) produced at second order in perturbations by isocurvature fluctuations. The subject of scalar-induced SGWB by adiabatic fluctuations is very well developed by now (see [111–117] and the comprehensive review [50]). Much less studied are SGWB induced by isocurvature modes -the case relevant for us since we study vector longitudinal modes corresponding to iso-curvature fluctuations. However, it has been demonstrated that, similar to the well studied adiabatic case, a peaked spectrum of longitudinal iso-curvature modes (with a maximum at scale k_*), enhanced to the non-slowroll phase, is expected to significantly boost the generation of gravitational waves- potentially to an amplitude detectable by future experiments. In particular, the amplitude of the gravitational wave spectrum increases with the parameter Π_0. Since a large value of Π_0 is permitted in the regime of small vector mass, ultralight dark matter is particularly relevant for our purposes [98].

6.5.1 Ultralight Dark Matter and Primordial Black Holes

An intriguing feature of this framework is its potential ability to simultaneously generate both longitudinal vector dark matter and primordial black holes, offering a unified mechanism for producing a two-component dark matter model from a common inflationary source.

The common ingredient is the brief violation of slow-roll conditions during inflation. While our analysis has focused on how this non-slow-roll phase induces rapid variations in the effective vector mass -leading to enhanced production of longitudinal modes-, the same mechanism also amplifies adiabatic curvature perturbations. These enhanced perturbations can, in turn, collapse into primordial black holes during the radiation-dominated era.

This opens the possibility of a mixed dark matter scenario, composed of both ultralight vector modes and primordial black holes, with the black hole mass spectrum determined by the properties of the non-slow-roll phase. Such a framework may help evade stringent observational constraints that arise when each dark matter candidate is considered in isolation. In addition, it predicts a gravitational wave background with a bimodal structure, featuring two distinct peaks at different frequencies -one sourced by amplified isocurvature fluctuations and the other by amplified adiabatic perturbations.

Chapter 7

Conclusions

In this work we have presented a new framework for the generation of ultralight vector dark matter during inflation. The central ingredient is a temporary departure from slow-roll dynamics, which we modeled as a brief non-slow-roll (NSR) phase. When the mass of the vector field depends on the inflaton velocity, the large time derivatives of the inflaton during this epoch induce rapid variations of the effective mass. As a consequence, the infrared behavior of the longitudinal spectrum is dramatically modified: instead of the k^2 scaling typical of slow-roll inflation, we find a much steeper k^6 growth.
This modification has noteworthy consequences. Thanks to the NSR phase, the power spectrum is strongly amplified, and the enhancement opens up new regions of parameter space that would otherwise be excluded in the standard slow-roll setup. In particular, it allows the vector field mass to be as small as

$$m \lesssim 10^{-19}\ \text{eV}\,,$$

while still accounting for a sizeable fraction of the observed dark matter abundance in the form of longitudinal vector bosons. Moreover, the same dynamics responsible for this enhancement can also leave imprints in complementary observables. The steepened small-scale spectrum acts as a source of scalar-induced gravitational waves at second order, generating a stochastic background of potentially detectable amplitude. In addition, the interplay between the NSR-induced growth and the breaking of conformal invariance by the longitudinal modes points to intriguing possibilities for a unified inflationary origin of multiple relics: ultralight vector dark matter and primordial black holes.

We first motivated our study by focusing our attention on a novel mechanism for producing dark matter, which has attracted growing interest in recent years: inflation provides a minimal and elegant mechanism for dark matter production, since quantum fluctuations during the primordial epoch can naturally seed relic abundances without requiring additional post-inflationary dynamics. Inflation naturally provides the conditions for generating dark matter as a consequence of quantum fluctuations in the primordial universe. We emphasize that this represents a refined and self-contained production mechanism: it does not rely on additional assumptions beyond the inflationary dynamics itself and the presence of a massive field.

In this respect, vector fields stand out as particularly promising candidates. Unlike scalars or tensors, whose nearly scale-invariant spectra are tightly constrained by CMB data, we have seen

that a massive vector acquires a distinctive peaked spectrum around a characteristic scale k_* and the CMB constraints are not restrictive because they primarily affect much larger scales. Moreover, the massive vector field is particularly appealing because its longitudinal degree of freedom breaks conformal invariance, ensuring an efficient population of the mode which can account for the dark matter density, and the generation of a significant dark matter abundance. We thus computed the energy density of the vector candidate and recovered the results of [15], indicating that for standard slow-roll dynamics a viable mass scale is $m \sim 10^{-6}\,\mathrm{eV}$.

We then explored how this prediction is modified in the presence of non-standard inflationary dynamics. While earlier works have focused on the effects of reheating on the relic abundance, our goal was instead to investigate departures from slow-roll *during* inflation itself. Motivated by studies of primordial black hole formation, which require NSR phases to trigger the large amplification of fluctuations needed for collapse, we asked whether a similar mechanism could affect the production of ultralight vector dark matter. Remarkably, we found that the enhancement induced by the NSR epoch modifies the spectrum in an analogous way: both in the PBH case and in our setup the growth is steep, scaling as k^4. This parallel opens the possibility of a common inflationary origin for both ultralight vector dark matter and PBHs.

To analyze this setup, we relied on the analytical approach developed in [104], based on a gradient expansion for cosmological perturbations during brief NSR phases. At leading order in the small parameter controlling the NSR duration, we solved the equations of motion exactly, yielding compact expressions for the mode functions. These depend only on the slope α of the pump field during the NSR interval and on the timescale $\Delta\tau$ of the departure from slow-roll. In particular, these parameters fully determine the overall amplification and the scale dependence of the fluctuation spectrum, controlling how the spectrum interpolates between large and small momentum modes. The resulting power spectra reproduce a transient dip, and a region of rapid growth toward small scales. These properties closely match what has been observed in detailed numerical studies of concrete inflationary scenarios with brief non-slowroll periods.

We then supposed that such a scenario could be obtained by considering a time-dependent mass M, whose mass changes rapidly in a very short period of time $\Delta\tau$. This approach is powerful because it does not require to explicitly specify how the mass changes to see how the mode functions evolve during the NSR phase; we just need to match the solutions at the end of the NSR phase with the standard slow-roll inflationary solution in order to delineate a spectrum which describes the consequences of adding a non-slow-roll phase. This procedure allows us to construct a spectrum that reflects the impact of including a brief non-slow-roll period.

It is important to emphasize that the mechanism we propose differs fundamentally from the conventional misalignment scenario for producing ultralight dark matter. In our framework, the relic abundance is generated directly during inflation through the dynamics of the longitudinal vector modes, without relying on the oscillations of a background field around its potential minimum: the dark matter abundance is produced directly by the inflationary dynamics of longitudinal modes.

Moreover, as we have already emphasized, an intriguing aspect of this framework is its potential to simultaneously generate both longitudinal vector dark matter and primordial black holes, thereby offering a unified mechanism for producing a two-component dark matter model.

A second key implication is that this mechanism significantly amplifies the small-scale spectrum, which in turn drives the production of scalar-induced gravitational waves. Indeed, the rapid growth at small scales naturally generates a stochastic background of gravitational waves with a potentially observable amplitude. These waves are produced at second order in perturbation theory and are sourced by the enhanced small-scale vector spectrum. The predicted signal peaks at ultra-low frequencies, $f \sim 10^{-15}$–10^{-13} Hz [98], outside the range of pulsar timing arrays but possibly accessible through alternative probes such as galaxy shape correlations and intrinsic alignments. This constitutes a distinctive observational signature of our framework, testable even if dark matter interacts with the Standard Model only gravitationally.

In conclusion, the scenario we developed shows that a short NSR phase during inflation is a valuable mechanism for the production of ultra-light dark matter vector bosons, which could account for the abundance of dark matter in our universe. Moreover, this framework simultaneously enhance the production of ultralight vector dark matter and generate observable relics such as PBHs and a stochastic gravitational wave background. This opens up the intriguing possibility of a unified inflationary origin for multiple dark components of the universe.

The question of what dark matter is and how it can be produced is still open and astonishingly interesting. The work presented in this thesis is intended to contribute to the growing body of knowledge in this area, providing a foundation for future investigations, collaborations and potential breakthroughs. Several directions remain open for future research: identifying explicit realizations of this ultralight vector dark matter scenario, potentially within extensions of the Standard Model that accommodate very light vector bosons, refining the predictions for PBH abundances and exploring novel detection strategies for ultra-low-frequency gravitational waves. We leave these questions to forthcoming work.

By continuing to push the boundaries of our understanding, we take meaningful steps toward unrevealing the fundamental mysteries of the universe -shedding light on the hidden dynamics of the primordial cosmos and opening new pathways for discovery at the frontiers of cosmology and high-energy physics. In this pursuit, we do not merely seek answers, but participate in the timeless human endeavour to comprehend the grand design of nature itself.

We look forward, searching for a light within the darkness of the primordial universe, hoping that this will bring us closer to understanding the true nature of our origin.

Appendix A

Action of the Massive Vector Boson in terms of transversal and longitudinal modes

In this Appendix, we present a reformulation of the action 5.3, expressed in terms of the transverse and longitudinal components of the vector field A_μ. This decomposition is useful as it separates the physical degrees of freedom from the remaining components, thereby providing a clearer understanding of the underlying dynamics and simplifying the subsequent analysis. In this way, we recover Eq. 5.6.
We start from the action

$$S = \int d^4x \, \sqrt{-g} \left(-\frac{1}{4} F_{\mu\nu} F^{\mu\nu} - M^2 A_\mu A^\mu \right) \, . \tag{A.1}$$

Here,

$$F_{\mu\nu} = \partial_\mu A_\nu - \partial_\nu A_\mu \, , \tag{A.2}$$

$$A_\mu = \left(A_0, \, \partial_i \varphi + A_i^T \right) \quad , \tag{A.3}$$

and

$$A_i = A_i^{\mathrm{T}} + \partial_i \varphi \, , \qquad \text{with} \qquad \partial_i A_i^{\mathrm{T}} = 0 \, . \tag{A.4}$$

Furthermore, we work in a FWR spacetime:

$$ds^2 = a^2(\tau) \left(-d\tau^2 + \delta_{ij} dx^i dx^j \right) \, . \tag{A.5}$$

We first evaluate the field strength component. Starting from:

$$F_{\mu\nu} F^{\mu\nu} = F_{\mu\nu} g^{\mu\alpha} g^{\nu\beta} F_{\alpha\beta} \tag{A.6}$$

we obtain:

$$\begin{aligned} F_{0i} F^{0i} &= -\frac{1}{a^4} F_{0i} F_{0i} \, , \\ F_{ij} F^{ij} &= \frac{1}{a^4} F_{ij} F_{ij} \, . \end{aligned} \tag{A.7}$$

Thus:

$$F_{\mu\nu} F^{\mu\nu} = \frac{2}{a^4} \left(-F_{0i} F_{0i} + \frac{1}{2} F_{ij} F_{ij} \right) \, . \tag{A.8}$$

We now write the latter in terms of the transversal and longitudinal components, by expressing:

$$F_{0i}F_{0i} = A_i^{T'^2} - A_0\nabla^2 A_0 - \varphi'\nabla^2\varphi' + 2A_0\nabla^2\varphi' \ , \tag{A.9}$$

$$F_{ij}F_{ij} = -2A_i^T\nabla^2 A_i^T \ . \tag{A.10}$$

Therefore, the first piece of the integral is:

$$S_{EM} = -\frac{1}{4}\int d^4x\sqrt{-g}\ F_{\mu\nu}F^{\mu\nu} \tag{A.11}$$

$$= \frac{1}{2}\int d^4x\left[A_i^{\mathrm{T}\prime}A_i^{\mathrm{T}\prime} + A_i^{\mathrm{T}}\Delta A_i^{\mathrm{T}} + 2A_0\Delta\varphi' - A_0\,\Delta A_0 - \varphi'\,\Delta\varphi\right] \ . \tag{A.12}$$

On the other hand, the mass term gives the contribution:

$$M^2A_\mu A^\mu = M^2g^{\mu\nu}A_\mu A_\nu = -\frac{M^2}{a^2}A_0^2 + \frac{M^2}{a^2}(A_i^TA_i^T - \varphi\nabla^2\varphi) \ . \tag{A.13}$$

Thus,

$$S_{mass} = \frac{1}{2}\int d^4x\ M^2a^2\Big(A_0^2 + \varphi\,\Delta\varphi - A_i^{\mathrm{T}}A_i^{\mathrm{T}}\Big) \ . \tag{A.14}$$

Bringing everything together:

$$S = \frac{1}{2}\int d^4x\left[A_i^{\mathrm{T}\prime}A_i^{\mathrm{T}\prime} + A_i^{\mathrm{T}}\Delta A_i^{\mathrm{T}} + 2A_0\,\Delta\varphi' - A_0\,\Delta A_0 - \varphi'\,\Delta\varphi' + M^2a^2\Big(A_0^2 + \varphi\,\Delta\varphi - A_i^{\mathrm{T}}A_i^{\mathrm{T}}\Big)\right] \tag{A.15}$$

which is Eq. 5.6.

Appendix B

Analytical solutions of Eq.5.37

The evolution equation for for the transfer functions $\mathcal{T}$ during RD has analytical solutions for *small* y and *large* y, which can be approximate as follow, if we work in the two regimes $x_* \ll 1$ and $x_* \gg 1$ [95]:

1. Range $x_* \ll 1$:

$$T_{\rm early} = \frac{\sin(x_* y)}{x_* y}, \quad \text{valid for } y \ll 1, \tag{B.1}$$

$$T^{(A)}_{\rm late} = \frac{1}{\sqrt{y}}\left[c_1^A \cos\left(\frac{y^2}{2}\right) + c_2^A \sin\left(\frac{y^2}{2}\right)\right], \quad \text{valid for } y \gg 1, \tag{B.2}$$

with

$$c_1^A = -\sin(1/2)\cos x_\star + \left(\cos(1/2) + \frac{1}{2}\sin(1/2)\right)\frac{\sin x_\star}{x_\star}, \tag{B.3}$$

$$c_2^A = \cos(1/2)\cos x_\star + \left(\sin(1/2) - \frac{1}{2}\cos(1/2)\right)\frac{\sin x_\star}{x_\star}. \tag{B.4}$$

2. Range $x_* \gg 1$:

$$T_{\rm early} = \frac{\sin(x_* y)}{x_* y}, \quad \text{valid for } y \ll x_*, \tag{B.5}$$

$$T^{(B)}_{\rm late} = \frac{1}{\sqrt{y}}\left[c_1^B \cos\left(\frac{y^2}{2}\right) + c_2^B \sin\left(\frac{y^2}{2}\right)\right], \quad \text{valid for } y \gg x_*, \tag{B.6}$$

with

$$c_1^B \simeq \frac{\sin(x_*^2/2)}{x_*^{3/2}}\left(1 + \frac{\sin x_*^2}{2x_*^2}\right), \tag{B.7}$$

$$c_2^B \simeq \frac{\cos(x_*^2/2)}{x_*^{3/2}}\left(1 - \frac{\sin x_*^2}{2x_*^2}\right). \tag{B.8}$$

The choice of y-independent coefficients $c_{1,2}^{A/B}$ ensures that the analytic approximation for $\mathcal{T}$, together with its derivative $\frac{\partial \mathcal{T}}{\partial y}$, remains continuous across these transition boundaries.
An extension of the domain of validity of these expressions to include the transition regions at $y = 1$ and $x_* = 1$, can be obtained by replacing the strict inequalities $\ll$ and $\gg$ with the relaxed bounds $\leq$ and $\geq$, respectively.

Appendix C

The values of s_1 and s_2 in Eq. 6.60

In this Appendix we provide the explicit expressions for the functions $s_1(\sigma)$ and $s_2(\sigma)$ appearing in Eq. (6.60). Here, Ci denotes the cosine integral function and γ_E is the Euler–Mascheroni constant.

$$
\begin{aligned}
s_1(\sigma) = \frac{1}{16\sigma^2(\sigma^2-1)^2}\Bigg[& 4\Big(-3+\sigma^2\big(4+5\gamma_E(\sigma^2-1)^2-\sigma^2(2+\sigma^2)\big)+3\cos(2\sigma) \\
& +\sigma\Big(\sigma\big(-6+\cos(2)+\sigma^2(3+\cos(2))\big)\cos(2\sigma) \\
& \quad +(\sigma^2-1)^2\big(-6\,\mathrm{ArcCoth}(\sigma)+3\sigma\cos(2)-5\sigma\,\mathrm{Ci}(2)\big)\Big)\Big) \\
& +2\sigma\Big[-4\sigma(\sigma^2-1)\cos(2\sigma)\sin(2) \\
& \quad +(\sigma^2-1)^2\Big((-6+5\sigma)\,\mathrm{Ci}(2(1-\sigma))+6\,\mathrm{Ci}(2(1+\sigma)) \\
& \qquad +\sigma\big(-10\,\mathrm{Ci}(2\sigma)+5\,\mathrm{Ci}(2(1+\sigma))+\log(1024)+10\log(\sigma)-5\log(\sigma^2-1)+4\sin(2)\big)\Big)\Big] \\
& -2\big[(\sigma^2-1)(7-5\cos(2)+\sigma^2(-7+3\cos(2)))+2(1-3\sigma^2+\sigma^4)\sin(2)\big]\sin(2\sigma)\Bigg],
\end{aligned}
\tag{C.1}
$$

$$
\begin{aligned}
s_2(\sigma) = \frac{1}{8\sigma^2(1-\sigma^2)^2}\Bigg[& -15+30\sigma^2-17\sigma^4-2\sigma^6+2\gamma_E(1-\sigma^2)^2(4+5\sigma^2) \\
& +(1-\sigma^2)^2(5+6\sigma^2)\cos(2)+\big(15(1-\sigma^2)^2+(-5+8\sigma^2+\sigma^4)\cos(2)\big)\cos(2\sigma) \\
& +12\,\mathrm{Ci}(2)-2\sigma^2(17-16\sigma^2+5\sigma^4)\mathrm{Ci}(2) \\
& +(1-\sigma^2)^2(-6+5\sigma^2)\mathrm{Ci}(2(1-\sigma))-2(1-\sigma^2)^2(4+5\sigma^2)\mathrm{Ci}(2\sigma) \\
& -6\,\mathrm{Ci}(2(1+\sigma))+\log(256)+8\log(\sigma)+6\log(1-\sigma^2)-2\sin(2)-2(1-\sigma^4)\cos(2\sigma)\sin(2) \\
& +\sigma^2\Big[(17-16\sigma^2+5\sigma^4)\mathrm{Ci}(2(1+\sigma))+2(-3-6\sigma^2+5\sigma^4)\log(2\sigma) \\
& \quad +(-17+16\sigma^2-5\sigma^4)\log(1-\sigma^2)+2(4-5\sigma^2+2\sigma^4)\sin(2)\Big] \\
& -2\sigma\big[(1-\sigma^2)(7-5\cos(2)+\sigma^2(-7+3\cos(2)))+2(2-4\sigma^2+\sigma^4)\sin(2)\big]\sin(2\sigma)\Bigg].
\end{aligned}
\tag{C.2}
$$

These functions vanish in the limit $\sigma \to 0$, and for $\sigma \to \infty$ they asymptote to a constant, as shown in the left panel of Fig. 6.3.

References

[1] Andrew R. Liddle and D. H. Lyth. *Cosmological inflation and large scale structure*. 2000.

[2] Edward W. Kolb and Michael S. Turner. *The Early Universe*, volume 69. Taylor and Francis, 5 2019.

[3] Vera C. Rubin and W. Kent Ford, Jr. Rotation of the Andromeda Nebula from a Spectroscopic Survey of Emission Regions. , 159:379, February 1970.

[4] K. C. Freeman. On the Disks of Spiral and S0 Galaxies. , 160:811, June 1970.

[5] Heinz Andernach and Fritz Zwicky. English and spanish translation of zwicky's (1933) the redshift of extragalactic nebulae, 2017.

[6] F. Zwicky. Nebulae as gravitational lenses. *Phys. Rev.*, 51:290, 1937.

[7] C. L. Bennett, D. Larson, J. L. Weiland, N. Jarosik, G. Hinshaw, N. Odegard, K. M. Smith, R. S. Hill, B. Gold, M. Halpern, E. Komatsu, M. R. Nolta, L. Page, D. N. Spergel, E. Wollack, J. Dunkley, A. Kogut, M. Limon, S. S. Meyer, G. S. Tucker, and E. L. Wright. Nine-year wilkinson microwave anisotropy probe (wmap) observations: Final maps and results. *The Astrophysical Journal Supplement Series*, 208(2):20, September 2013.

[8] Henk Hoekstra, H. K. C. Yee, and Michael D. Gladders. Properties of Galaxy Dark Matter Halos from Weak Lensing. , 606(1):67–77, May 2004.

[9] Douglas Clowe, Maruša Bradač, Anthony H. Gonzalez, Maxim Markevitch, Scott W. Randall, Christine Jones, and Dennis Zaritsky. A direct empirical proof of the existence of dark matter*. *The Astrophysical Journal*, 648(2):L109, aug 2006.

[10] Gianfranco Bertone, Dan Hooper, and Joseph Silk. Particle dark matter: Evidence, candidates and constraints. *Phys. Rept.*, 405:279–390, 2005.

[11] Jonathan L. Feng. Dark Matter Candidates from Particle Physics and Methods of Detection. *Ann. Rev. Astron. Astrophys.*, 48:495–545, 2010.

[12] Daniel Baumann. Tasi lectures on primordial cosmology, 2018.

[13] Daniel Baumann. Tasi lectures on inflation, 2012.

[14] Antonio Riotto. Inflation and the theory of cosmological perturbations, 2017.

[15] Peter W. Graham, Jeremy Mardon, and Surjeet Rajendran. Vector Dark Matter from Inflationary Fluctuations. *Phys. Rev. D*, 93(10):103520, 2016.

[16] Andrei Linde. Particle physics and inflationary cosmology, 2005.

[17] L. H. Ford. Gravitational Particle Creation and Inflation. *Phys. Rev. D*, 35:2955, 1987.

[18] Ogan Özsoy and Gianmassimo Tasinato. On the slope of the curvature power spectrum in non-attractor inflation. *JCAP*, 04:048, 2020.

[19] Pedro Carrilho, Karim A. Malik, and David J. Mulryne. Dissecting the growth of the power spectrum for primordial black holes. 2019.

[20] Christian T. Byrnes, Philippa S. Cole, and Subodh P. Patil. Steepest growth of the power spectrum and primordial black holes. *JCAP*, 06:028, 2019.

[21] Elisa G. M. Ferreira. Ultra-light dark matter. *The Astronomy and Astrophysics Review*, 29(1), September 2021.

[22] Andrew Eberhardt and Elisa G. M. Ferreira. Ultralight fuzzy dark matter review. 7 2025.

[23] Mar Bastero-Gil, Jose Santiago, Lorenzo Ubaldi, and Roberto Vega-Morales. Vector dark matter production at the end of inflation. *JCAP*, 04:015, 2019.

[24] Yohei Ema, Kazunori Nakayama, and Yong Tang. Production of purely gravitational dark matter: the case of fermion and vector boson. *JHEP*, 07:060, 2019.

[25] Yuichiro Nakai, Ryo Namba, and Ziwei Wang. Light Dark Photon Dark Matter from Inflation. *JHEP*, 12:170, 2020.

[26] Aqeel Ahmed, Bohdan Grzadkowski, and Anna Socha. Gravitational production of vector dark matter. *JHEP*, 08:059, 2020.

[27] Edward W. Kolb and Andrew J. Long. Completely dark photons from gravitational particle production during the inflationary era. *JHEP*, 03:283, 2021.

[28] Borna Salehian, Mohammad Ali Gorji, Hassan Firouzjahi, and Shinji Mukohyama. Vector dark matter production from inflation with symmetry breaking. *Phys. Rev. D*, 103(6):063526, 2021.

[29] Takeo Moroi and Wen Yin. Light Dark Matter from Inflaton Decay. *JHEP*, 03:301, 2021.

[30] Asimina Arvanitaki, Savas Dimopoulos, Marios Galanis, Davide Racco, Olivier Simon, and Jedidiah O. Thompson. Dark QED from inflation. *JHEP*, 11:106, 2021.

[31] Takanori Sato, Fuminobu Takahashi, and Masaki Yamada. Gravitational production of dark photon dark matter with mass generated by the Higgs mechanism. *JCAP*, 08(08):022, 2022.

[32] Basabendu Barman, Nicolás Bernal, Ashmita Das, and Rishav Roshan. Non-minimally coupled vector boson dark matter. *JCAP*, 01(01):047, 2022.

[33] Michele Redi and Andrea Tesi. Dark photon Dark Matter without Stueckelberg mass. *JHEP*, 10:167, 2022.

[34] Ogan Özsoy and Gianmassimo Tasinato. Vector dark matter, inflation, and non-minimal couplings with gravity. *JCAP*, 06:003, 2024.

[35] Haipeng An, Maxim Pospelov, Josef Pradler, and Adam Ritz. Direct Detection Constraints on Dark Photon Dark Matter. *Phys. Lett. B*, 747:331–338, 2015.

[36] Samuel D. McDermott and Samuel J. Witte. Cosmological evolution of light dark photon dark matter. *Phys. Rev. D*, 101(6):063030, 2020.

[37] Vincent S. H. Lee, Andrea Mitridate, Tanner Trickle, and Kathryn M. Zurek. Probing Small-Scale Power Spectra with Pulsar Timing Arrays. *JHEP*, 06:028, 2021.

[38] Mustafa A. Amin, Mudit Jain, Rohith Karur, and Philip Mocz. Small-scale structure in vector dark matter. *JCAP*, 08(08):014, 2022.

[39] Nils Siemonsen, Cristina Mondino, Daniel Egana-Ugrinovic, Junwu Huang, Masha Baryakhtar, and William E. East. Dark photon superradiance: Electrodynamics and multi-messenger signals. *Phys. Rev. D*, 107(7):075025, 2023.

[40] William E. East. Vortex String Formation in Black Hole Superradiance of a Dark Photon with the Higgs Mechanism. *Phys. Rev. Lett.*, 129(14):141103, 2022.

[41] Aaron Pierce, Keith Riles, and Yue Zhao. Searching for Dark Photon Dark Matter with Gravitational Wave Detectors. *Phys. Rev. Lett.*, 121(6):061102, 2018.

[42] Kimihiro Nomura, Asuka Ito, and Jiro Soda. Pulsar timing residual induced by ultralight vector dark matter. *Eur. Phys. J. C*, 80(5):419, 2020.

[43] Yu-Mei Wu, Zu-Cheng Chen, Qing-Guo Huang, Xingjiang Zhu, N. D. Ramesh Bhat, Yi Feng, George Hobbs, Richard N. Manchester, Christopher J. Russell, and R. M. Shannon. Constraining ultralight vector dark matter with the Parkes Pulsar Timing Array second data release. *Phys. Rev. D*, 106(8):L081101, 2022.

[44] Caner Unal, Federico R. Urban, and Ely D. Kovetz. Probing ultralight scalar, vector and tensor dark matter with pulsar timing arrays. 9 2022.

[45] Jiang-Chuan Yu, Yue-Hui Yao, Yong Tang, and Yue-Liang Wu. Sensitivity of Space-based Gravitational-Wave Interferometers to Ultralight Bosonic Fields and Dark Matter. 7 2023.

[46] Eleni Bagui, Sebastien Clesse, Valerio De Luca, Jose María Ezquiaga, Gabriele Franciolini, Juan García-Bellido, Cristian Joana, Rajeev Kumar Jain, Sachiko Kuroyanagi, Ilia Musco, Theodoros Papanikolaou, Alvise Raccanelli, Sébastien Renaux-Petel, Antonio Riotto, Ester Ruiz Morales, Marco Scalisi, Olga Sergijenko, Caner Unal, Vincent Vennin, and David Wands. Primordial black holes and their gravitational-wave signatures, 2023.

[47] Samuel Passaglia and Misao Sasaki. Primordial black holes from CDM isocurvature perturbations. *Phys. Rev. D*, 105(10):103530, 2022.

[48] Sabino Matarrese, Ornella Pantano, and Diego Saez. General relativistic dynamics of irrotational dust: Cosmological implications. *Phys. Rev. Lett.*, 72:320–323, 1994.

[49] Keisuke Inomata and Takahiro Terada. Gauge Independence of Induced Gravitational Waves. *Phys. Rev. D*, 101(2):023523, 2020.

[50] Guillem Domènech. Scalar Induced Gravitational Waves Review. *Universe*, 7(11):398, 2021.

[51] Elisa G. M. Ferreira. Ultra-light dark matter. *Astron. Astrophys. Rev.*, 29(1):7, 2021.

[52] Alan H. Guth. Inflationary universe: A possible solution to the horizon and flatness problems. *Phys. Rev. D*, 23:347–356, Jan 1981.

[53] Andrei D. Linde. A New Inflationary Universe Scenario: A Possible Solution of the Horizon, Flatness, Homogeneity, Isotropy and Primordial Monopole Problems. *Phys. Lett. B*, 108:389–393, 1982.

[54] Alan H. Guth. The Inflationary Universe: A Possible Solution to the Horizon and Flatness Problems. *Phys.Rev.*, D23:347–356, 1981.

[55] David H. Lyth, David Roberts, and Michael Smith. Cosmological consequences of particle creation during inflation. *Physical Review D*, 57(12):7120–7129, June 1998.

[56] David Langlois and Sebastien Renaux-Petel. Perturbations in generalized multi-field inflation. *JCAP*, 0804:017, 2008.

[57] Antonio Riotto. Inflation and the theory of cosmological perturbations. *ICTP Lect. Notes Ser.*, 14:317–413, 2003.

[58] U. A. Yajnik. GRAVITATIONAL PARTICLE PRODUCTION IN INFLATION: A FRESH LOOK. *Phys. Lett. B*, 234:271–275, 1990.

[59] Andrei D. Linde. A New Inflationary Universe Scenario: A Possible Solution of the Horizon, Flatness, Homogeneity, Isotropy and Primordial Monopole Problems. *Phys.Lett.*, B108:389–393, 1982.

[60] Andrei D. Linde. Chaotic Inflation. *Phys. Lett. B*, 129:177–181, 1983.

[61] Andrei D. Linde. Axions in inflationary cosmology. *Phys. Lett. B*, 259:38–47, 1991.

[62] Edmund J. Copeland, Andrew R. Liddle, David H. Lyth, Ewan D. Stewart, and David Wands. False vacuum inflation with Einstein gravity. *Phys. Rev. D*, 49:6410–6433, 1994.

[63] Juan García-Bellido. Massive Primordial Black Holes as Dark Matter and their detection with Gravitational Waves. *J. Phys. Conf. Ser.*, 840(1):012032, 2017.

[64] Juan Garcia-Bellido and Ester Ruiz Morales. Primordial black holes from single field models of inflation. *Phys. Dark Univ.*, 18:47–54, 2017.

[65] Guillermo Ballesteros and Marco Taoso. Primordial black hole dark matter from single field inflation. *Phys. Rev.*, D97(2):023501, 2018.

[66] Hayato Motohashi and Wayne Hu. Primordial Black Holes and Slow-Roll Violation. *Phys. Rev.*, D96(6):063503, 2017.

[67] Cristiano Germani and Tomislav Prokopec. On primordial black holes from an inflection point. *Phys. Dark Univ.*, 18:6–10, 2017.

[68] Konstantinos Dimopoulos. Ultra slow-roll inflation demystified. *Phys. Lett.*, B775:262–265, 2017.

[69] Samuel M Leach, Misao Sasaki, David Wands, and Andrew R Liddle. Enhancement of superhorizon scale inflationary curvature perturbations. *Phys. Rev. D*, 64:023512, 2001.

[70] Osamu Seto, Jun'ichi Yokoyama, and Hideo Kodama. What happens when the inflaton stops during inflation. *Phys. Rev. D*, 61:103504, 2000.

[71] Samuel M. Leach and Andrew R. Liddle. Inflationary perturbations near horizon crossing. *Phys. Rev. D*, 63:043508, 2001.

[72] David H. Lyth. What would we learn by detecting a gravitational wave signal in the cosmic microwave background anisotropy? *Phys.Rev.Lett.*, 78:1861–1863, 1997.

[73] Edward W. Kolb and Andrew J. Long. Cosmological gravitational particle production and its implications for cosmological relics. *Rev. Mod. Phys.*, 96(4):045005, 2024.

[74] David Langlois. Inflation, quantum fluctuations and cosmological perturbations. In *Cargese School of Particle Physics and Cosmology: the Interface*, pages 235–278, 5 2004.

[75] Viatcheslav F. Mukhanov, H.A. Feldman, and Robert H. Brandenberger. Theory of cosmological perturbations. Part 1. Classical perturbations. Part 2. Quantum theory of perturbations. Part 3. Extensions. *Phys.Rept.*, 215:203–333, 1992.

[76] Edward W. Kolb and Andrew J. Long. Superheavy dark matter through Higgs portal operators. *Phys. Rev. D*, 96(10):103540, 2017.

[77] Michael S. Turner and Lawrence M. Widrow. Inflation Produced, Large Scale Magnetic Fields. *Phys. Rev. D*, 37:2743, 1988.

[78] Vera C. Rubin and W. Kent Ford, Jr. Rotation of the Andromeda Nebula from a Spectroscopic Survey of Emission Regions. , 159:379, February 1970.

[79] Leszek Roszkowski, Enrico Maria Sessolo, and Sebastian Trojanowski. Wimp dark matter candidates and searches—current status and future prospects. *Reports on Progress in Physics*, 81(6):066201, May 2018.

[80] R. D. Peccei and Helen R. Quinn. CP conservation in the presence of pseudoparticles. *Phys. Rev. Lett.*, 38:1440–1443, Jun 1977.

[81] Daniel J.H. Chung. Classical inflation field induced creation of superheavy dark matter. *Phys.Rev.*, D67:083514, 2003.

[82] Daniel J. H. Chung, Edward W. Kolb, and Antonio Riotto. Superheavy dark matter. *Phys. Rev. D*, 59:023501, 1998.

[83] Marco Fabbrichesi, Emidio Gabrielli, and Gaia Lanfranchi. The Dark Photon. 5 2020.

[84] Wayne Hu, Rennan Barkana, and Andrei Gruzinov. Fuzzy cold dark matter: The wave properties of ultralight particles. *Phys. Rev. Lett.*, 85:1158–1161, Aug 2000.

[85] Francesca Chadha-Day, John Ellis, and David J. E. Marsh. Axion dark matter: What is it and why now? *Science Advances*, 8(8):eabj3618, 2022.

[86] Bernard Carr, Florian Kühnel, and Marit Sandstad. Primordial black holes as dark matter. *Phys. Rev. D*, 94:083504, Oct 2016.

[87] Misao Sasaki, Teruaki Suyama, Takahiro Tanaka, and Shuichiro Yokoyama. Primordial black hole scenario for the gravitational-wave event gw150914. *Physical Review Letters*, 117(6), August 2016.

[88] Bernard Carr and Florian Kühnel. Primordial black holes as dark matter: Recent developments. *Annual Review of Nuclear and Particle Science*, 70(1):355–394, October 2020.

[89] Stephen Hawking. Gravitationally collapsed objects of very low mass. *Monthly Notices of the Royal Astronomical Society*, 152(1):75–78, 04 1971.

[90] B. J. Carr and S. W. Hawking. Black holes in the early universe. *Monthly Notices of the Royal Astronomical Society*, 168(2):399–415, 08 1974.

[91] Burak Himmetoglu, Carlo R. Contaldi, and Marco Peloso. Instability of the ACW model, and problems with massive vectors during inflation. *Phys. Rev. D*, 79:063517, 2009.

[92] Vittoria Demozzi, Viatcheslav Mukhanov, and Hector Rubinstein. Magnetic fields from inflation? *Journal of Cosmology and Astroparticle Physics*, 2009(08):025–025, August 2009.

[93] Alisha Marriott-Best, Marco Peloso, and Gianmassimo Tasinato. New gravitational wave probe of vector dark matter. *Phys. Rev. D*, 111(10):103511, 2025.

[94] Bill Atkins, Debika Chowdhury, Alisha Marriott-Best, and Gianmassimo Tasinato. Inflationary magnetogenesis beyond slow-roll and its induced gravitational waves. 7 2025.

[95] Gianmassimo Tasinato Alisha Marriott-Best, Marco Peloso. New gravitational wave probe of vector dark matter. *arxiv.org*, 2025.

[96] Peter W. Graham, David E. Kaplan, Jeremy Mardon, Surjeet Rajendran, and William A. Terrano. Dark Matter Direct Detection with Accelerometers. *Phys. Rev. D*, 93(7):075029, 2016.

[97] Joseph H.P. Jackson, Hooshyar Assadullahi, Andrew D. Gow, Kazuya Koyama, Vincent Vennin, and David Wands. The separate-universe approach and sudden transitions during inflation. *Journal of Cosmology and Astroparticle Physics*, 2024(05):053, May 2024.

[98] Martina La Rosa and Gianmassimo Tasinato. Ultralight dark matter from non-slowroll inflation, 2025.

[99] William H. Kinney. Horizon crossing and inflation with large eta. *Phys. Rev.*, D72:023515, 2005.

[100] Jerome Martin, Hayato Motohashi, and Teruaki Suyama. Ultra Slow-Roll Inflation and the non-Gaussianity Consistency Relation. *Phys. Rev.*, D87(2):023514, 2013.

[101] Hayato Motohashi, Alexei A. Starobinsky, and Jun'ichi Yokoyama. Inflation with a constant rate of roll. *JCAP*, 09:018, 2015.

[102] Shogo Inoue and Jun'ichi Yokoyama. Curvature perturbation at the local extremum of the inflaton's potential. *Phys. Lett. B*, 524:15–20, 2002.

[103] Konstantinos Tzirakis and William H. Kinney. Inflation over the hill. *Phys. Rev.*, D75:123510, 2007.

[104] Gianmassimo Tasinato. An analytic approach to non-slow-roll inflation. *Phys. Rev. D*, 103(2):023535, 2021.

[105] Ogan Özsoy and Gianmassimo Tasinato. Inflation and Primordial Black Holes. *Universe*, 9(5):203, 2023.

[106] Gerard 't Hooft. A Planar Diagram Theory for Strong Interactions. *Nucl. Phys. B*, 72:461, 1974.

[107] Gianmassimo Tasinato. A large $|\eta|$ approach to single field inflation, 2023.

[108] P.A.R. Ade et al. Planck 2015 results. XIII. Cosmological parameters. 2015.

[109] Neal Dalal and Andrey Kravtsov. Excluding fuzzy dark matter with sizes and stellar kinematics of ultrafaint dwarf galaxies. *Phys. Rev. D*, 106(6):063517, 2022.

[110] Tim Zimmermann, James Alvey, David J. E. Marsh, Malcolm Fairbairn, and Justin I. Read. Dwarf Galaxies Imply Dark Matter is Heavier than 2.2×10-21 eV. *Phys. Rev. Lett.*, 134(15):151001, 2025.

[111] Sabino Matarrese, Ornella Pantano, and Diego Saez. A General relativistic approach to the nonlinear evolution of collisionless matter. *Phys. Rev. D*, 47:1311–1323, 1993.

[112] Kishore N. Ananda, Chris Clarkson, and David Wands. The Cosmological gravitational wave background from primordial density perturbations. *Phys. Rev. D*, 75:123518, 2007.

[113] Daniel Baumann, Paul J. Steinhardt, Keitaro Takahashi, and Kiyotomo Ichiki. Gravitational Wave Spectrum Induced by Primordial Scalar Perturbations. *Phys. Rev. D*, 76:084019, 2007.

[114] Ryo Saito and Jun'ichi Yokoyama. Gravitational-Wave Constraints on the Abundance of Primordial Black Holes. *Prog. Theor. Phys.*, 123:867–886, 2010. [Erratum: Prog.Theor.Phys. 126, 351–352 (2011)].

[115] Edgar Bugaev and Peter Klimai. Induced gravitational wave background and primordial black holes. *Phys. Rev.*, D81:023517, 2010.

[116] José Ramón Espinosa, Davide Racco, and Antonio Riotto. A Cosmological Signature of the SM Higgs Instability: Gravitational Waves. *JCAP*, 1809(09):012, 2018.

[117] Kazunori Kohri and Takahiro Terada. Semianalytic calculation of gravitational wave spectrum nonlinearly induced from primordial curvature perturbations. *Phys. Rev. D*, 97(12):123532, 2018.